10-18-2018 3:30 PM

Thioindigo-Based Photoswitchable Hydrogen Bond Arrays

Fereshteh Davoud, *The University of Western Ontario*

Supervisor: Dr. James A. Wisner, *The University of Western Ontario*

A thesis submitted in partial fulfillment of the requirements for the Master of Science degree in Chemistry
© Fereshteh Davoud 2018

Abstract

In the context of hydrogen bonded materials, most efforts have been focusing on designing and synthesizing acceptor and donor arrays that in their original forms are capable of hydrogen bonding. However, less attention has been paid to the molecules that potentially act as viable acceptors or donors upon exposure to external stimuli.

This thesis describes the design, synthesis and photophysical properties of photochromic thioindigo derivatives as potential acceptors. Illumination of light can induce photoisomerization of thioindigo derivatives where they can change their orientation to generate linear hydrogen bond arrays (AAA). This linear arrangement accounts for the formation of hydrogen bonded complexes with different donor arrays (AAA-DD(D)). The stability of the complexes was determined by using ^{1}H NMR titration procedure where the most stable complex showed a K_a of 2.3 x 10^{-5} M^{-1}.

Keywords

Co-Authorship Statement

Jeffrey S. Pleizier is credited for the synthesis of **D4** and **D5**. Doug Hairsine (manager of mass spectrometry facility) has collected all the mass spectrometry data presented in this work. The crystallographic studies described in Chapter 2 was written in collaboration with Dr. Iamnica Janic Linares Mendez. Dr. Paul D. Boyle (X-Ray facility manager) is credited for x-ray crystallographic studies data collection and structure refinement. All of the remaining work in this thesis has been done by the author herself.

Acknowledgments

I would like to thank all the people who have helped me through these two years of my graduate program at Western University.

First and foremost, I have to give a big thank to my supervisor professor James A. Wisner for giving me this opportunity to work under his supervision and for always pushing me to do my best. His understanding, encouragement, and patience towards my performance during these two years have created a significant impact on my personal and professional development. I have learned so much during my studies that shaped me into the researcher I am today for which I am truly grateful.

Likewise, I am thankful to the members of the examination committee: Dr. Paul Ragogna, Dr. Viktor Staroverov, and Mark S. Workentin for your taking the time reading and outlining the areas where I can improve the quality of the work presented. I need to thank Dr. Michael A. Kerr for teaching the heterocycle course. You were always encouraging us during the course where you openly and patiently answered all the questions. I would also like to thank Dr. Joe Gilroy for his precious advice during the course and pushing me to think outside the box to face the real world. He has been a very caring person who offered help when I did not even ask for.

I would like to thank present group members, Jeffrey S. Pleizier and Dr. Iamnica Janic Linares Mendez. In particular, Jeffrey S. Pleizier who provided laboratory training when I first joined the group and assisted me in developing experimental procedures throughout my research. He has always been very kind and supportive. I just can say thank you, Jeff, for being there whenever things did not go well in the lab. You have always been encouraging and inspiring especially when I felt down. Janic, I am truly thankful for all the experiences and knowledge you have been sharing with me during my studies.

I would also like to extend my appreciation to all the faculty and staff at the Chemistry Department. In particular, many thanks to Mathew Willans (NMR facility manager) for his immeasurable help during titration procedures. Thank you, Matt, for being such an incredible person who tried to explain all the small details of working with NMR spectrometer. Without your help, it could have been difficult for me to get the results. Likewise, thanks to Doug Hairsine (Mass Spec facility manager) and Paul D. Boyle (X-Ray facility manager) for their aid towards the characterization of the compounds obtained.

پدرم و مادرم، حسن رضا و میترا، بهترین ها و عزیزترین های زندگیم، برای تمام سال ها و لحظاتی که تلاش کردید تا هر آنچه که برای رسیدن به آرزوهام نیاز بود رو فراهم کنید خاضعانه و با تمام وجودم سپاسگزارم. پدرم برای تمام باور قلبی که به من و توانایی های من نه تنها به عنوان یک دانشجو بلکه به عنوان یک انسان داشتی از صمیم قلب سپاسگزارم. برای تمام لحظاتی که تلاش کردی تا باور کنم از پس سخت ترین مشکلات بر میام ممنونم. برای تمام حمایت ها، توجه ها و برای تمام صبوری ها ممنونم. مادر مهربونم، برای تلاش های بی دریغت، برای تمام صبوری هات، برای همه از خود گذشتگی هات، برای تمام فداکاریات با همه وجودم ممنونم. بدون شک، بدون شما رسیدن به این نقطه غیر ممکن بود. ممنونم که غیر ممکن زندگیم رو برام ممکن کردین و من میتونم با افتخار بگم هر آنچه دارم به خاطر وجود پدر و مادر نازنینی مثل شماست. خواهرم فریبا، به خاطر تمام لحظاتی که کنارم بودی چه زمانی که ایران بودم و چه طی این دو سال ممنونم. ممنونم که همیشه مثل یه دوست در بدترین شرایط بودن تو باعث دلگرمی بود. فرزانه و مهدی، از اینکه با بودنتون باعث شدین زندگی ما معنی بهتری بگیره ممنونم. به خاطر تمام حس های قشنگتون و بودنتون ممنونم.

و در آخر همسرم، فرسامم، به خاطر تمام لحظات قشنگی که برام رقم زدی ممنونم. به خاطر تشویق ها، حمایت ها، بودن ها، اهمیت دادن ها و باور داشتن ها ممنونم. در کنار تو بودن قشنگ ترین و بهترین اتفاقی بود که میتونست برای من بیوفته. سپری کردن این دو سال با همه سختی هاش و به دور از خونواده بودن فقط با بودن تو ممکن بود. دوستت دارم مرد مهربونم.

Table of Contents

List of Tables

List of Figures

List of Schemes

List of Abbreviations

A	hydrogen bond acceptor
$BArF^{-1}$	tetrakis(3,5-bis(trifluoromethyl)phenyl)borate
$CDCl_3$	deuterated chloroform
$CDCl_2$	deuterated dichloromethane
Cy	cyclohexane
D	donor
d	doublet
dd	doublets of doublets
Δ	heat
ΔG	change in Gibbs free energy
δ	chemical shift
δ_{bound}	chemical shift of completely bound donor
δ_{free}	chemical shift of free donor
δ_{obs}	chemical shift observed
DCM	dichloromethane
DMF	N,N'-dimethylformamide
DNA	deoxyribonucleic acid
E	entgegen or cis
EI-HRMS	Electron Impact Ionization High Resolution Mass Spectrometry
eq.	equivalent
EtOH	ethanol

g	grams
gCOSY	gradient Correlation Spectroscopy
h	hours
hν	frequency
Hz	hertz
HMBC	Heteronuclear Multiple-Bond Correlation Spectroscopy
HSQCAD	Heteronuclear Signal Quantum Coherence Spectroscopy Adiabatic Version
i-PrOH	isopropanol
IUPAC	International Union of Pure and Applied Chemistry
J	coupling constant
K	Kelvin
K_a	association constant
kJ	kilojoules
λ_{max}	maximum wavelength
m	multiplet
M	molar
M^{-1}	per molar
mM	millimolar
min	minutes
μL	microliters
mL	milliliters
mol^{-1}	per mole
mmol	millimoles

MHz	megahertz
nm	nanometers
NMR	Nuclear Magnetic Resonance
˚C	Celsius degree
π	pi orbital
pH	minus logarithm of proton concentration
ppm	parts per million
Py	pyridine
R.T.	room temperature
s	singlet
t	triplet
T	temperature
THF	tetrahydrofuran
TLC	thin layer chromatography
TMS	tetramethylsilane
UV	ultra violet
Vis	visible
Vs.	versus
Z	zusammen or cis

Chapter 1

1   Introduction

1.1   Polymers

Polymers are one of the most ubiquitous materials that can be found in every aspect of human's lives. They have shown a myriad of applications in different fields ranging from industrial to biological systems. Polymer refers to a macromolecule with high molecular mass that encompasses large number of repeating units where they are held together by covalent bonds that endow specific physical and chemical characteristics to the polymer. These monomers are not limited to carbon and hydrogen. In fact, a wide range of heteroatoms such as nitrogen, oxygen, sulfur, chlorine, and phosphine can be incorporated in the polymer structure. Depending on the polymerization method and the types of monomers involved, polymers can exhibit basic structures of linear, branched and network (cross-linked) connectivity that delivers different properties and applications. The ongoing demand for synthesizing new polymers with unique applications, has led to the introduction of supramolecular polymers.

1.2   Supramolecular Polymers

Supramolecular polymers are a result of the interplay of supramolecular chemistry and polymer science that was first brought to attention by Jean-Marie Lehn and coworkers.[1a-c] They developed a polymer wherein the monomers were connected using hydrogen bonding to generate a liquid crystalline supramolecular polymer.

In contrast to traditional conventional polymers where the monomers are covalently bonded together,[2] supramolecular polymers are composed of building blocks brought together via reversible and often highly directional noncovalent interactions.[3] In fact, directional interactions are the driving force for the construction of supramolecular

polymers that lead to their polymeric characteristics, both in solution and bulk.[4] In addition, they impart a dynamic character to the structure where there is an equilibrium between the interacting monomers in the polymer .[5] The intrinsic dynamics are responsible for some interesting features of supramolecular polymers such as the ability to self-heal, high responsiveness to different external stimuli and environmental adaptivity.[4,5] Regarding their responsiveness to external stimuli, supramolecular polymers can be categorized in several groups containing but not limited to pH-responsive,[6] solvent-responsive,[7] photo-responsive,[8] electricity-responsive,[9] and thermally responsive materials.[10] Given these unusual features, supramolecular polymers can be elaborated to develop the next-generation of smart materials.

Depending on the non-covalent interactions involved in the formation of supramolecular polymers such as hydrogen bonding, metal coordination bonds, and aromatic donor-acceptor interactions (π-π stacking), these complexes can be divided into different categories.[4] Although each category displays distinctive properties and applications that can be easily differentiated, there are some supramolecular polymers that take advantage of incorporating multiple types of secondary interactions spontaneously. Utilizing these multiple driving forces allows precise control over the structure and functionality of the supramolecular polymers.

1.3   Non-Covalent Interactions

In the context of supramolecular polymer chemistry what holds the building blocks together are non-covalent or intermolecular interactions. These interactions are different from covalent interactions in two major senses. First, while covalent interactions are short range (approximately 2Å for covalent bonds), non-covalent interactions are longer range.[11] Secondly, instead of only sharing electrons, intermolecular interactions include a wide range of attractive and repulsive forces. They are normally much weaker than covalent interactions and vary from 2 kJ mol^{-1} for dispersion interactions to 300 kJ mol^{-1} for ion-ion interactions.[12-17] However, the use of multiple noncovalent bonds and their facile transformation can produce stable supramolecular entities with high binding energies.[11,18]

At a molecular level, the interplay of these non-covalent interactions can regulate physical and chemical properties of macromolecules such as boiling point, viscosity, vapor pressure, surface tension and density.

Table 1.1 Different types of intermolecular interactions and their features.[19,20]

Interaction	Strength (kJ mol^{-1})	Example	Distance dependence	Relative stability
Ion-ion	200-300	Tetrabutylammonium chloride	$1/r$	High
Ion-dipole	50-200	Sodium[15]crown-5	$1/r^2$, $1/r^4$	High
Dipole-dipole	5-50	Acetone	$1/r^3$, $1/r^6$	Low
Hydrogen bonding	4-120	Different examples based on their strength (Table 2)	See Table 2	Medium
Cation-π	5-180	K^+ in benzene	$1/r^2$, $1/r^4$	Medium
π-π	0-50	Benzene and graphite	$1/r^3$, $1/r^6$	Low
van der Waals	<5, variable depending on surface area	Argon, packing in molecular crystals	$1/r^6$	Low
Hydrophobic	Related to solvent-solvent interaction energy	Cyclodextrin inclusion compounds	-	High

Intermolecular interactions are of great importance in bio-disciplines as they are responsible for maintaining the three-dimensional structure of biopolymers such as nucleic

acids (RNA and DNA) and proteins.[11,21] Molecular recognition processes and drug design, are also governed predominantly by non-covalent interactions.[21,22] Furthermore, these interactions can play a pivotal role in the development of different fields of sensing, material science, and crystal engineering.[23-27]

Some of these supramolecular interactions are listed in Table 1.1, of which hydrogen bonding is one of the most extensively explored interactions as its existence is crucial for sustaining life. In order to comply with the requirements to have stable and directional self-assembled supramolecular polymers solely formed by hydrogen bonding, the minimum association constant or dimerization constant (K_a) has to be higher than 10^4 M^{-1} and 10^3 M^{-1} for reaching a degree of polymerization (DP) of 100 at 0.05 M and 1 M, respectively.
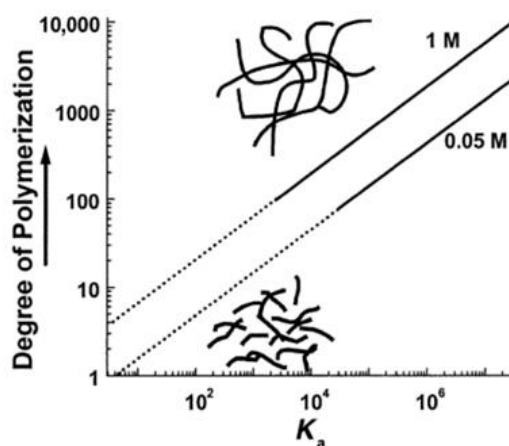
Figure 1.1 Degree of polymerization as a function of concentration and association constant for a main chain supramolecular polymer.

Figure 1.1,[3] explicitly indicates that concentration and inter-monomer association constants are two main factors that regulate the degree of polymerization. There is a linear relationship between the degree of polymerization and the association constant that varies at different concentrations. Higher concentration facilitates binding interactions between

monomers and result in longer chains. Likewise, a high association constant is needed to attain long enough polymer chains to exhibit polymer properties.

1.4 Hydrogen Bonding

Hydrogen bonding is a pervasive noncovalent interaction that offers extensive applications due to its defining characteristics of directionality, specificity and strength tunability. DNA is one of the spectacular examples of biological supramolecular polymers wherein two polynucleotide strands flawlessly intertwine by using hydrogen bonding in a highly specific and reversible manner (Figure 1.2).
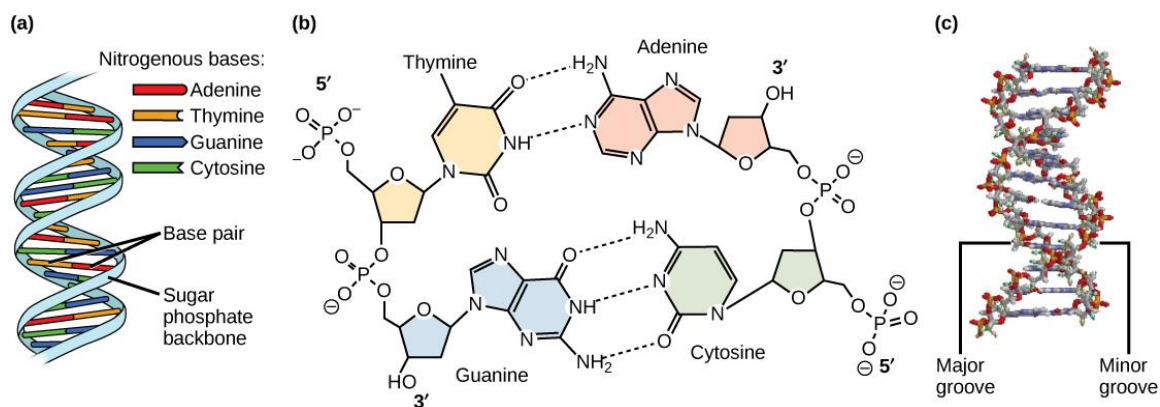
Figure 1.2 A cartoon of polynucleotide strands of DNA held together by hydrogen bonding between pairing bases.[28]

1.4.1   Definition

The term hydrogen bonding was first coined in 1939 by Linus Pauling in his book entitled "The Nature of the Chemical Bond" where he described it as: *"under certain conditions an atom of hydrogen is attracted by rather strong forces to two atoms, instead of only one, so that it may be considered to be acting as a bond between them. This is called the hydrogen bond".*[29] The rationale behind this definition as proposed by Pauling was that

because the H atom cannot have more than one covalent bond, the second interaction might be as a result of ionic forces.[30] Thus, as typical for ionic interactions, hydrogen bonding can solely occur in the presence of highly electronegative atoms.

However, years after establishing the concept of hydrogen bonding by Pauling, there were some examples of hydrogen bonding that did not fall within his definition. Therefore, in an attempt to find a comprehensive definition that can be applied to the context of modern chemistry, IUPAC, in 2011 reported a universal definition of hydrogen bonding *The hydrogen bond is an attractive interaction between a hydrogen atom from a molecule or a molecular fragment X–H in which X is more electronegative than H, and an atom or a group of atoms in the same or a different molecule, in which there is evidence of bond formation.*[31] This definition is simply represented in Figure 1.3 where H is covalently bonded to X and noncovalently to Y.

$$X{-}H \; + \; Y \; \rightleftharpoons \; X{-}H{-}{-}{-}{-}{-}Y$$
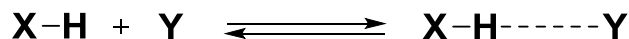
Figure 1.3 The concept of hydrogen bonding based on the definition provided by IUPAC.

Although this definition is widely accepted, Desiraju,[32] one of the influential IUPAC task group members, still believed that a hydrogen bonding consists of four atoms (or group of atoms), X, H, Y and Z and their arrangement as X-H⋯Y-Z can properly represent the hydrogen bonding. He argued that each part of the entire species (X-H, H⋯Y, and Y-Z) can mutually affect the other part and it is misleading to only consider the H⋯Y part as hydrogen bond. The nature of X, Y, Z can define the strength (energy) of hydrogen bond that lies in the range of 2.1 to 167 kJ mol^{-1}. It can be inferred that the strongest hydrogen bonds are stronger than the weakest covalent bonds, yet the weakest hydrogen bonds cannot be practically differentiated from van der Waals interactions.

1.4.2   Classifications

There have been several attempts to classify hydrogen bonding to obtain a better understanding of their behaviour in different contexts including but not limited to organic chemistry, supramolecular chemistry and biological systems. Two well-established classifications are based on the strength of hydrogen bond, and the spatial arrangement of the atoms involved in hydrogen bonding.

Regarding the first classification, hydrogen bonds can be categorized into three different groups as very strong, strong and weak. This classification first introduced by Desiraju and Steiner used various criteria such as geometrical, energetic, spectroscopic, or functional that tend to be distinctive in different strength of hydrogen bond (Table 1.2).[33] As Desiraju stated, it is a broad guide that can be used accurately in particular contexts of crystal engineering and supramolecular chemistry. However, in biological literature where bonds such as O-H$\cdots$O-H and specifically O_w-H$\cdots$$O_w$-H are not considered strong, another terminology has been employed to describe the hydrogen bonding interactions. In this context, Jeffrey preferred to use the terminology of strong, moderate and weak.[34] Table 1.2 lists the criteria used by two terminologies and shows how different these criteria are in each group of hydrogen bonds.[13,33-36]

Table 1.2 Classification of hydrogen bond strength relative to various criteria.

	Very strong or strong	Strong or moderate	weak
Examples	[F⋯H⋯F]⁻ [N⋯H⋯N]⁺	O-H⋯O=C N-H⋯O=C	C-H⋯O O-H⋯π
Bond energy (kJ mol^{-1})	60-170	15-60	<15
Length of X-H (Å)	0.05-0.2	0.01-0.05	≤0.01
D (X…Y) range (Å)	2.2-2.5	2.5-3.2	3.0-4.0
d (H…Y) range (Å)	1.2-1.5	1.5-2.2	2.0-3.0
θ (X-H…Y) range (°)	175-180	130-180	90-180
Effect on crystal packing	Strong	Distinctive	Variable
Covalency	Pronounced	Weak	Vanishing
Electrostatics	Significant	Dominant	Moderate
IR v_s relative shift	>25%	2-25%	<5%
^{1}H Chemical shift downfield (ppm)	14-22	<14	-

The second classification of hydrogen bonds is on the basis of the different geometries they exhibit, mainly in the solid state.[37] What makes hydrogen bonds distinguishable from other interactions such as van der Waals is their preference for linearity.[35] However, not all hydrogen bonds are linear. In fact, they are able to change their geometry to form more complex arrays of hydrogen bondings wherein the atom or molecule containing the H-X fragment is donor (D), and the other fragment (Y) is acceptor (A). These spatial

arrangements of linear, bent, donating bifurcated, accepting bifurcated, trifurcated, and three centers bifurcated are shown in Figure 1.4 wherein their corresponding angles are significantly deviated from the linear arrangement. These distortions from linearity explain why these geometries of hydrogen bonds cannot be present in very strong hydrogen bond interactions.
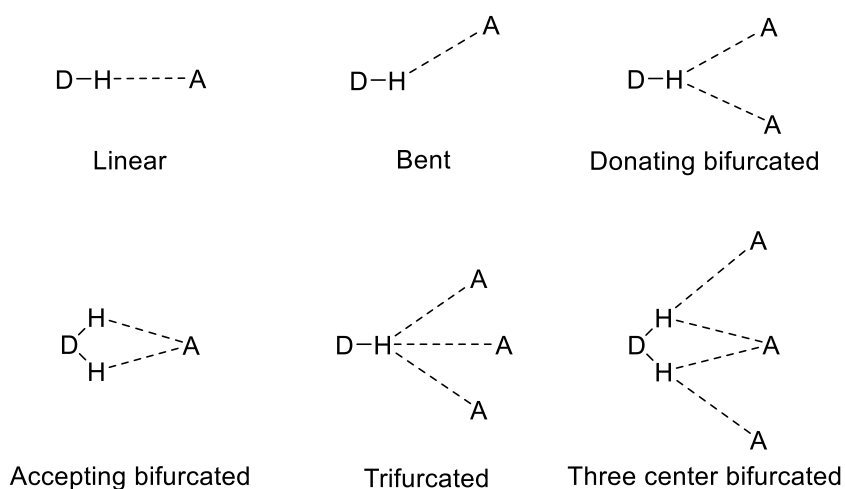
Figure 1.4 Various types of hydrogen bond arrays.[38,39]

1.4.3   Hydrogen Bond Strength in Supramolecular Complexes

Among non-covalent interactions, hydrogen bonding has been most extensively used in designing and constructing supramolecular complexes. These supramolecular complexes often include a large number of hydrogen bond interactions between donor and acceptor fragments such that their overall effect can regulate the stability of the complex. Therefore, to gain a deeper insight into the nature of hydrogen bonded supramolecular arrays and modulate their strength and properties to the application(s) of interest, it is essential to identify the elements that contribute to the strength of hydrogen bonding in supramolecular complexes. These elements are:

 1.   Number of hydrogen bonding sites

2. Sequence or arrangement of acceptor and donor hydrogen bond sites if adjacent to one another

3. Proximal functional groups and substituents (nature of acceptor and donor). For example, the presence of electron donating or electron withdrawing groups within the acceptor or donor fragments.

1.4.3.1   Number of Hydrogen Bonding Sites

The first contributing factor to the stability of complexes incorporating multiple hydrogen bond arrays is the number of hydrogen bonding sites that form the complementary complex. There is a positive correlation between the number of hydrogen bonds and complex stability. As the number of hydrogen bonds increases, the well-established concept of cooperativity that refers to the overall effect of hydrogen bonds results in higher stability of the complex.[20,40] This contributing factor was studied by Zimmerman and Murry, wherein they chose hydrogen bond complexes with different number of contiguous hydrogen bond acceptor-donor arrangements of DD-AA, DD-AAA, DDD-AA, and DDD-AAA.[41,42] As shown in Figure 1.5, the highest association constant (K_a) belongs to triply hydrogen bond complex DDD-AAA ($\geq 10^5$ M^{-1}), while the DD-AA forms the least stable complex with $K_a = 260$ M^{-1}. Comparing DD-AAA and DDD-AA, they pointed out that the effect of incorporating an extra hydrogen donor site on complex stability is greater than that was observed for one with extra hydrogen acceptor.

Figures and affinities shown in figure:

DD-AA
K_a = 260 M^{-1}

DD-AAA
K_a = 848 M^{-1}

DDD-AA
K_a = 3 x 10^3 M^{-1}

DDD-AAA
$K_a \geq$ 10^5 M^{-1}
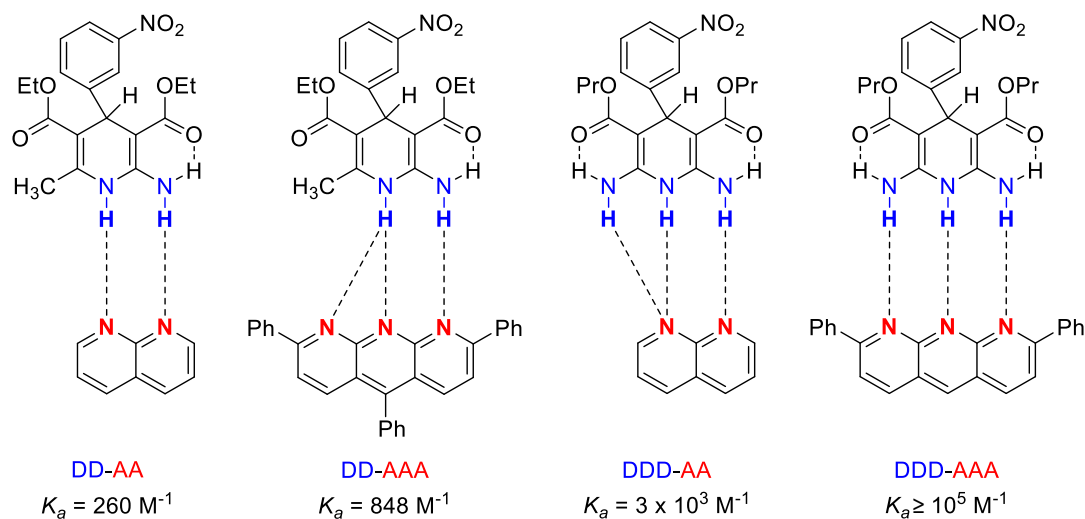
Figure 1.5 Hydrogen bond complexes with different numbers of hydrogen bonding sites in both acceptor and donor entities studied in CDCl$_3$ at 298 K by Zimmerman and Murry.[41,42]

1.4.3.2 Sequence or Arrangement of Acceptor and Donor Hydrogen Bond Sites

The binding affinity can also be affected by the sequence of adjacent donor and acceptor sites. The importance of this feature, that can lead to a large variation in the association constants of supramolecular complexes, was first recognized by Jorgenson (Figure 1.6).[43,44] Evaluating the association constants of different hydrogen bond complexes of nucleotide bases,[43,45-47] he noted that even with a similar number of primary hydrogen bonds in each system, the variation in the association constants could be a result of the different arrangements of the hydrogen bonding sites that lead to different secondary electrostatic interactions.
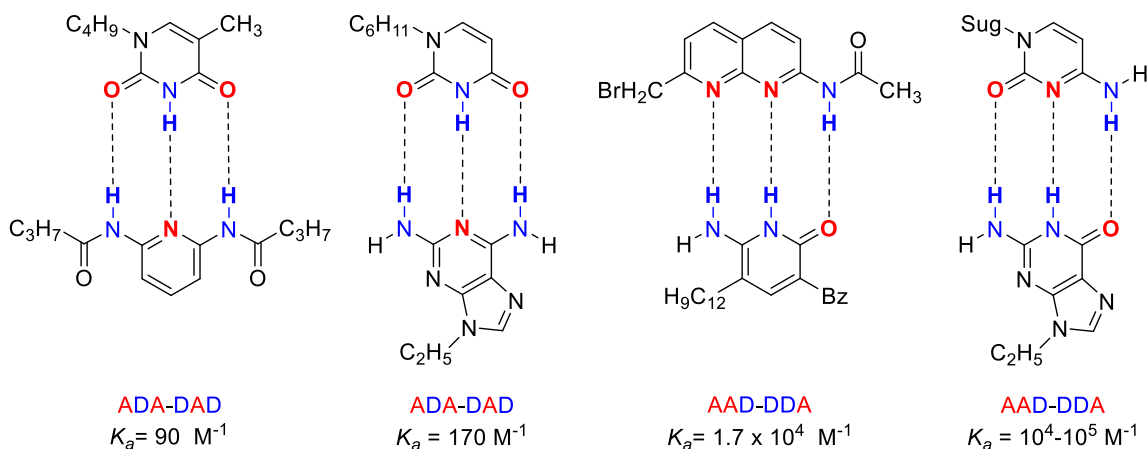
Figure 1.6 Triply hydrogen bonded systems studied by Jorgenson to introduce the concept of secondary hydrogen bonds.[43,44]

Inspired by that finding, Zimmerman and co-workers, in an attempt to test the generality of the proposed analysis examined new triply hydrogen bonded complexes.[48] The results obtained from their study further confirmed the substantial effect of secondary interactions on the stability of hydrogen bond complexes. Their findings led to the introduction of attractive and repulsive secondary interactions resulting from the adjacent donor and acceptor groups (Figure 1.7). Although all three complexes depicted in Figure 1.7 have three hydrogen bonding sites, ADA-DAD (**a**) exhibits a 10^2-10^3 M^{-1} association constant, while in the AAD-DDA (**b**) arrangement this value is approximately 10^4-10^5 M^{-1}. The highest association constant exceeding 10^5 M^{-1} belongs to (**c**) wherein the active hydrogen bonding sites are arranged in an AAA-DDD manner which means solely attractive secondary interactions are present.
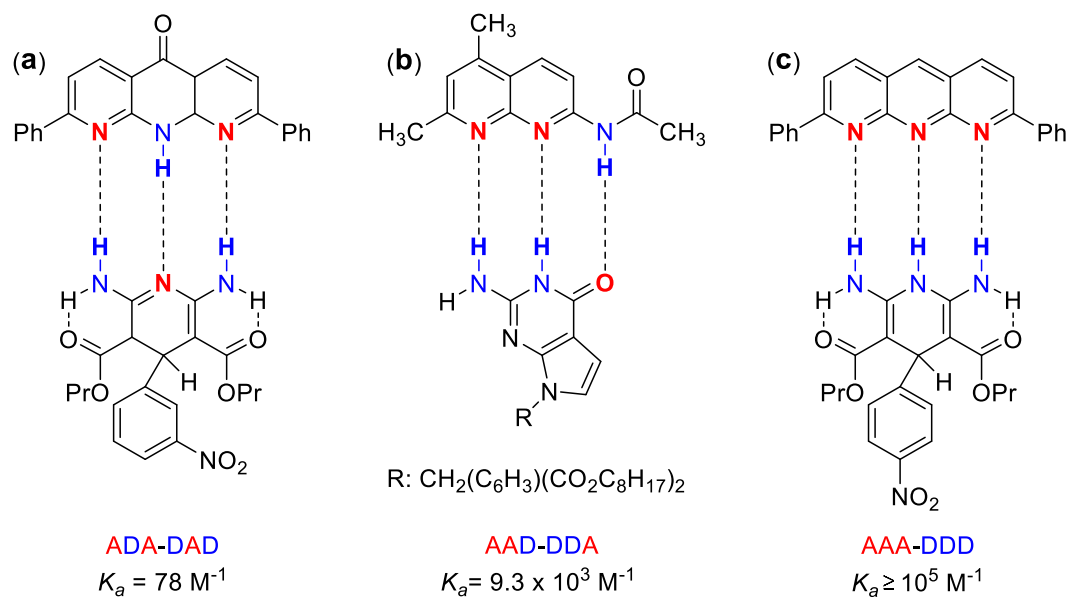
Figure 1.7 The effect of secondary hydrogen bond interactions on the association constant of triply hydrogen bond complexes.

Indeed, as the number of attractive interactions increases between the acceptors and donors the resulting hydrogen bond systems tend to be more stable. This concept of secondary hydrogen bond interactions is simplified in Figure 1.8 in the same order given above for the complexes.
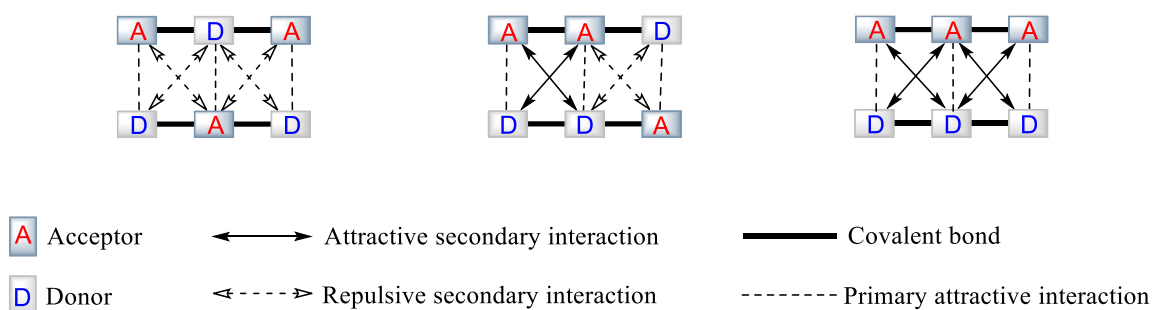
Figure 1.8 Simplified analysis of secondary hydrogen bond interactions.

Analysis of dozens of complexes resulted in average values for primary and secondary interactions of 7.9 and 2.9 kJ mol^{-1}, respectively.[49]

1.4.3.3   Nature of Acceptor (A) and Donor (D)

Ideally, for the formation of hydrogen bond complexes, the hydrogen atoms of donor sites need to be positively polarized, while on the other side, the acceptors need to be electron rich. Therefore, the last factor to consider is the influence of substitution on acceptors and donors on complex stability. Considering the previous results obtained by Jorgensen and Zimmerman to design various multiple hydrogen bond motifs, Wisner and coworkers,[50] targeted an AAA-DDD triple complex and further modified the donor to study any changes in the association constants. Figure 1.9 highlights the important effect of substitution of the donor structure that in turn results in different binding affinities.

X	Y	K_a (M[-1])
H	H	3.7×10^3
Br	H	7×10^3
H	CO$_2$Et	1.1×10^4
Br	CO$_2$Et	2.6×10^4
H	CN	2.9×10^4
CN	Br	4.9×10^4
CO$_2$Et	CO$_2$Et	5.4×10^4
CN	CN	1.1×10^5

DDD-AAA
CDCl$_3$, 298 K
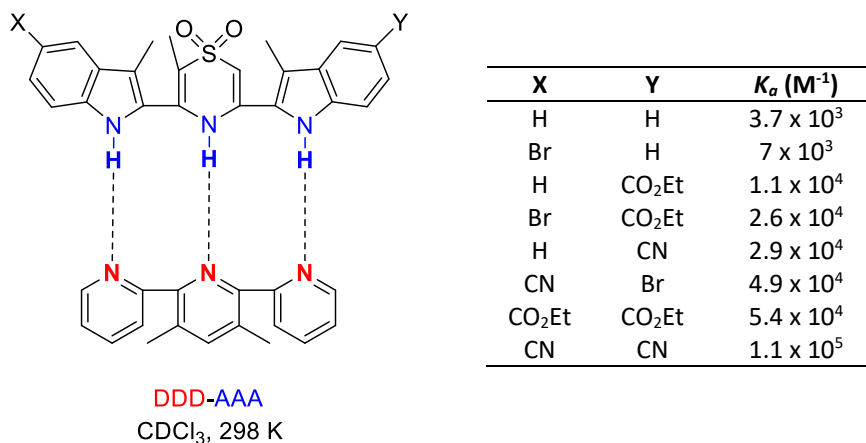
Figure 1.9 Modified supramolecular AAA-DDD complex and the corresponding K_a in CDCl$_3$ at 298 K.[50]

They observed that the highest association constant obtained where two strong electro withdrawing groups were introduced in the donor fragment ($K_a = 1.1 \times 10^5$). Two CN

groups pull electron density away from the donor hydrogen atoms through induction and resonance to make them more electropositive.

1.5   Photoswitches

Molecular photoswitches are small molecules that encompass a chromophoric core in their structure. Upon irradiation with light, these photochromic or photoswitching molecules can undergo reversible changes between at least two (meta) stable states. These two forms show different physicochemical properties such as polarity,[51] refractive indices,[52] dielectric constant,[53] charge distribution,[54] color and reactivity solely by absorbing light.[55] Light as an external stimulus shows several advantages over other stimuli; it is non-invasive over a wide range of wavelengths, it can be delivered with high spatial-temporal precision, and no additional reagent is required to proceed the reaction. In addition, the wavelength and intensity of this stimulus can be precisely tuned to guarantee the preferred properties and applications.[51,56]

Some of the most important photoswitches that have been extensively studied are shown in Schemes 1.1 and 1.2.[57] The reversible interconversion of these photoswitches can occur through either *cis*/*tr*ans (*E*/*Z*) double bond photoisomerization or cyclization/ring-opening reactions. Intramolecular hydrogen transfer, dissociation processes, intramolecular group transfer and electron transfer (oxidation-reduction) are other examples of photochromic processes that can produce two photoisomers, Scheme 1.3-1.6).[57]

These molecular photoswitches, depending on their thermal stability, can be categorized into two different classes of thermally reversible (T-type) and bistable (P-type or photochemically reversible type).[51,58] Most photoswitches belong to T-type class wherein they revert thermally to their initial state in the absence of light. On the other hand, P-type photochromic molecules (e.g. diarylethenes and furylfulgide, Scheme 1.2) are thermally stable with no tendency to convert back to the initial state even if high temperature is applied.[59-61]
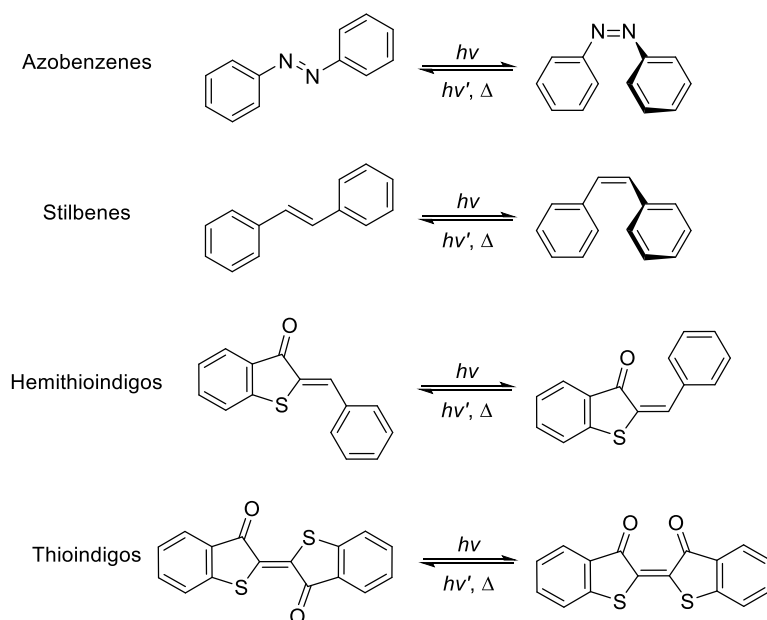
Scheme 1.1 Photochromic switches performing conversion by *cis/trans* (*E/Z*) photoisomerization.
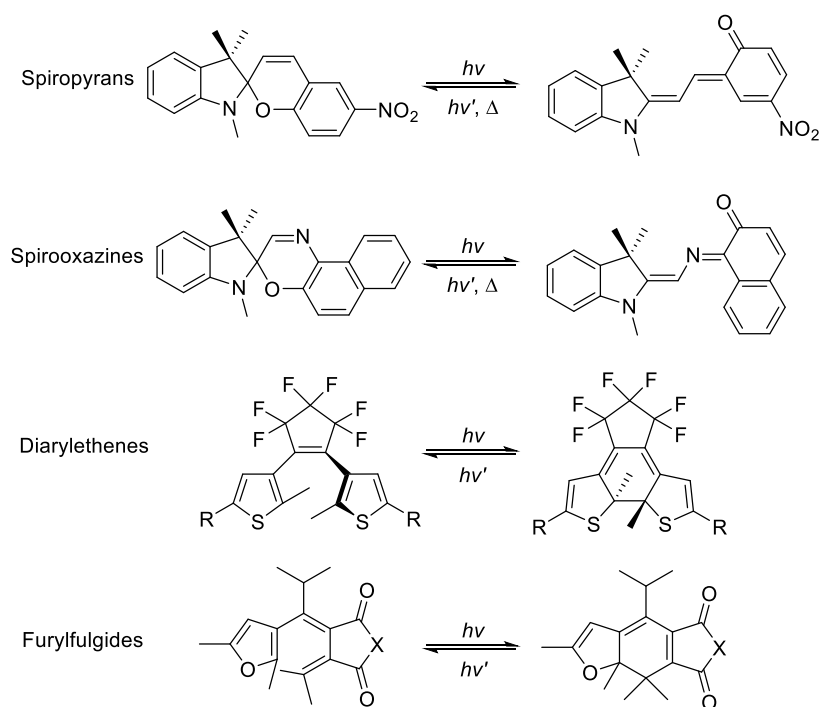
Scheme 1.2 Photochromic switches performing conversion by cyclization/ring-opening. (diarylethenes and furylfulgides are p-type photochromic molecules that do not convert thermally).[59]

Viologens
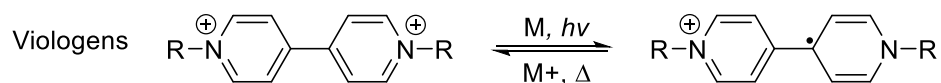
Scheme 1.3 A photochromic switch performing conversion by electron transfer and reduction.

Triarylmethanes
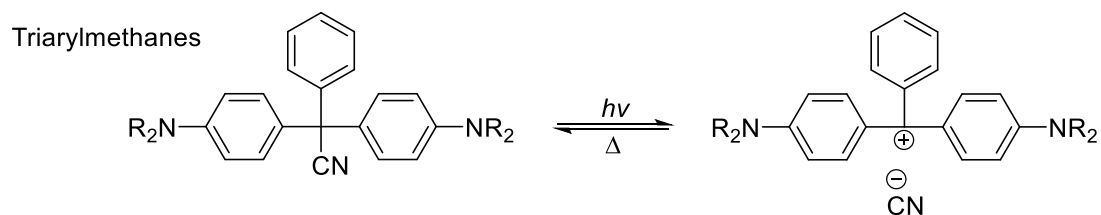
Scheme 1.4 A photochromic switch performing conversion by a dissociation process.

Perimidinespirocyclohexadienones
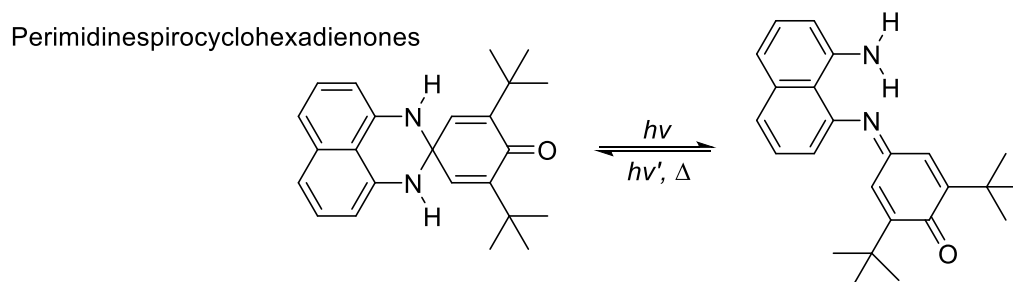
Scheme 1.5 A photochromic switch performing conversion by intramolecular hydrogen transfer.

Polycyclic quinones (periaryloxyquinones)
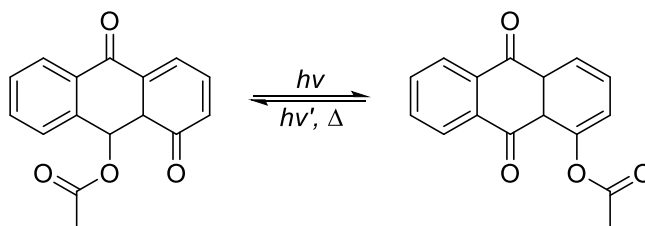
Scheme 1.6 A photochromic switch performing conversion by intramolecular group transfer.

There are a variety of procedures that take advantage of using photoswitches. The most important example of these procedures in biological systems is vision. The underlying concept of vision is *cis/trans* isomerization of the rhodopsin chromophore (11-*cis*-retinylidene (1)) to all-*trans*-retinylidene that takes place in the presence of light.[62] Based on this process, different vision-restoration strategies have been developed to restore visual function to the blind retina by using light sensitive azobenzene-based photoswitches.[63] Other biological applications of photoswitches are biomedical imaging and drug delivery.[64] In addition, incorporating photoswitches in a variety of materials has shown promising results in different fields of optical devices, smart materials, catalysis, surface chemistry, polymers and supramolecular polymers.[65-68] Scheme 1.7 shows an example of photochromic diarylethene polymers wherein the closed isomer is photostable under ambient light, and by applying heat above 150 °C, photocoloration and rapid thermal bleaching occurred. This polymer can be potentially used in rewritable display materials and image recordings by a write-by-light/erase-by-heat system as the reversible isomerization between colored isomer (the closed form) and colorless isomer (the open form) can be modulated by irradiation of light and thermal conversion.[69]
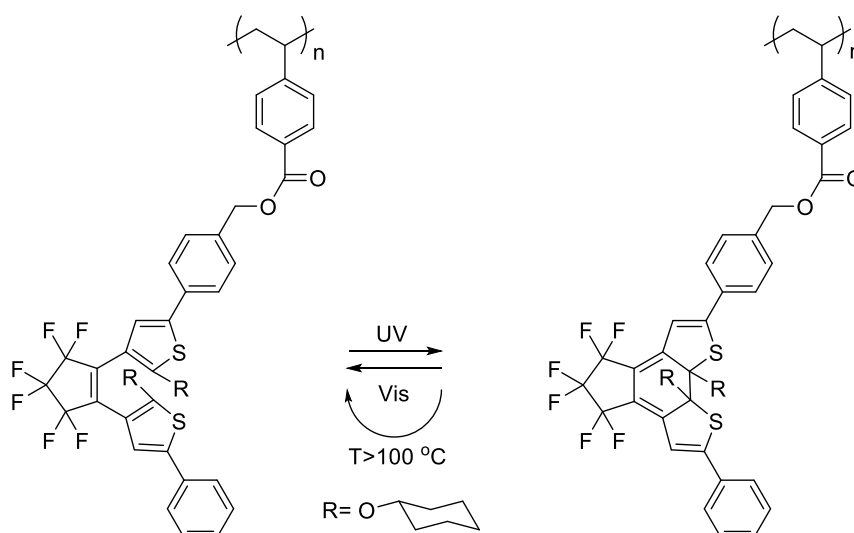
Scheme 1.7 Photocoloration and thermal bleaching of the diarylethenes derivatives.

1.6 Photoswitchable Hydrogen Bonded Supramolecular Polymers

Photoswitchable hydrogen bonded supramolecular polymers contain photochromic compounds that upon irradiation can switch between two states, where these states exhibit differences in the formation of hydrogen bonds. Typically, one state (before photoisomerization) is unable to form effective hydrogen bonds as the geometry of the molecule prevents any favorable arrangement. However, after irradiation, in a new orientation, the arrangements of hydrogen bonding sites match to result in a stable complex. These photoswitchable entities can be covalently or non-covalently incorporated in the structure of supramolecular polymers. They can be either the monomeric building blocks of the main chain or a pendant side chain.[70] In pioneering work conducted by Takeshita,[71] photoswitchable diarylethene was implemented between monomeric units of ureido-pyrimidinone (UPy) to form a hydrogen bonded supramolecular polymer where UPys are self-assembled by quadruple hydrogen bonding. As illustrated in Scheme 1.8, using different wavelengths (UV and visible room light), the supramolecular polymer can reversibly transform back and forth between open and closed forms wherein the particle sizes of the isomers are different.
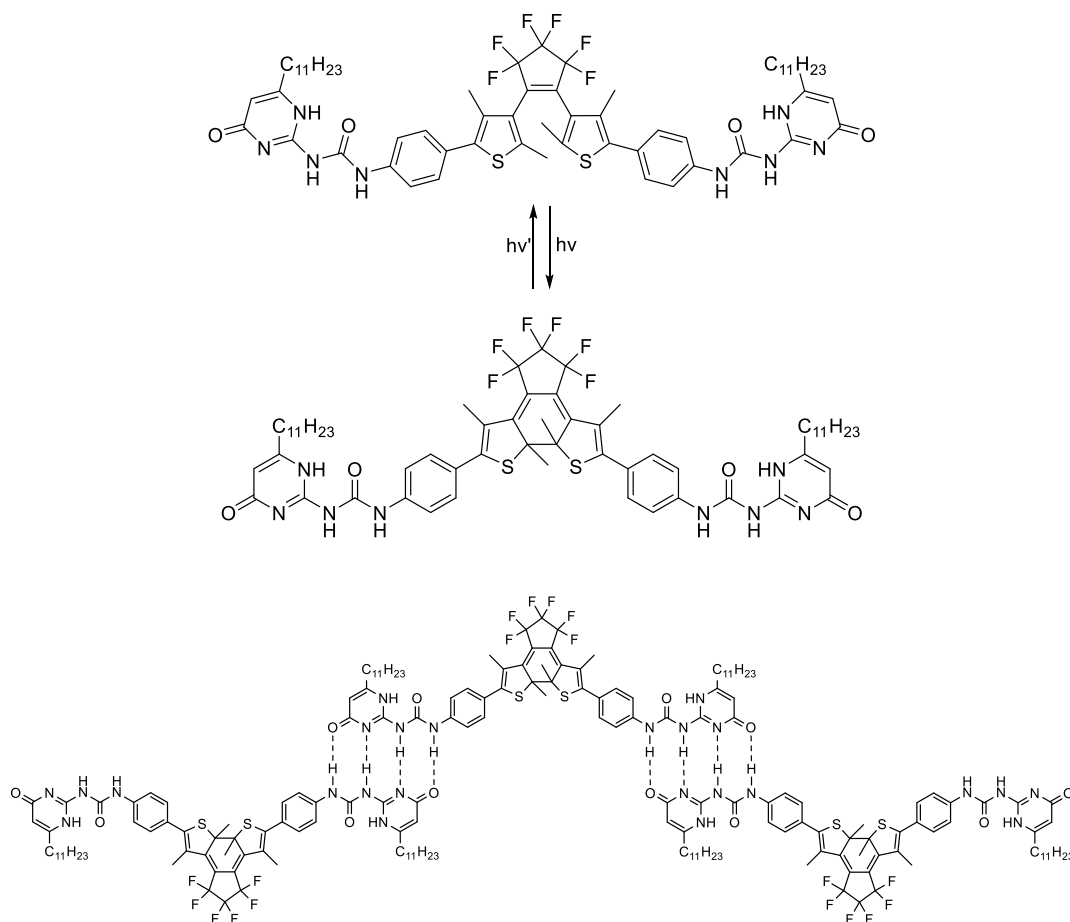
Scheme 1.8 Quadruple hydrogen bonded supramolecular polymer of dialkylethenes and UPy.
The closed (lower) form exists as large aggregates. The open (upper) form does not.

Following the previous report, in 2013, Yang and coworkers,[72] reported another photoresponsive supramolecular polymer wherein the monomeric units including a stiff stilbene and two ureidopyrimidinone moieties were connected via hydrogen bonding. Photoisomerization of the stilbene resulted in two isomeric forms with different self-assembly behaviors and physical properties. The photo generated *Z*- and *E*-isomers proved to have different polymerization mechanisms of ring-chain and isodesmic growth, respectively. The former isomer polymerized to form fluorescent nanofibers by electrospinning, while the latter one produced a multi-responsive gel. Scheme 1.9, pictures the concept of photoswitching for this stiff stilbene-based supramolecular polymer where the ureidopyrimidinone parts of the monomer provided a linear arrangement of quadruple

hydrogen bonding sites in both isomers but with different proximities and spatial relationships.
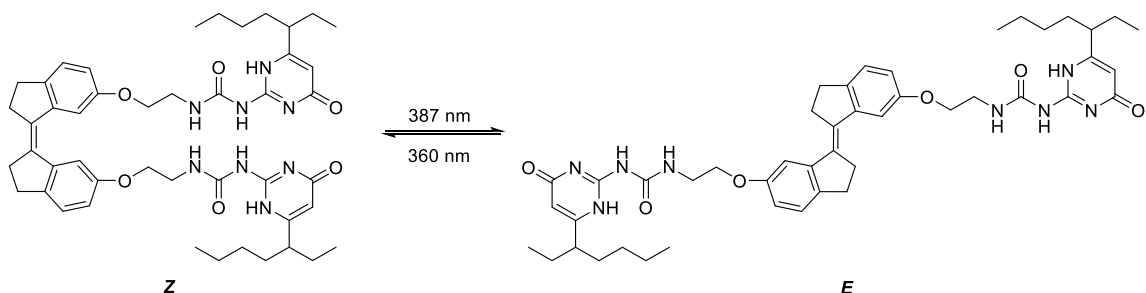
Scheme 1.9 *E/Z* photoisomerization of the stiff stilbene-based supramolecular polymer.

Photoswitches can also perform as side chain pendants of supramolecular polymers. These pendant groups can covalently or noncovalently attach to the main chain.[73,74] A good example in this class is the work conducted in Zhao's group wherein poly(4-vinyl pyridine) was functionalized by photochromic 7-(carboxymethoxy)-4-methylcoumarin as a pendant group.[73] The formation of non-covalent hydrogen bonds between the pyridyl and carboxylic acid groups yield a hydrogen bonded photoswitchable supramolecular network polymer (Scheme 1.10). Due to the presence of hydrogen bonds, the films of this supramolecular polymers exhibit large-scale photoinduced bending. A plausible mechanism would be the photodimerization of coumarin pendants along the polymer chains that produce imbalanced surface stress and thereby the film bend. These photodeformable polymers can offer some interesting applications in shape-memory materials, artificial muscles, and remotely photocontrolled devices.[75-78]
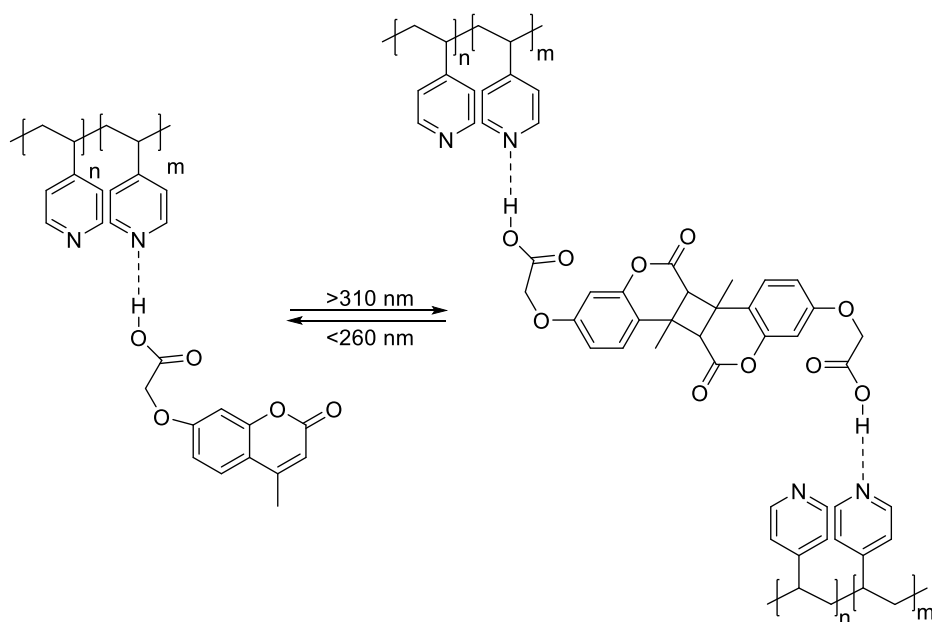
Scheme 1.10 The formation of hydrogen bonds between the main chain poly(4-vinyl pyridine) and 7-(carboxymethoxy)-4-methylcoumarin as a photoswitchable pendant.

1.7 Photoswitchable Thioindigo

Indigo and its sulfur analog, thioindigo, are compounds that have been used as vat dyestuff to color textiles from ancient time. Indigo is a symmetrical molecule comprised of two indolin-3-one moieties that are bridged by a central double bond. Its sulfur analog, thioindigo, has the same symmetrical structure where the two NH groups are replaced with sulfur atoms (benzo[b]thiophen-3(2H)-one) (Scheme 1.11).
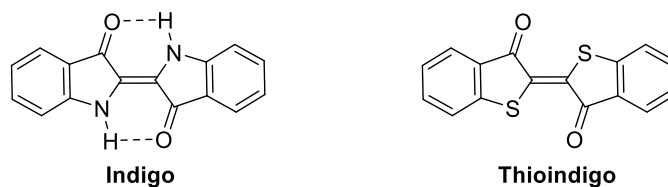
Scheme 1.11 Structures of indigo and thioindigo.

This small modification accounts for remarkable differences in photophysical properties and applications of these two molecules. The most substantial difference is their ability to isomerize upon irradiation with light. Indigo is locked in its *trans* form due to the presence of hydrogen bonding between NH groups and nearby CO groups. However, thioindigo can undergo appreciable and reversible *cis/trans* photoisomerization. This photoisomerizability of thioindigo is due to the loss of hydrogen bonding resulting from the replacement of NH groups with sulfur atoms. In general, the *trans*-isomer of thioindigo is the thermodynamically more stable form. Upon irradiation the double bond character of the central bond reduced, and the molecule can switch and relax back to the ground state of the *cis*-isomer. In the absence of light, the c*is*-isomer is to be less stable and at room temperature, it can thermally revert to the *trans* isomeric form. The thermal conversion is slow; however, irradiation at a shorter wavelength (480 nm) can facilitate the reversion to *trans* form (Scheme 1.12).
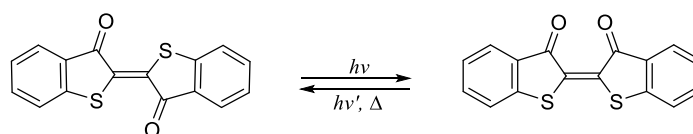
Scheme 1.12 General *cis/trans* isomerization for thioindigos.

In terms of their absorption spectra,[79,80] the *trans*-isomer displays three maxima: two at shorter wavelengths that correspond to symmetry allowed $\pi \rightarrow \pi^*$ transitions to produce the S_1 and S_2 excited states, and another absorption band at longer wavelength (approximately 548 nm) that corresponds to a $n \rightarrow \pi^*$ transition to yield the T_1 excited state. After irradiation and isomerization to *cis*-isomer, two maxima of $\pi \rightarrow \pi^*$ transitions overlap to form a band at approximately the same wavelength, whereas the $n \rightarrow \pi^*$ transition shows a blueshift (hypsochromic shift). In terms of the photoisomerization mechanism, after years of debate, it has been agreed that the mechanism involves a small $S_1 \rightarrow S_0$ (singlet excited state)

followed by an intersystem crossing to the triplet state $S_1 \rightarrow T_1$ (a triplet excited states). [81-85]

A number of thioindigo derivatives have been studied both theoretically and experimentally to deliver a better understanding of physical and photophysical properties of this class of photoswitches. Generally, a bathochromic shift for the largest-wavelength absorption band can be expected by an electron donating substitution at the 5-position of the phenyl ring. Introducing electron-donating groups at the order of C-5> C-4> C-7> C-6 can continuously shift the absorption band bathochromically. Meanwhile, incorporating electron-withdrawing groups in the structure of thioindigo can result in a hypsochromic shift of the largest-wavelength. [86,87]

Making a library of thioindigo derivatives have not been limited to the substitution of different functional groups on the peripheral rings. Thioindigoids refer to thioindigo-based photochromic compounds that comprise of only one half of thioindigo, benzo[b]thiophen-3(2H)-one. The other half could be an isatin (I), thioquinone (II),[88] stilbene (III),[89] or acenaphthylene-1,2-dione (IV) group. These thioindigoids are also known as hemithioindigos and are equally photoresponsive as they contain a central double bond (Scheme 1.13).
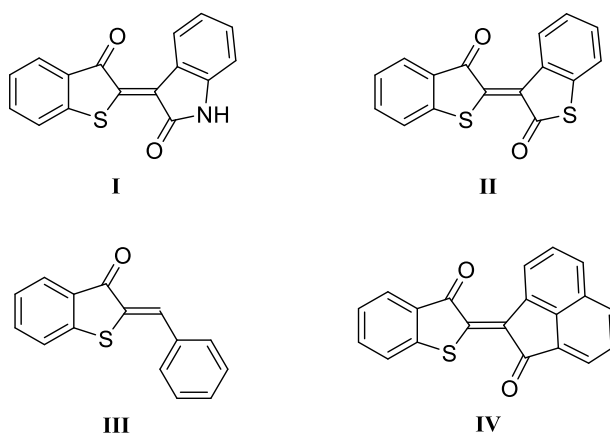
Scheme 1.13 Different derivatives of thioindigo.

Thioindigos have been predominantly known as dyestuff and have been used to dye textiles. However, they have received more attention once their photoswitchability was determined. Due to their ability to reversibly switch upon irradiation, they can render interesting applications in different fields of sensors, liquid crystal films (as one of the first on/off switches),[90,91] solar cells,[92] ion transport,[93] and inorganic supports.[94] More importantly, as this class of photoswitch performs *cis/trans* isomerization under ambient light, they can be attractive candidates for biological applications.[95]

1.8 Scope of Thesis

The main purpose of this project was to develop new complementary hydrogen bond complexes wherein a photoswitch (thioindigoid) was introduced as a hydrogen bond acceptor array. What illustrates the novelty of the project is the employment of light as an external stimulus that can modulate the hydrogen bond array's geometry of the photochromic acceptor by inducing an *E/Z* isomerization. This photoisomerization plays a key role in determining the stability of the hydrogen bond arrays as only one isomer is able to form hydrogen bonding and thereby a stable complex. Therefore, the main challenge was measuring the degree of stability of these photoresponsive hydrogen bonds complexes upon irradiation. Chapter 2 will discuss the design, synthesis, and characterization of different photo-responsive AAA-DD(D) complementary hydrogen bond complexes.

1.9 References

1. (a) Fouquey, C.; Lehn, J. M.; Levelut, A. M. *Adv. Mater.* **1990**, *5*, 254-257. (b) Lehn, J. M. *Angew. Chem. Int. Ed.* **1990**, *29*, 1304-1319. (c) Lehn, J. M. *Science* **1993**, *260*, 1762-1763.

2. Staudinger, H. *Berichte Dtsch. Chem. Ges. B Ser.* **1920**, *53*, 1073-1085.

3. Brunsveld, L.; Folmer, B. J. B.; Meijer, E. W.; Sijbesma, R. P. *Chem. Rev.* **2001**, *101,* 4071-4097.

4. Yang, L.; Tan, X.; Wang, Z.; Zhang, X. *Chem. Rev.* **2015**, *115*, 7196-7239.

5. Bochicchio, D.; Pavan, G. M. *Adv. Phys. X*, **2018**, *3*, 315-337.

6. Ma, L.; Kang, H.; Liu, R.; Huang, Y.; *Langmuir*, **2010**, *26*, 18519-18525.

7. Wang, J-H.; Li, M.; Li, D. *Chem. Sci.*, **2013**, *4*, 1793-1801.

8. Lendlein, A.; Jiang, H. Y.; Jünger, O.; Langer, R. *Nature*, **2005**, *434*, 879-882.

9. Biggs, J.; Danielmeier, K.; Hitzbleck, J.; Krause, J.; Kridl, T.; Nowak, S.; Orselli, E.; Quan, X.; Schapeler, D.; Sutherland, W.; Wagner, J. *Angew. Chem. Int. Ed. Engl.*, **2013**, *52*, 9409-9421.

10. Lagoudas, D. C. *Shape Memory Alloys: Modeling and Engineering Applications,* Boston: Springer-Verlag, 2008.

11. Müller-Dethlefs, K.; Hobza, P. *Chem. Rev.* **2000**, *100*, 143-168.

12. Pihko, P. M. *Hydrogen bonding in organic synthesis*, Wiley-VCH, Weinheim, 2009.

13. Gilli, P.; Gilli, G. *The nature of the hydrogen bond*, Oxford: Oxford University Press, 2009.

14. Hobza, P.; Müller-Dethlefs, K. *Non-covalent interactions: theory and experiment*, Cambridge, UK: Royal Society of Chemistry, 2010.

15. Gale, P. A.; Steed, J. W. *Supramolecular chemistry: from molecules to nanomaterials*, Chichester: John Wiley & Sons, Ltd, 2012.

16. Baev, A. K. *Specific intermolecular interactions of organic compounds*, Heidelberg: Springer, 2012.

17. Baev, A. K. *Specific intermolecular interactions of nitrogenated and bioorganic compounds*, Heidelberg: Springer, 2014.

18. Lodish, H.; Berk, A.; Zipursky, S. L.; Matsudaira, P.; Baltimore, D.; Darnell, J. *Molecular cell biology,* New York: W. H. Freeman, 2000.

19. Goshe, A. J.; Steele, I. M.; Ceccarelli, C.; Rheingold, A. L.; Bosnich, B. *Proc. Natl. Acad. Sci. U.S.A.* **2002**, *99*, 4823-4829.

20. Steed, J. W.; Turner, D. R.; Wallace, K. *Core concepts in supramolecular chemistry and nanochemistry*, John Wiley & Sons, Inc., 2007.

21. Černý, J.; Hobza, P. *Phys. Chem. Chem. Phys.* **2007**, *9*, 5291-5303.

22. Konteatis, Z. D.; Klon, A. E.; Zou, J.; Meshkat, S. *Methods Enzymol.* **2011***, 493,* 357-380.

23. Schneider, H. J. *Angew. Chem. Int. Ed.* **2009**, *48*, 3924-3977.

24. Osada, Y.; De Rossi, D. E. *Polymers, Sensors, Actuators,* Berlin: Springer, 2000.

25. Hatada, K. *Macromolecular design of polymeric materials*, New York: Marcel-Dekker, Inc., 1997.

26. Moulton, B; Zaworotko, M. J. *Chem. Rev.* **2001**, *101*, 1629-1658.

27. Aakeroy, C. B.; Seddon, K. R. *Chem. Soc. Rev.* **1993**, *22*, 397-407.

28. https://courses.lumenlearning.com/suny-osbiology2e/chapter/dna-structure-and-sequencing/

29. Pauling, L. *The nature of the chemical bond and the structure of molecules and crystals: an introduction to modern structural chemistry,* New York: Cornell University Press, 1960.

30. Smith, D. A. *In modeling the hydrogen bond*, Washington: ACS Symposium Series, American Chemical Society, 1994.

31. Arunan, E.; Desiraju, G. R.; Klein, R. A.; Sadlej, J.; Scheiner, S.; Alkorta, I.; Clary, D. C.; Crabtree, R. H.; Dannenberg, J. J.; Hobza, P.; Kjaergaard, H. G.; Legon, A. C.; Mennucci, B.; Nesbitt, D. J. *Pure Appl. Chem.* **2011**, *83*, 1637-1641.

32. Desiraju, G. R. *Angew. Chem. Int. Ed.* **2011**, *50*, 52-59.

33. Desiraju, G, R.; Steiner, T. *The weak hydrogen bond in structural chemistry and biology,* Oxford: New York: Oxford University Press, 1999.

34. Jeffrey, G. A. *An introduction to hydrogen bonding*, New York: Oxford University Press, 1997.

35. Steiner, T. *Angew. Chem. Int. Ed. Engl.,* **2002**, *41*, 48-76.

36. Marechal, Y. *The hydrogen bond and the water molecule: the physics and chemistry of water, aqueous and bio-media*, Elsevier Science, 2006.

37. Mills, J. E. J.; Dean, P. M. *J. Comput. Aided Mol. Des.* **1996,** *10*, 607-622.

38. Taylor, R.; Kennard, O. *Acc. Chem. Res.* **1984**, *17,* 320-326.

39. Taylor, R.; Kennard, O.; Versichel, W. *Acta Cryst.* **1984**, *40*, 280-288.

40. (a) Prins, L. J.; Reinhoudt, D. N.; Timmerman, P. *Angew. Chem. Int. Ed.* **2001**, *40*, 2382-2426; (b) Cooke, G.; Rotello, V. M. *Chem. Soc. Rev.* **2002**, *31*, 275-286; (c) Hunter, C. A.; Anderson, H. L. *Angew. Chem. Int. Ed.* **2009**, *48*, 7488-7499; (d) Misuraca, M. C.; Grecu, T.; Freixa, Z.; Garavini, V.; Hunter, C. A.; van Leeuwen, P. W. N. M.; Segarra-Maset, M. D.; Turega, S. M. *J. Org. Chem.* **2011**, *76*, 2723-2732.

41. Zimmerman, S. C.; Murray, T. J. *Tetrahedron Lett.* **1994**, *35*, 4077-4080.

42. Zimmerman, S. C.; Murray, T. J. *Phil. Trans. Roy. Soc. London. A.* **1993**, *345*, 49-56.

43. Jorgensen, W. L.; Pranata, J. *J. Am. Chem. Soc.* **1990**, *112*, 2008-2010.

44. Pranata, J.; Wierschke, S. G.; Jorgensen, W. L. *J. Am. Chem. Soc.* **1991**, *113*, 2810-2819.

45. Hamilton, A. D.; Van Engen, D. J. *J. Am. Chem. Soc.* **1987**, *109*, 5035-5036.

46. Kelly, T. R.; Maguire, M. P. *J. Am. Chem. Soc.* **1987**, *109,* 6549-6551.

47. Kyogoku, Y.; Lord, R. C.; Rich, A. *Proc. Natl. Acad. Sci. U.S.A.* **1967**, *57*, 250-257.

48. Murray, T. J.; Zimmerman, S. C. *J. Am. Chem. Soc.* **1992**, *114*, 4010-4011.

49. Sartorius, J.; Schneider, H-J. *Chem. Eur. J.* **1996**, *2*, 1446-1452.

50. Wang, H.; Mudraboyina, B. P.; Wisner, J. A. *Chem. Eur. J.* **2012**, *18*, 1322-1327.

51. Lerch, M. M.; Szymański, W.; Feringa, B. L. *Chem. Soc. Rev.* **2018**, *47*, 1910-1937.

52. Hoshino, M., Ebisawa, F.; Yoshida, T.; Sukegawa, K. *J. Photochem. Photobiol, A: Chem.*, **1997**, *105*, 75-81.

53. Kurihara, S.; Ikeda, T.; Tazuke, S. *Jpn. J. Appl. Phys.*, *part 2* **1988**, *27*, L1791-L1792.

54. Bouas-Laurent, H.; and Durr, H. *Pure Appl. Chem.* **2001**, *73*, 639-665.

55. Barachevsky, V. A. *Proc. SPIE* **1995**, *2208*, 184-195.

56. Zhang, X.; Hou, L.; Samorì, P. *Nat. Comm.* 2016, DOI: 10.1038/ncomms11118.

57. Bouas-Laurent, H.; Durr, H. *Pure Appl. Chem.* **2001**, *73*, 639-665.

58. Feringa, B. L.; Browne, W. R. *Molecular Switches*, Wiley-VCH, 2011.

59. Bossi, M. L.; Aramendía, P. F. *J. Photochem. Photobiol. C*, **2011**, *12*, 154-166.

60. Heller, H. G.; Harris, S. A.; Oliver, S. N. *J. Chem. Soc. Perkin 1*, **1991**, 3258.

61. Irie, M.; Uchida, K. *Bull. Chem. Soc. Jpn.* **1998**, *71*, 985-996.

62. Kiser, P. D.; Golczak, M.; Palczewski, K. *Chem. Rev.* **2014**, *114*, 194-232.

63. Tochitsky, I.; Helft, Z.; Meseguer, V.; Fletcher, R. B.; Vessey, K. A.; Telias, M.; Denlinger, B.; Malis, J.; Fletcher, E. L.; Kramer, R. H. *Neuron*. **2016**, *92*, 100-103.

64. Del Canto, E.; Natali, M.; Movia, D.; Giordani, S. *Phys. Chem. Chem. Phys.* **2012**, *14*, 6034-6043.

65. Russew, M-M.; Hecht, S. *Adv. Mater.* **2010**, *22*, 3348-3360.

66. Velema, W. A.; Szymanski, W.; Feringa, B. L. *J. Am. Chem. Soc.* **2014**, *136*, 2178-2191.

67. Broichhagen, J.; Frank, J. A.; Trauner, D. *Acc. Chem. Res.* **2015**, *48*, 1947-1960.

68. Lerch, M. M.; Hansen, M. J.; van Dam, G. M.; Szymanski, W.; Feringa, B. L. *Angew. Chem. Int. Ed.* **2016**, *55*, 10978-10999.

69. Kobatake, S.; Yamashita, I. *Tetrahedron*, **2008**, *64*, 7611-7618.

70. Yao, X.; Li, T.; Wang, J.; Ma, X.; Tian, H. *Adv. Optical Mater.* **2016**, DOI: 10.1002/adom.201600281.

71. Takeshita, M.; Hayashi, M.; Kadota, S.; Mohammed, K. H.; Yamato, T. *Chem. Commun.* **2005**, 761-763.

72. Xu, J-F.; Chen, Y-Z.; Wu, D.; Wu, L-Z.; Tung, C-H.; Yang, Q-Z. *Angew. Chem. Int. Ed.* **2013**, *52*, 9738-9742.

73. He, J.; Zhao, Y.; Zhao, Y. *Soft Matter* **2009**, *5*, 308-310.

74. Yu, Z.; Zheng, Y.; Parker, R. M.; Lan, Y.; Wu, Y.; Coulston, R. J.; Zhang, J.; Scherman, O. A.; Abell, C. *ACS Appl. Mater. Interfaces.* **2016**, *8*, 8811-8820.

75. Li, M.; Keller, P.; Yang, J.; Albouy, P. A. *Adv. Mater.* **2004**, *16*, 1922-1925.

76. Kondo, M.; Yu, Y.; Ikeda, T. *Angew. Chem., Int. Ed.* **2006**, *45*, 1378-1382.

77. Ikeda, T.; Mamiya, J.; Yu, Y. *Angew. Chem., Int. Ed.* **2007**, *46*, 506-528.

78. Mamiya, J.; Yoshitake, A.; Kondo, M.; Yu, Y.; Ikeda, T. *J. Mater. Chem.* **2008**, *18*, 63-65.

79. Wyman, G. M.; Brode, W. R. *J. Am. Chem. Soc.* **1951**, *73*, 1487-1493.

80. Rogers, D. A.; Margerum, J. D.; Wyman, G. M. *J. Am. Chem. Soc.* **1957**, *79*, 2464-2468.

81. Karstens, T.; Kobs, K.; Memming, R. *Ber Bunsenges. Phys. Chem.* **1979**, *83*, 504-510.

82. Kirsch, A. D.; Wyman, G. M. *J. Phys. Chem.* **1977**, *81,* 413-420.

83. Karstens, T.; Kobs, K.; Memming, R.; Schroppel, F. *Chem. Phys. Lett.* **1977**, *48*, 540-544.

84. Maeda, Y.; Okada, T.; Mataga, N. *J. Phys. Chem.* **1984,** *88,* 1117-1119.

85. Rondão R.; de Melo, J. S. S. *J. Phys. Chem. C.* **2013**, *117*, 603-614.

86. Zollinger, H. *Color Chemistry: Syntheses, properties, and applications of organic dyes and pigments*, John Wiley & Sons, 2003.

87. Jacquemin, D.; Preat, J.; Wathelet, V.; Fontaine, M.; Perpète, E. A. *J. Am. Chem. Soc.* **2006**, *128*, 2072-2083.

88. Harley-Mason, J.; Mann, F. G. *J. Chem. Soc.* **1942**, 404-415.

89. Konieczny, M. T.; Konieczny, W. *Heterocycles* **2005**, *65*, 451-464.

90. Vlahakis, J. Z.; Wand, M. D.; Lemieux, R. P. *J. Am. Chem. Soc.* **2003**, *125*, 6862-6863.

91. Lemieux, R. P. *Chem. Rec.* **2004**, *3*, 288-295.

92. Hosseinnezhad, M.; Moradian, S.; Gharanjig, K. *Dyes and Pigments* **2015**, *123*, 147-153.

93. Irie, M.; Kato, M. *J. Am. Chem. Soc.* **1985**, *107*, 1024-1028.

94. Ramirez, A.; Sifuentes, C.; Manciu, F. S.; Komarneni, S.; Pannell, K. H.; Chianelli, R. R. *Appl. Clay Sci.* **2011**, *51*, 61-67.

95. Seki, T.; Tamaki, T.; Yamaguchi, T.; Ichimura, K. *Bull. Chem. Soc. Jpn.* **1992**, *65*, 657-663. (b) Eggers, K.; Fyles, T. M.; Montoya-Pelaez, P. J. *J. Org. Chem.* **2001**, *66*, 2966-2977. (c) Lougheed, T.; Borisenko, V.; Hennig, T.; Rück-Braun, K.; Woolley, G. A. *Org. Biomol. Chem.* **2004**, *2*, 2798-2801. (d) For a review on the use of hemithioindigos in chromopeptides, see: Kitzig, S.; Thilemann, M.; Cordes, T.; Rück-Braun, K. *Chem. Phys. Chem.* **2016**, *17*, 1252-1263.

Chapter 2

2   Synthesis, Characterization and Supramolecular Study of Photoswitchable Thioindigoid as a Hydrogen Bond Acceptor Array

2.1   Design of **A2**: Photoswitchable Hydrogen Bond Acceptor Array (AAA)

What defines a viable hydrogen bond acceptor in the context of supramolecular assemblies is the ability of the group or molecule to interact with a hydrogen bond donor. To fulfill this requirement in a hydrogen bonded complex, the acceptor has to provide an electron rich region favorable for the polarized hydrogen atom of a donor moiety. It can be obtained by considering two factors when it comes to design an acceptor. The first element is the presence of electron donating groups in the structure of the acceptor that may increase the electron density of the heteroatom through resonance or induction. The second element to consider is the arrangement of the hydrogen bonding sites. A molecule with more than one adjacent hydrogen bonding site can act as a hydrogen bond array that in turn may improve the stability of a complementary complex.

Following previous work in our group designing and synthesizing different hydrogen bond acceptor and donor moieties to build supramolecular complexes,[1,2] we were interested in incorporating a stimuli responsive acceptor in a complementary hydrogen bond complex. Thioindigo is a photoswitchable molecule with two carbonyl groups in its chromophoric core that captured our attention. This molecule can reversibly change its configuration to form an AAA hydrogen bond array modulated by light as an external stimulus. When photoisomerization from *E-* to *Z*-thioindigo takes place, the two carbonyl groups are arranged next to each other in the new geometry to produce an electron rich linear array. In fact, this new geometry creates a new hydrogen bond acceptor site (AAA) that enhances the stability of the complex. Whereas, in the absence of light no complexation is expected as the acceptor sites are no longer arranged closely in space (Scheme 2.1).
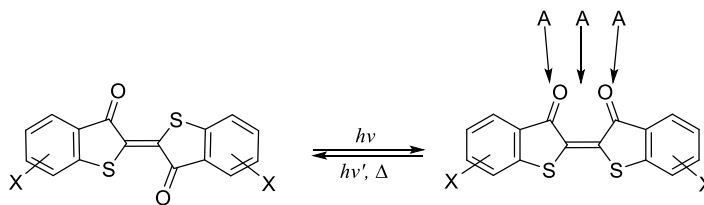
Scheme 2.1 General *E*/*Z* isomerization for thioindigo derivatives.

This idea was supported by a report from Rosengaus and Willner wherein they observed a hydrogen bonded assembly of (*E*)-6,6'-diethoxy-3*H*,3'*H*-[2,2'-bibenzo[*b*]thiophenylidene]-3,3'-dione (6,6'-diethoxythioindigo) with 2,3-Bis(aminocyclohexyl)-6-methoxy-1,3,5-triazine, using UV-Vis spectroscopy (Scheme 2.2).[3] In our hands, no evidence of hydrogen bonding could be detected by ^{1}H NMR in this system.
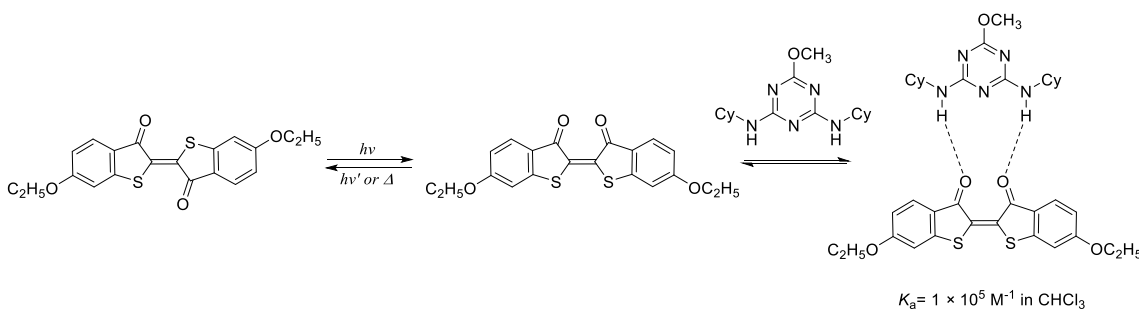
Scheme 2.2 Photoswitchable hydrogen bond complexes of 6,6'-diethoxythioindigo and 2,3-bis(aminocyclohexyl)-6-methoxy-1,3,5-triazine.

Regardless, we decided to further test the idea using more complementary donor array designs. With this goal in mind, 6,6'-dihexyloxythioindigo (hereafter referred to **A1**; Scheme 2.3) as an AAA acceptor was synthesized and evaluated with a complementary hydrogen bond donor array to evaluate its binding affinity. Although it exhibited promising results in terms of generating a stable supramolecular assembly, its extremely low and capricious solubility in non-polar solvents together with low synthetic yield in the final

step limited the scope of the project. Therefore, we turned our attention to another thioindigo derivative, (*Z*)-6-(hexyloxy)-2-(2-oxoacenaphthylen-1(2H)-ylidene)benzo[b]thiophen-3(2H)-one (hereafter referred to **A2**; Scheme 2.3). This new derivative of thioindigo offered two marked advantages over **A1**. Firstly, **A2** was obtained in a much improved yield through the synthetic procedure depicted in Scheme 2.3. Secondly, in comparison with **A1**, **A2** proved to be significantly easier to handle in the sense that it was freely soluble up to approximately 8 mM in commonly employed non-polar organic solvents such as $CHCl_3$, CH_2Cl_2 and toluene.

2.2 Synthesis of Hydrogen Bond Acceptor **A1** and **A2**

A1 and **A2** were synthesized in six steps as depicted in Scheme 2.3.
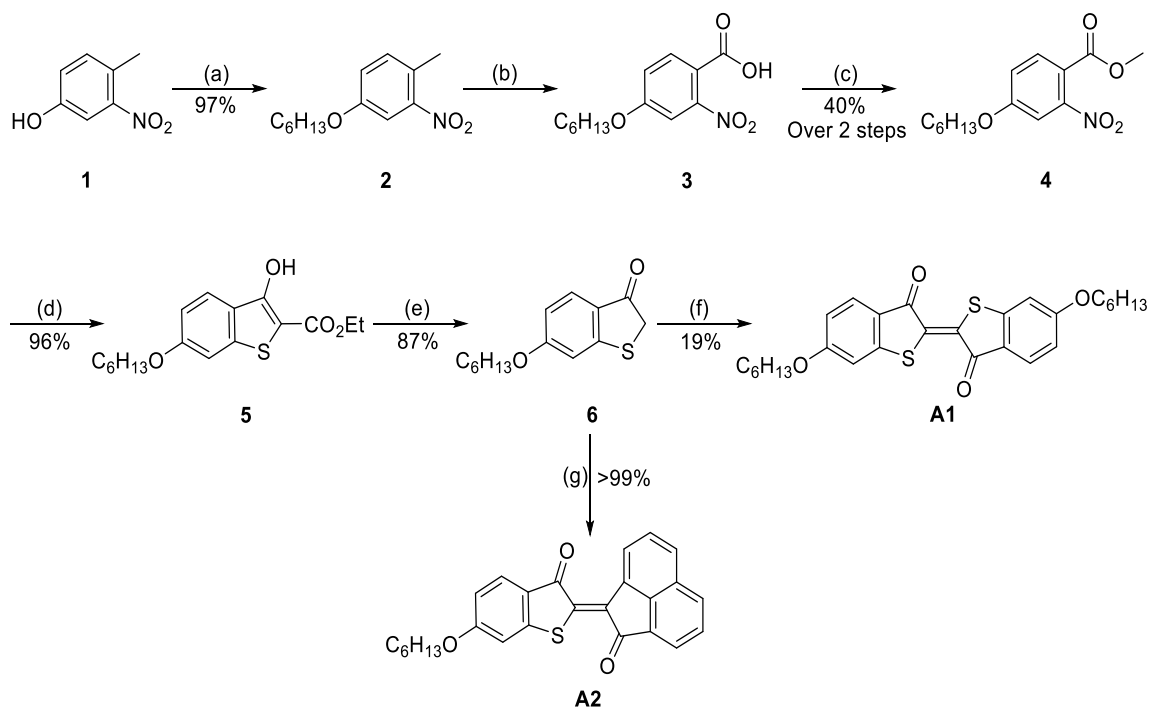
Scheme 2.3 Synthesis of photoresponsive **A1** and **A2**. Reagents and conditions: (a) 1.1 eq. IC_6H_{13}, 1.2 eq. K_2CO_3, DMF, N_2, 50 ˚C, 18 h. (b) 5 eq. $KMnO_4$, H_2O-Py (1:1), 100 ˚C. (c) 1.1 eq. Me_2SO_4, 1.1 eq. K_2CO_3, acetone, reflux, 2 h. Yields obtained from two steps (d) 1.6 eq. $HSCH_2CO_2Et$, 3.5 eq. KOH, DMF, N_2, 0 ˚C, then R.T., 4 h. (e) 15% KOH, H_2O-EtOH, N_2, reflux, 13 h. (f) 4 eq. piperidine, 4 eq. $K_3Fe(CN)_6$, *i*-PrOH/H_2O, N_2, 70 ˚C, 30 min, R.T., 30 min, (g) 1 eq. acenaphthylene-1,2-dione, 1 eq. K_2CO_3, DMF, N_2, R.T., 2-3 h.

The precursor 4-methyl-3-nitrophenol produced an alkylated phenol **2** via an S_N2 reaction between the deprotonated phenol and 1-iodohexane (also referred as a Williamson-ether synthesis).[4] In the second step, the methyl group in the *para* position was oxidized to a carboxylic acid **3** using $KMnO_4$.[5] This conversion was carried out in a (1:1) solution of pyridine and water. To avoid any aldehyde formation, an excess of potassium permanganate was used. The crude product proved to be a mixture of compound **2** and **3** which was used for the following step without any further purification. The mixture was refluxed in acetone with dimethyl sulfate under basic condition to esterify and produce intermediate **4**.[6] Compound **4** was then treated with ethyl mercaptoacetate and potassium carbonate to cyclize and form the benzothiophene ester **5**.[7] Subsequently, intermediate **5** was submitted to a saponification and thermal decarboxylation using KOH to yield benzothiophenone (**6**).[8] Once intermediate **6** was isolated, **A1** and **A2** were generated through different synthetic routes: **A1** was achieved through the oxidative dimerization of compound **6** utilizing $K_3Fe(CN)_6$ and piperidine;[9] meanwhile, **A2** was obtained by an aldol condensation with acenaphthylene-1,2-dione in a basic environment. Unlike **A1**, **A2** was obtained with an excellent yield of over 99% as a fine red powder in only one isomeric form, presumably the *Z*-isomer.

2.3 Photoisomerization Studies of **A2** using ^{1}H NMR and UV-Vis Spectroscopy

Compound **A2** obtained from the synthetic procedure was isolated as only a single isomer whose configuration needed to be identified. This isomeric form of **A2**, is stable in the solid state as a red powder that does not isomerize after exposure to ambient light for a week. Conversely, when freshly prepared **A2** is in solution under ambient light, photoisomerization takes place, wherein **A2** reaches an ~1:1 *E/Z* ratio at the photostationary state (Figure 2.1).

Comparing the ^{1}H NMR spectra in Figure 2.1, it was assumed that the isomer obtained from the synthetic procedure was the *Z*-isomer (the thermodynamically stable product, hereafter referred to as *Z*-**A2**). This interpretation was based on the presence of a signal at 9.53 ppm that corresponds to proton **H$_a$**. The deshielding effect over this proton is due to an intramolecular interaction between this proton and the closest carbonyl group. This effect would not be observed in the other isomeric form (hereafter referred as *E*-**A2**) as the **H$_a$** is far away from carbonyl group in this orientation and less crowded by the opposing thiophenone ring.
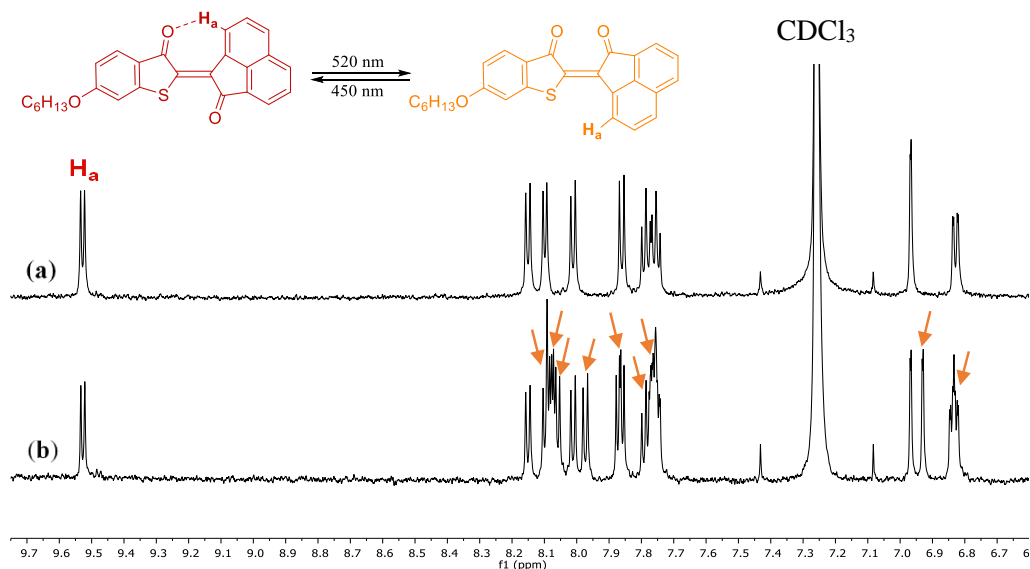
Figure 2.1 ^{1}H NMR Spectra of **A2** in CDCl$_3$ at 298 K. (a): **A2** as obtained from synthetic procedure, (b): **A2** at the photostationary state under ambient illumination (~1:1 *E*/*Z* ratio), orange arrows indicate resonances due to second isomeric form of **A2**.

Interested in purifying and characterizing *E*-**A2**, a pure *Z*-**A2** solution in CHCl$_3$ was irradiated at 520 nm under an N$_2$ atmosphere to prevent any side reaction that might occur due to the presence of O$_2$ (Scheme 2.4). After reaching the maximum conversion (63%), the putative *E*-isomer was isolated in the dark via thin layer chromatography with chloroform as eluent.
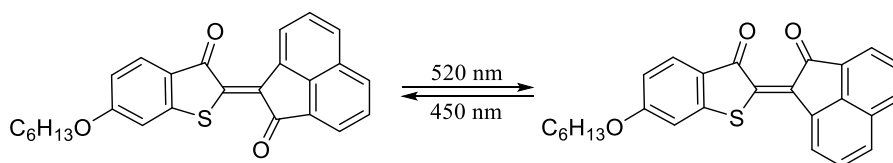
Scheme 2.4 Photoisomerization of **A2** in CHCl$_3$ with specific wavelengths (520 nm and 450 nm to obtain *E*- and *Z*-isomers, respectively).

In order to properly identify the chemical shifts of the different protons in both isomers, 2D NMR spectra (gCOSY, HSQC and HMBC, Appendices) were obtained. On the basis of the correlations, Figure 2.2 details the full assignment of the ^{1}H NMR signals of both isomers.
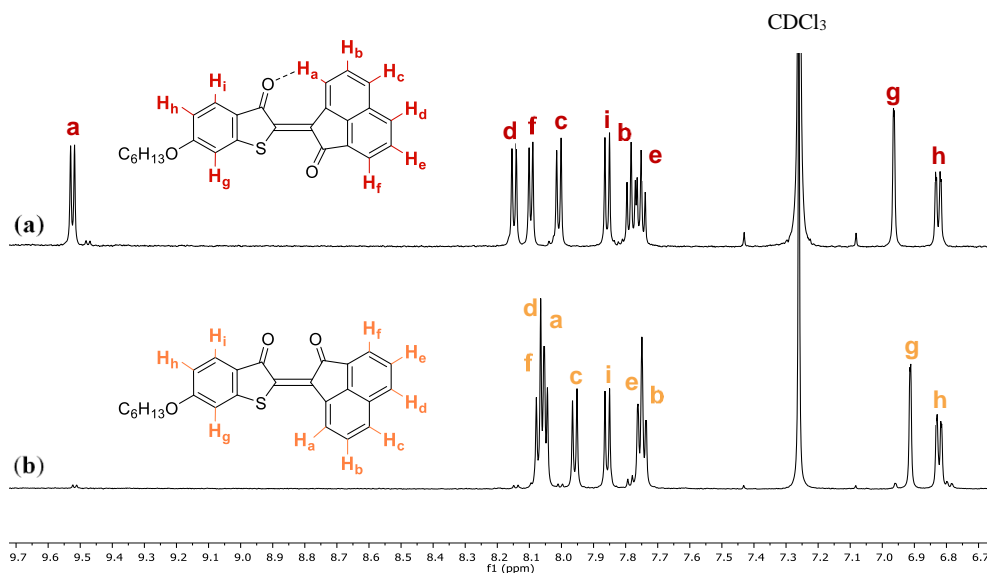
Figure 2.2 ^{1}H NMR (600 MHz) of (a) *Z*-**A2** and (b) *E*-**A2** in CDCl$_3$ at 298 K.

The photophysical properties of **A2** were studied through UV-Vis spectroscopy. As shown in Figure 2.3, there are three maxima in the UV-Vis absorption spectrum of the *Z*-isomer: one at 500 nm, that corresponds to n→π* transition; and two absorption bands at 365 nm and 310 nm corresponding to π→π* transitions. A similar absorption pattern was observed

for the *E*-isomer where the distinctive change was a blueshift (hypsochromic) of the n→π* band to 458 nm.
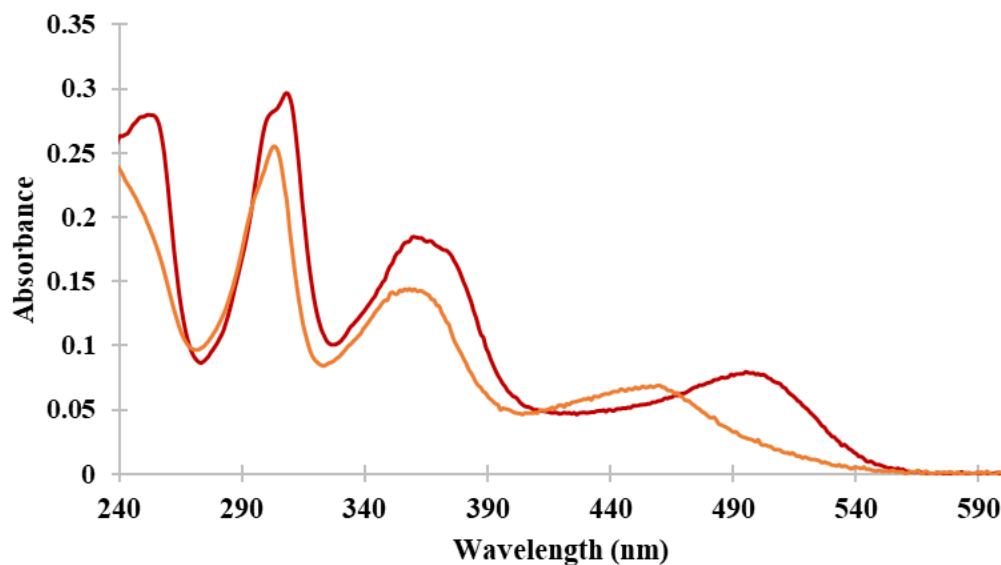
Figure 2.3 The UV-Vis absorption spectra of *Z*-**A2** (red) and *E*-**A2** (orange). The spectra were recorded in CHCl$_3$ at 1×10^{-5} M solution at 298 K.

The spectral overlap between the two isomeric forms hinders the complete conversion of one form into another. To verify this observation, a ^{1}H NMR study was performed wherein a 2 mM solution of **A2** at photostationary state (∼1:1 *E/Z* rate) was first irradiated at 520 nm to reach the highest conversion to *E* and then irradiated at 450 nm to shift the isomerization back to *Z*. As illustrated in Figure 2.4, although irradiation can favor one isomer over the other, complete conversion is not attainable.
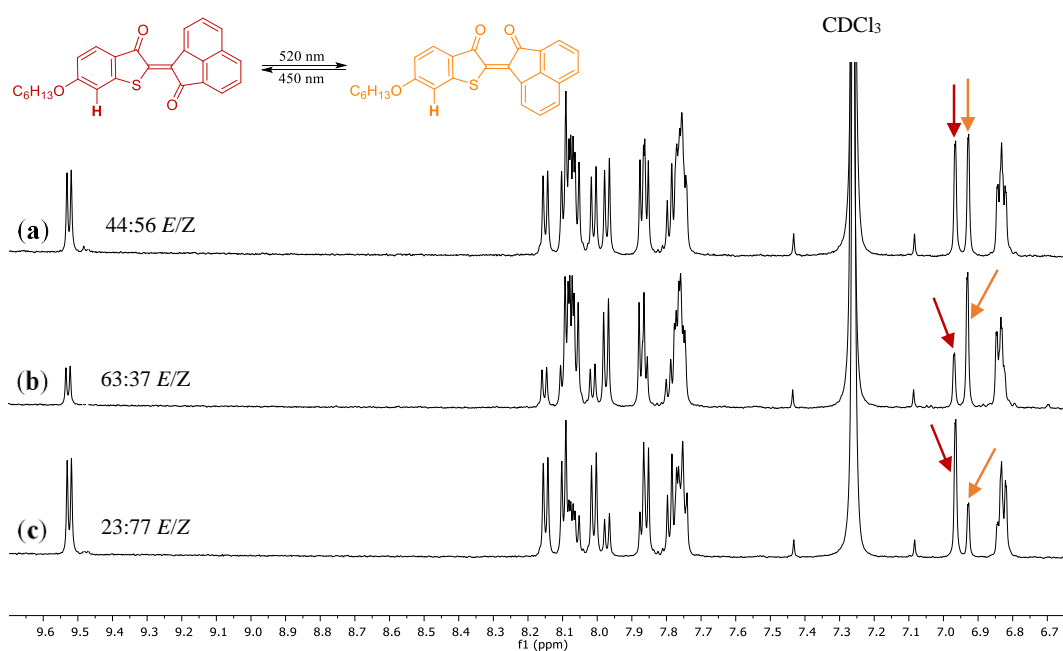
Figure 2.4 The photoisomerization of **A2**. ^{1}H NMR spectra (600 MHz) of (a) photostationary state under ambient light (44:56) (b) irradiated at 520 nm for 20 minutes (63% *E*-**A2**), and (c) irradiated at 450 nm for 20 minutes (77% *Z*-**A2**), in CDCl$_3$ at 298 K. Red arrows refer to *Z*-**A2** and orange arrows refer to *E*-**A2**.

2.4   X-ray Characterization of *Z*-**A2**

We attempted to obtain single crystals of **A2** in both isomeric forms through different crystallization techniques. However, we were only able to produce single crystals of the *Z*-isomer from the slow evaporation of a **A2** solution in dichloromethane (∼1:1 *E*/*Z* ratio) at room temperature. The *Z*-isomer of **A2** (*Z*-**A2**) crystalizes as red prisms in the triclinic space group $P\bar{1}$. Each unit cell comprises two symmetry related molecules. Table 2.1 lists the crystallographic parameters for *Z*-**A2**.

Table 2.1 Crystallographic parameters for *Z*-**A2.**

Crystal Parameter	*Z*-**A2**
Chemical Formula	$C_{26}H_{22}O_3S$
Formula Weight (*g.mol⁻¹*)	414.49
Crystal System	Triclinic
Space Group	$P\bar{1}$
a (Å)	9.2857(14)
b (Å)	9.4290(13)
c (Å)	12.6162(19)
α (°)	94.406(7)
β (°)	111.347(6)
γ (°)	99.496(9)
V (Å³)	1003.4(3)
Z	2
F(000)	436
Temperature (K)	110
λ (CuKα) (Å)	1.54178
ρ_{cal} (g/cm)	1.372
μ (cm⁻¹)	1.641
Reflections Collected	23386
Unique Reflections	3510
Absorption Correction	multi-scan
Refinement on	F^2
Parameters Refined	359
R (F₀) (*l*>2σ(*l*))	0.0412
R_w (F₀²) (*l*>2σ(*l*))	0.1072
R (F₀) (all data)	0.0495
R_w (F₀²) (all data)	0.1137
GOF on F^2	1.058

Overall, Z-**A2** in the solid state has a planar structure wherein the highest deviation from the least square plane of all heavy atoms in the backbone (without including the alkoxy group) is 0.12 Å. The hexyloxy group *meta* to the sulfur atom deviates from this plane by 8^0 (angle between least square planes of all heavy atoms in the backbone and the C(sp3)-O bond of the alkoxy group). It is noteworthy to outline the intramolecular hydrogen bond interaction between the carbonyl on the benzothiophenone moiety and the γ-carbonyl proton of the acenaphthylenone group (C-H⋯O = 2.89 Å, C-H⋯O = 2.16 Å, ∠C-H⋯O = 132.84^0), pictured in Figure 2.5. This is in agreement with the chemical shift observed at 9.53 ppm on the Z-**A2** ^{1}H NMR (i.e., downfield from the expected value for an aromatic proton).
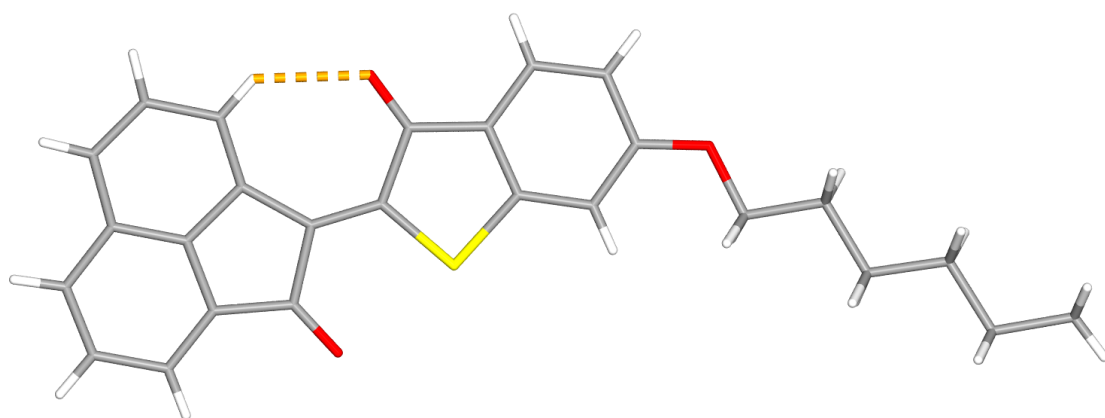
Figure 2.5 Stick representation of the X-ray crystal structure of Z-**A2** with an intramolecular C-H⋯O hydrogen bond indicated (dashed orange line). Grey, white, red and yellow correspond to carbon, hydrogen, oxygen and sulfur atoms, respectively.

Along the crystal lattice, Z-**A2** molecules are arranged in layers angled at 65^0 from the *bc* plane. Each layer comprises alkyl- and aromatic-dense regions (Figure 2.6 A). It is worth noting the presence of intermolecular C-H⋯O contacts between the carbonyl oxygens with β-carbonyl protons (C3-H3⋯O2 = 3.23 Å, C3-H3⋯O2 = 2.36 Å, ∠C3-H3⋯O2 = 155^0; and C16-H16⋯O1 = 3.33 Å, C16-H16⋯O1 = 2.46 Å, ∠C3-H3⋯O1 = 155^0) creating head-to-

tail chains within the layers (Figure 2.6 A and 2.6 B). Finally, the distance between layers ranges from 2.96 to 3.79 Å which suggest the presence of π-stacking interactions. Close examination confirms such interactions, specially between acenaphthylenone groups with a distance of 3.35 Å between the least square planes of all heavy atoms in the *Z*-**A2** backbone (Figure 2.7).

A)

B)

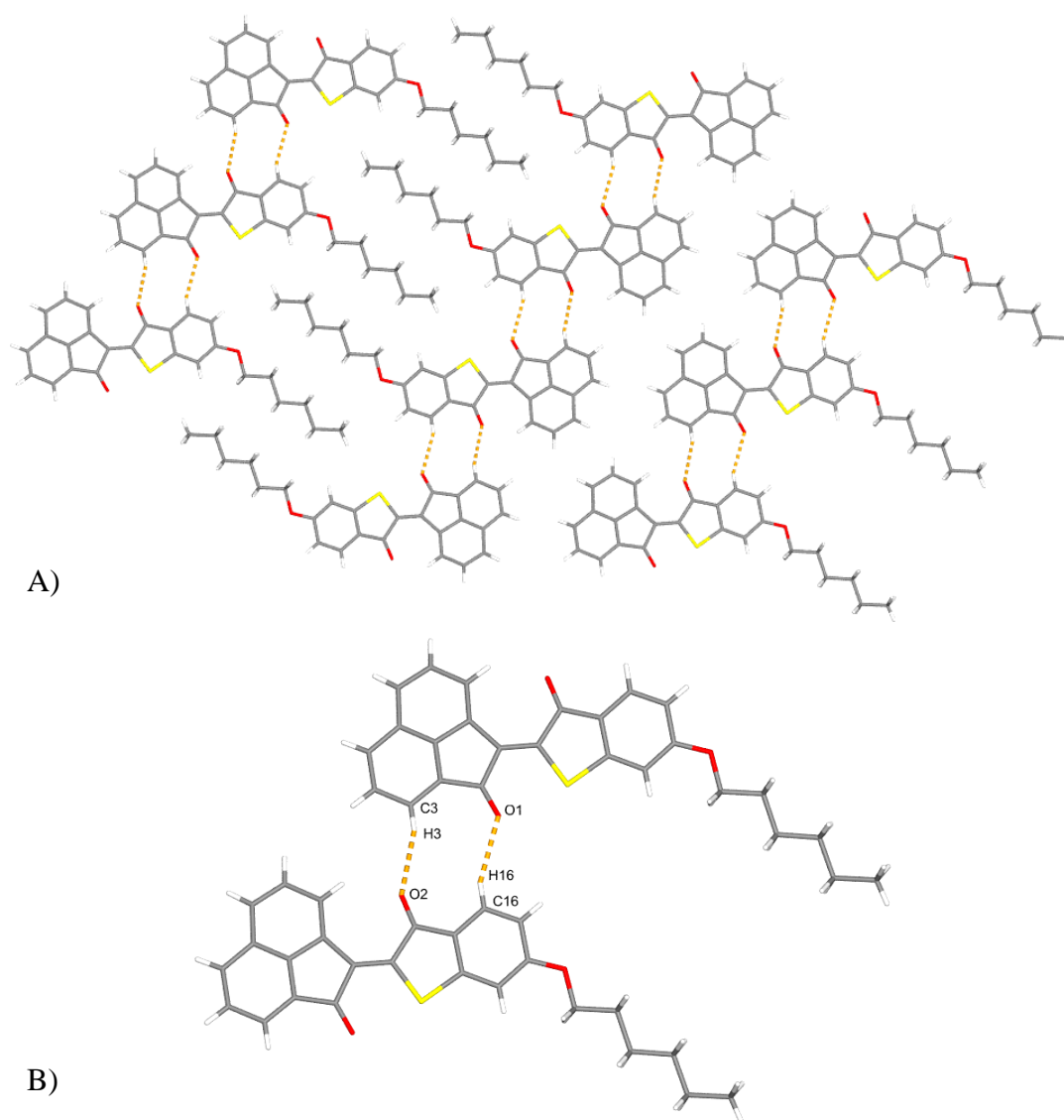**Figure 2.6** Stick representation of the X-ray crystal structure of *Z*-**A2** indicating CH⋯O contacts (dashed orange lines). Grey, white, red and yellow correspond to carbon, hydrogen, oxygen and sulfur atoms, respectively. A) *Z*-**A2** molecules displayed as a layer at a 65° angle from the *bc* plane; B) CH⋯O interactions between two *Z*-**A2** molecules within a layer.
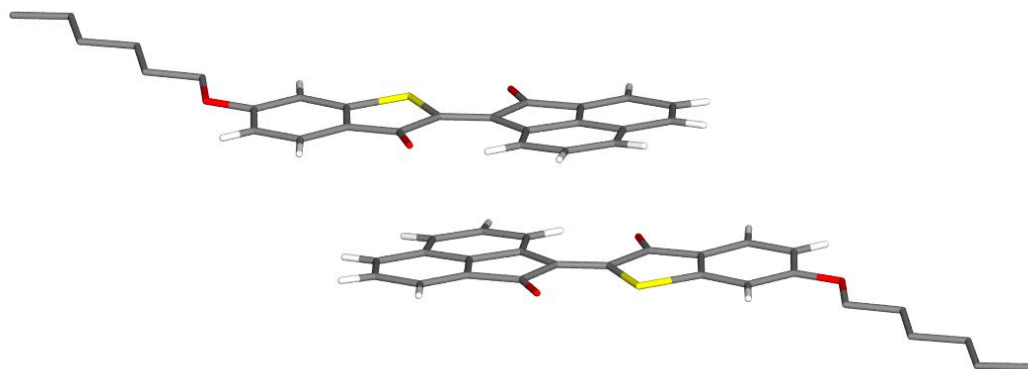
Figure 2.7 Stick representation of the X-ray crystal structure of Z-**A2**. p-stacking interaction between acenaphthylenone groups from two consecutive layers. Grey, white, red and yellow correspond to carbon, hydrogen, oxygen and sulfur atoms, respectively. Note: All Csp3 protons were removed for clarity.

2.5   Design and Complexation Studies of **A2** with Hydrogen Bond Donors

To this point, the main focus of the project was on the synthesis, characterization, and study of the photophysical properties of hydrogen bond acceptor **A2** with the aid of ^{1}H NMR spectroscopy, UV-Vis absorption spectra and X-ray crystallography. The results obtained support our contention that **A2** is a feasible photoswitchable hydrogen bond acceptor. However, its viability has to be examined when it comes to its behavior in a complex with a donor array. In addition, it was important to study the photochemical behavior of **A2** in a supramolecular complex and whether it can cause a meaningful change in the aggregation in solution. We began our assessment choosing a library of donors that have already been known and studied in our group and others. Scheme 2.5 depicts the donor systems employed to study the strength of **A2** as an acceptor, which are: 2,6-diaminopyridinium BArF (**D1⁺**), 2-amino-5-methylpyridinium BArF (**D2⁺**), 1,3-bis(3,5-bis(trifluoromethyl)phenyl)urea (**D3**), 1-(2-amino-5-nitro-6-(trifluoromethyl)-1H-indol-3-yl)-2,2,3,3,4,4,5,5,6,6,7,7,7-tridecafluoroheptan-1-one (**D4**), 1-(2-amino-5-(trifluoromethyl)-1H-indol-3-yl)-2,2,3,3,4,4,5,5,6,6,7,7,7-tridecafluoroheptan-1-one (**D5**) and diethyl 2,6-diamino-4-(3-nitrophenyl)-1,4-dihydropyridine-3,5-dicarboxylate (**D6**). It is important to note the variety of the donor arrays among the chosen systems.
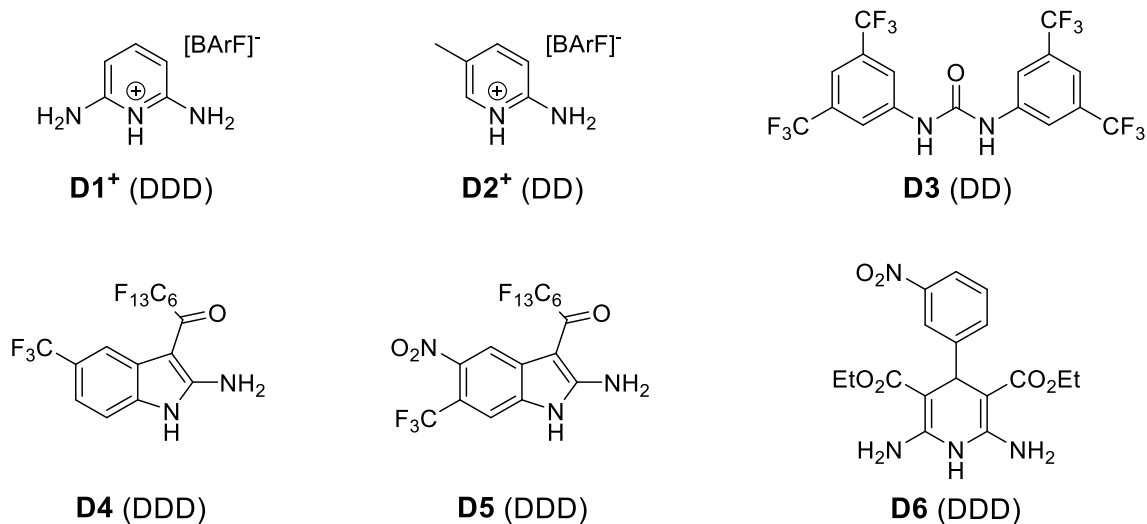
Scheme 2.5 Library of donors chosen for supramolecular complexes with **A2**.

Cationic **D1** and **D2** were prepared following a synthetic pathway described by Leigh and coworkers.[10] Trifluoromethyl substituted urea (**D3**), as a neutral donor, was obtained by condensing 1-isocyanato-3,5-bis(trifluoromethyl)benzene with 3,5-bis(trifluoromethyl)aniline.[11] **D4** and **D5** were obtained by an intramolecular Heck reaction followed by Curtius rearrangement performed by a group member as part of another research project.[12,13] Studies within our group have shown that both indoles can form stable supramolecular complexes but **D5** formed more stable complexes. The improved binding affinity of **D5** over **D4** is attributed to the presence of a nitro group that can add to the strength of the donor but has yet to be proved in our proposed complex system. The last proposed donor (**D6**), was synthesized according to a procedure reported by Zimmerman.[14]

2.5.1 ^{1}H NMR Titration Experiments: Stability of *E*-**A2•Dx** (AAA-DD(D))

Moving to the next step, we were determined to measure the complexation constants of our proposed systems (**A2•Dx**). In a typical titration, aliquots of a known-concentration acceptor solution are gradually added to a fixed-concentration donor solution in order to

quantify the stability of the supramolecular system. As the acceptor is added to the donor solution a change in the chemical shift (in the case of using ^{1}H NMR to quantify the response) is observed and recorded.[15] Then the data obtained is plotted versus the concentration of acceptor by an iterative fitting process to yield valuable information such as K_a, ΔG, δ_{bound} and δ_{free} of the complex. In this approach, the acceptor specie has to be completely stable in the solution and not prone to a change like degradation or isomerization to obtain accurate information. We performed a preliminary titration experiment of Z-**A2** with one of our donors taking a similar approach to obtain an association constant. However, the main challenge was that once the solution was exposed to ambient light (e.g. during transit to and from the spectrometer), interconversion of pure Z- to E-isomer and vice versa (pure E- to Z-) occurred. Therefore, the concentration of acceptor was inconsistent, and the results were no longer reliable. Apart from that, we speculated that only the E-isomer binds to the donor (**Dx**). Looking for a more accurate alternative to validate our assumption, we opted another titration strategy. Contrary to a typical titration, an excess of our acceptor in its Z-isomeric form was added all at once to obtain a 4:1 mixture of Z-**A2**•**Dx**. Once the solution of Z-**A2** and the selected donor (**Dx**) was exposed to light, the photoisomerization began, and as the amount of E increased in the solution the supramolecular interactions grew. In this way, which avoids systematical errors upon addition of aliquots, the E-isomer concentration gradually increased in the system. The solution was monitored over time by taking ^{1}H NMR spectra at regular intervals. NMR spectra were collected until compound **A2** reached the photostationary state. It was the point where maximum conversion from Z- to E-isomer in the solution occurred which was in agreement with the finding obtained from photophysical studies of the **A2** (i.e. photostationary state at 1:1). At that point, exposure to ambient light cannot induce more isomerization to E-**A2**, nor further changes in chemical shift.

The next step was to analyze the data acquired from ^{1}H NMR spectra. First, we looked at an observed physical change, chemical shift of a specific hydrogen donating site. Ideally, this proton has the largest chemical shift change during titration and should not be obscured by other peak(s). Depending on the donor employed in the complex system, we looked at either an NH$_2$ peak, NH peak or both. Then, we attempted to calculate the concentration of E-**A2** in each ^{1}H NMR spectrum taken. For this purpose, two proton signals were chosen:

the signal at 9.52 ppm assigned to the Z-isomer integrated to 1 as reference (P_1), and the signals between 7 and 6.8 ppm (P_2) whose integration indicated the total amount of E- and Z-**A2**. The concentration of E-**A2** can be measure by the following equation:

$$[E] = \frac{Integration\ of\ \mathrm{P_2} - 1}{Integration\ of\ \mathrm{P_2}}\ [Z]_i \tag{1}$$

Where $[E]$ is the concentration of E-**A2** formed in the system, $[Z]_i$ is the initial concentration of Z-**A2**, and P_2 is the total integration of two signals corresponding to E- and Z-**A2**.

During the ^{1}H NMR titration as the concentration of E-**A2** increases upon exposure to light, increased hydrogen bonding shifts the donor protons downfield. This correlation is important in the sense that the titration isotherm is plotted using these values. Titration analysis is a concentration dependant experiment wherein the association constant (K_a) would be defined by a set of equations concerning the concentration of acceptor (guest) and donor (host) species in the complex:

According to a 1:1 host-guest equilibrium, we have

$$H + G \rightleftharpoons HG \tag{2}$$

where [H], [G], and [HG] are the equilibrium concentrations of host, guest, and host-guest complex, respectively. Let us assume that we have a solution with total concentrations of guest ($[G]_0$) and host ($[H]_0$):

$$[H]_0 = [H] + [HG] \tag{3}$$

$$[G]_0 = [G] + [HG] \tag{4}$$

An association constant (K_a) is defined as,

$$K_a = \frac{[HG]}{[H][G]} \tag{5}$$

By substituting Eq. (3) and Eq. (4) in Eq. (5) and rearranging the equation,

$$[HG] = K_a\big(([H]_0 - [HG])([G]_0 - [HG])\big) \qquad (6)$$

Solving this equation for $[HG]$ yields Eq. 7:

$$[HG] = \frac{1 + K_a([H]_0 + [G]_0) - \sqrt{(1 + K_a[H]_0 + [G]_0)^2 - 4K_a{}^2[H]_0[G]_0}}{2K_a} \qquad (7)$$

and substituting the above equation in Eq. (3), leads to Eq. 8:

$$[H] = [H]_0 - \frac{1 + K_a([H]_0 + [G]_0) - \sqrt{(1 + K_a[H]_0 + [G]_0)^2 - 4K_a{}^2[H]_0[G]_0}}{2K_a} \qquad (8)$$

The observed chemical shift of the host is determined by the mole fraction weighted average

$$\delta_{\text{obs}} = \frac{[HG]}{[H]_0}\delta_{\text{bound}} + \frac{[H]}{[H]_0}\delta_{\text{free}} \qquad (9)[16]$$

Where,

δ_{obs} = the chemical shift of N-H proton of the donor (host) observed during titration analysis

δ_{free} = the chemical shift of N-H proton of the donor (host) in its uncomplexed form

δ_{bound} = chemical shifts of proton (N-H···O) in completely bound complex

Finally, δ_{obs} can be written as follow:

$$\delta_{\text{obs}} = \frac{1 + K_a([H]_0 + [G]_0) - \sqrt{\big(1 + K_a([H]_0 + [G]_0)\big)^2 - 4K_a{}^2[H]_0[G]_0}}{2K_a}\left(\frac{\delta_{\text{bound}}}{[H]_0}\right) \qquad (10)$$

$$+ \left([\text{H}]_0 - \frac{1 + K_a([\text{H}]_0 + [\text{G}]_0) - \sqrt{(1 + K_a([\text{H}]_0 + [\text{G}]_0))^2 - 4K_a{}^2[\text{H}]_0[\text{G}]_0}}{2K_a} \right) \left(\frac{\delta_{\text{free}}}{[\text{H}]_0} \right)$$

To quantify the stability of our systems, plotting the titration curve and calculating the K_a value based on the above 1:1 complexation model, was carried out using data analysis software (Origin™)[17,18] employing non-linear regression. Other information such as ΔG, chemical shift of the donor in its completely bound and unbound complex are also obtained from the titration fitting.

Experimentally, first we chose **D1**$^+$ to perform a titration since it has previously shown promising results in other complex systems.[10,19,20] The presence of two amine groups (NH$_2$), located symmetrically on both sides of a positively charged NH group that polarizes the electron density of hydrogen bonds, make it a strong DDD donor array. To calculate the binding affinity with **A2**, the chemical shifts of NH$_2$ protons versus the concentration of E-**A2** were fitted to a 1:1 binding curve. We disregarded the NH proton shift as it was obscured by other peaks in the crowded aryl region. A stacked plot of ^{1}H NMR spectra of the titration shows how increasing E formation causes the downfield shift of the NH$_2$ protons (Figure 2.8). The complexation constant (K_a) acquired from the **A2·D1**$^+$ data was 2.3×10^5 M^{-1} that can be converted to a free energy of $\Delta G = -30.6$ kJ mol^{-1} (Figure 2.9). The chemical shift of NH$_2$ protons at zero concentration of E-isomer is identical to the chemical shift of its free form. This implies that only E-**A2** interacts intermolecularly to produce an AAA-DDD complex.
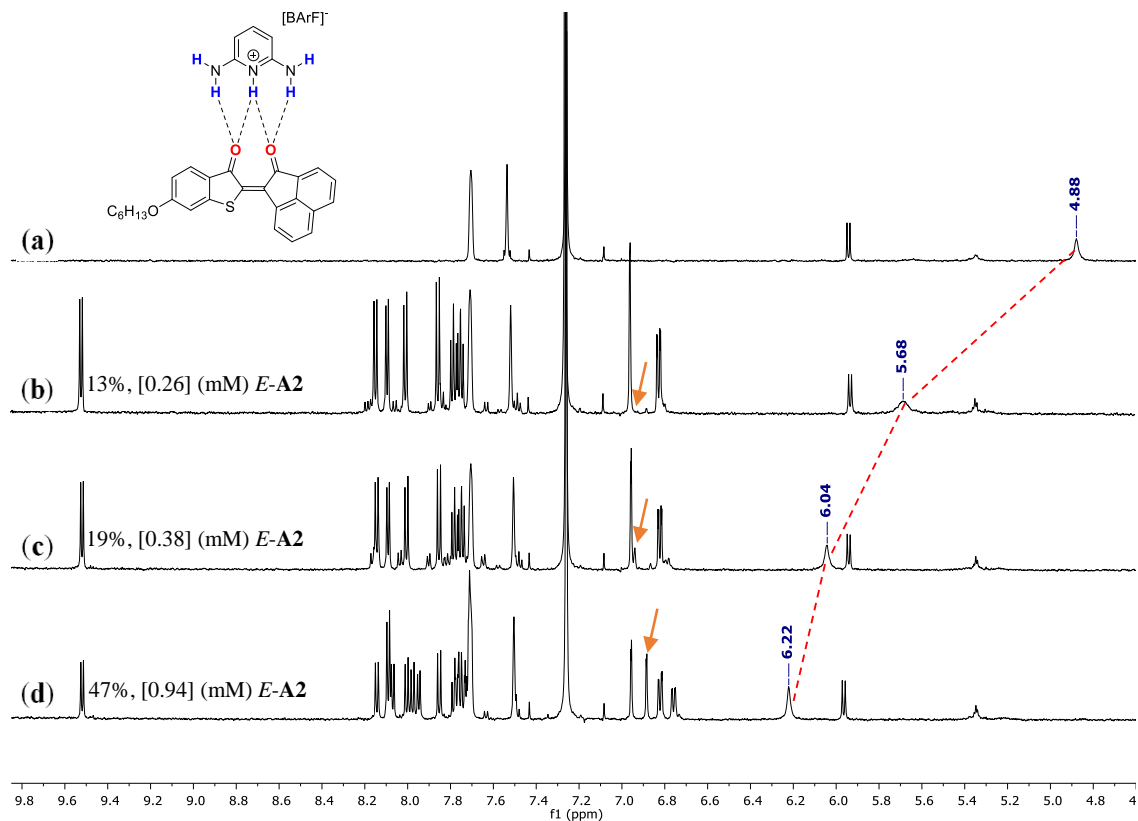
Figure 2.8 Stacked ¹H NMR plot of complementary **A2•D1⁺** in CDCl₃ at 298 K (600 MHz). (a) **D1⁺** in the absence of **A2**, (b), (c) and (d) in the presence of **A2**, indicate the gradual shrinking of *Z*-isomer while at the same time *E* concentration is increasing looking at percentages and concentrations, (*E*-**A2** shown with orange arrows).
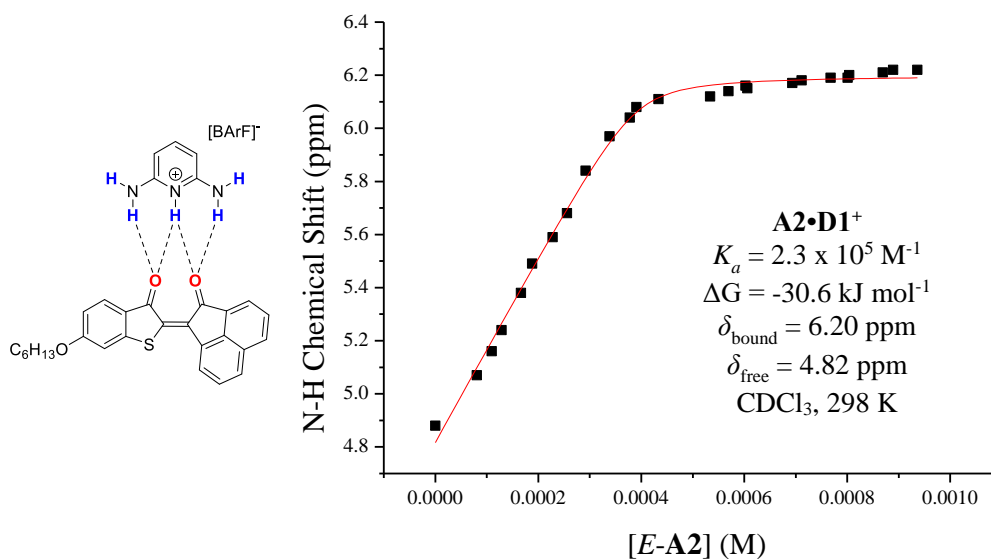
Figure 2.9 Calculated binding isotherm and ^{1}H NMR titration data of **A2•D1**$^+$ at 298 K in CDCl$_3$. The chemical shift of NH$_2$ protons of **D1**$^+$ was used.

A further question we asked was whether the presence of the donor array would alter the E/Z-isomeric ratio of **A2** due to binding. To determine this, a 2 mM solution f Z-**A2** was prepared and allowed to reach the photostationary state under ambient light wherein the ratio of E/Z is approximately 1:1. Then a generous amount of pure **D1**$^+$ in the solid form was added to the solution where it was monitored over time. The result is pictured in Figure 2.10. The ratios in each spectrum can be calculated using Eq. 1 that give values of 48.1:51.9 (a) and 45.5:54.5 (b), a difference of 2.6%. This value is near the error on the measurement and not a large effect.
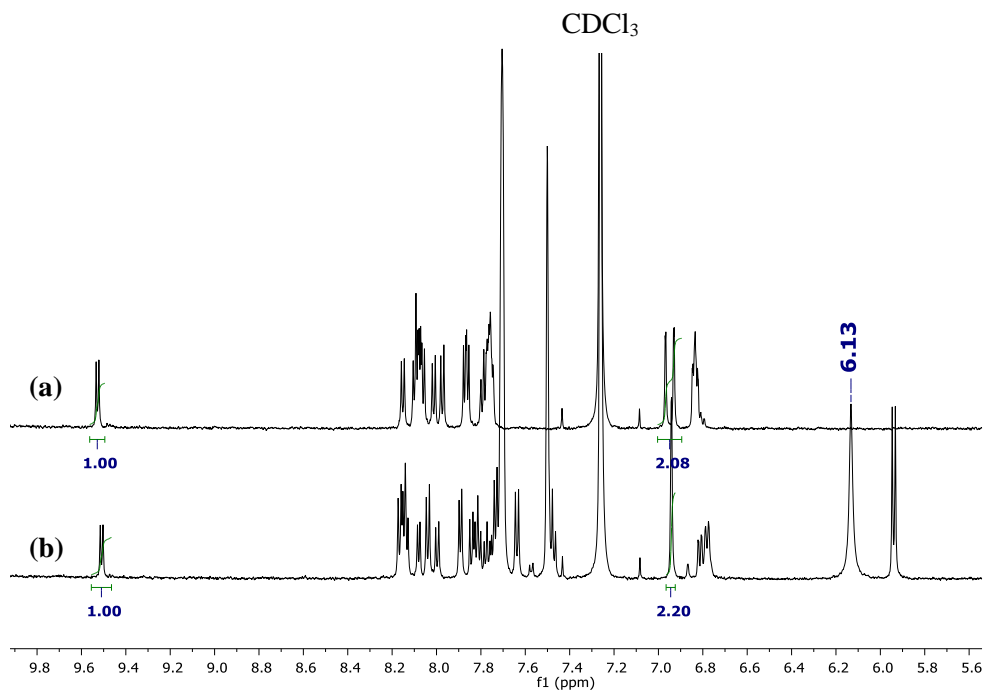
Figure 2.10 ^{1}H NMR (600 MHz) analysis of the ability of only one isomeric form (*E*-**A2**) to from a stable complex with **D1**$^+$ in CDCl$_3$ at 298 K under ambient light. (a) 2 mM solution of **A2** at photostationary state, (b) after 3.5 h in the presence of excess **D1**$^+$.

For the next experiment, we picked **D2**$^+$ with the assumption that this donor can form hydrogen bond complexes in a similar way as **D1**$^+$. The main difference between **D1**$^+$ and **D2**$^+$ is the lack of a second amine (NH$_2$) group in **D2**$^+$ structure that reduces the number of available hydrogen bond interactions and presumably the stability of the complex. This agrees with what we obtained from the fitted isotherms of this AAA-DD hydrogen bond complex ($K_a = 1.2$ x 10^5 M^{-1} of plotting chemical shift of NH against [*E*-**A2**]) (Figure 2.11). Again, the calculated δ_{free} was the same value as a solution of free donor.
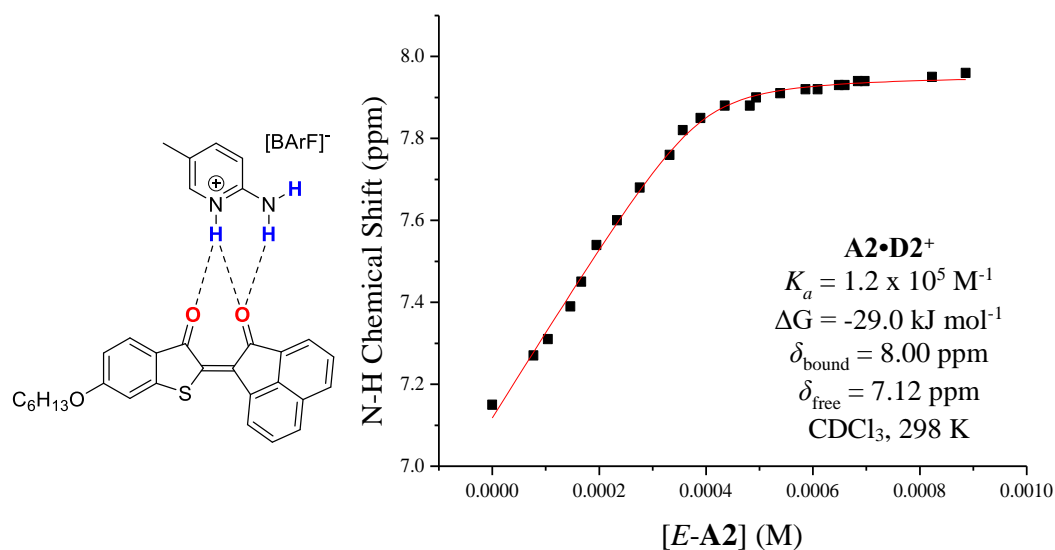
Figure 2.11 Calculated binding isotherm and ^{1}H NMR titration data of **A2•D2$^+$** at 298 K in CDCl$_3$. The chemical shift of NH proton of **D2$^+$** was used.

D3 is a symmetrically substituted urea containing two hydrogen bonding sites that can generate an AAA-DD complex with *E*-**A2** (**A2•D3**). Plotting the chemical shift of the NH protons against the concentration of *E*-**A2** to a 1:1 complexation model yields an isotherm with K_a = 7.0 x 10^3 M^{-1} and a free energy of complexation ΔG = -22.0 kJ mol^{-1} (Figure 2.12). The calculated uncomplexed chemical shifts of NH (δ_{free} = 7.12 ppm) that matches the chemical shift of **D3** in the absence of *E*-**A2**, lends further support for the conclusion that similar to **A2•D1$^+$** and **A2•D2$^+$**, this is only *E*-**A2** binding with **D3** to form an AAA-DD complex is observed.
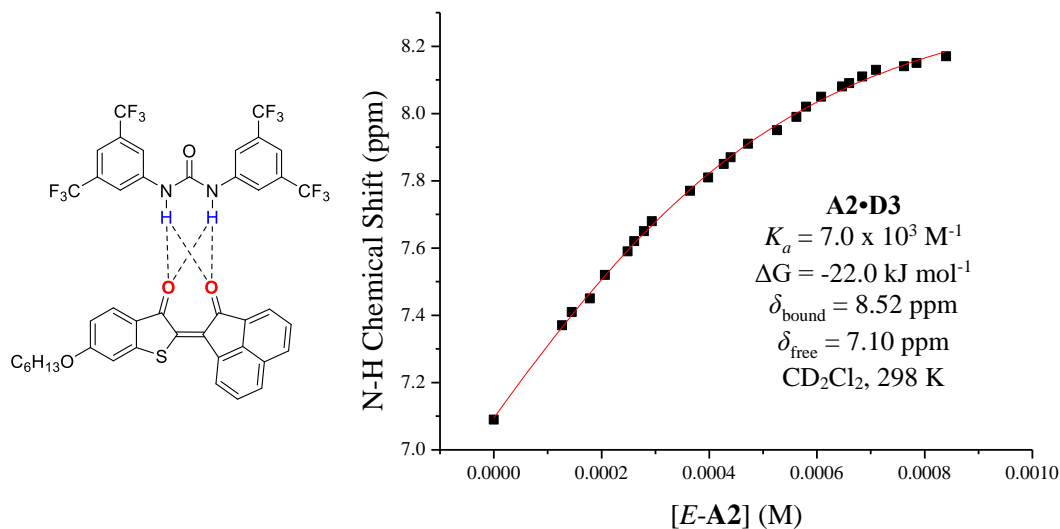
Figure 2.12 Calculated binding isotherm and ¹H NMR titration data of **A2•D3** at 298 K in CD₂Cl₂. The chemical shift of NH proton of **D3** was used.

Using an analogous processing and fitting method for the previously discussed complexes, the titration curves of **A2•D4**, **A2•D5** and **A2•D6** were plotted as illustrated in Figures 2.13 and 2.14, respectively. In the case of **D4** and **D5** (two substituted indoles with different binding strength), plots were obtained for the changes in chemical shifts of indole (NH) protons of **D4** and NH₂ protons of **D5** versus the concentration of *E*-**A2**. with the last donor studied (**A2•D6**), the chemical shift of the NH₂ protons were utilized. The corresponding data of K_a value, free energy (ΔG) and chemical shifts of bonded and nonbonded complexes were determined for these three AAA-DDD hydrogen bond complexes. Again, the chemical shift of NH or NH₂ protons at zero concentration of *E*-isomer are identical to the chemical shift of their free form. This implies that only *E*-**A2** interacts intermolecularly to produce AAA-DDD complexes.
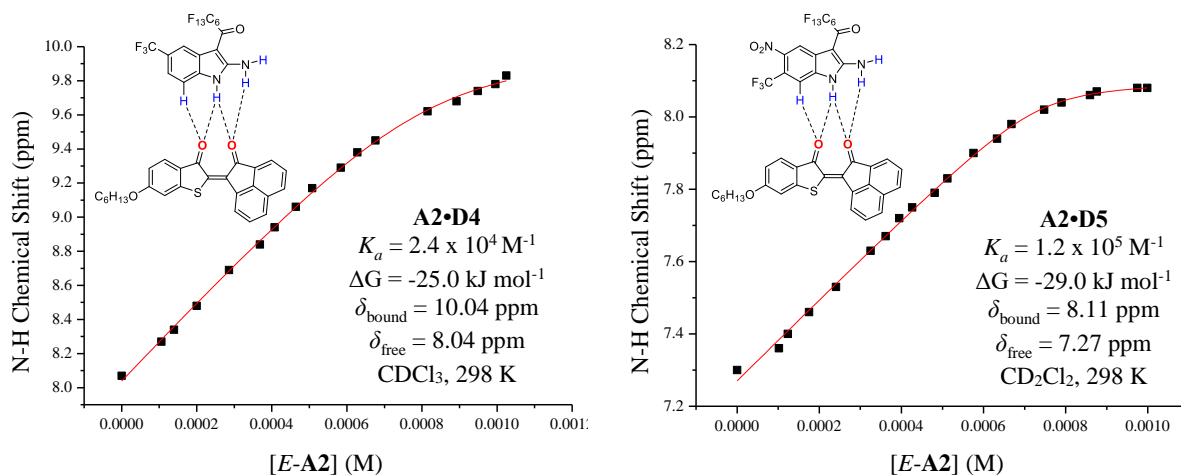
Figure 2.13 Calculated binding isotherms and ^{1}H NMR titration data of **A2•D4** and **A2•D5** at 298 K in CDCl$_3$ and CD$_2$Cl$_2$, respectively. The chemical shifts of the indole NH proton and NH$_2$ protons of **D4** and **D5** were used, respectively.
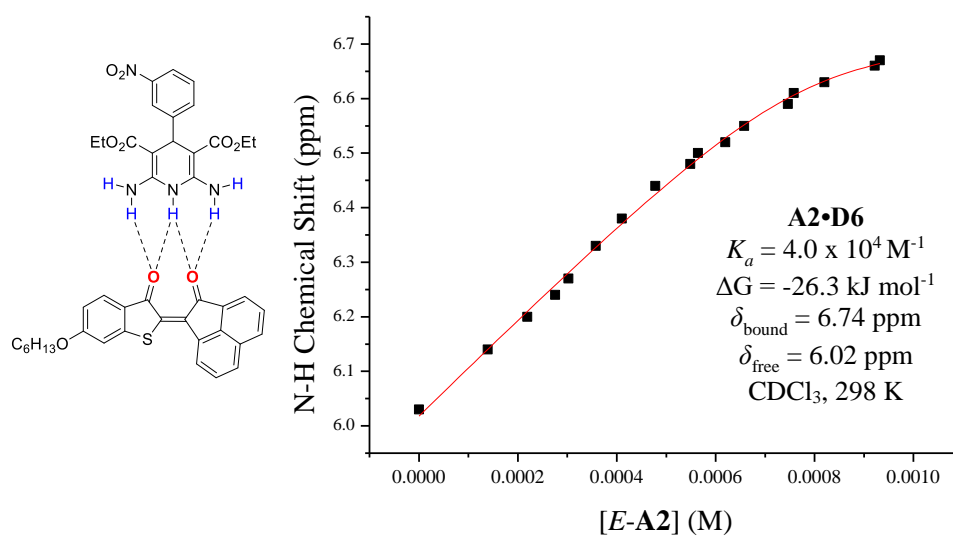

Figure 2.14 Calculated binding isotherm and ^{1}H NMR titration data of **A2•D6** at 298 K in CDCl$_3$. The chemical shift of NH$_2$ protons of **D6** was used.

As it can be observed from Figures 2.9, 2.11 and 2.13, the association constants of **A2•D1**$^+$, **A2•D2**$^+$ and **A2•D5** (2.3 x 10^5 M^{-1}, 1.2 x 10^5 M^{-1} and 1.2 x 10^5 M^{-1}, respectively) are

generally higher than those obtained for the remaining of complexes. **A2•D1**[+], with the highest value obtained, yielded an association constant two times greater than **A2•D2**[+] and **A2•D5**. This finding is in agreement with the fact that the positively charged species can pull the electron density away from the protons of NH and NH$_2$ which in turn enhance the strength of the donor moieties when it comes to form supramolecular interactions. In the case of **A2•D5**, that high association constant is a result of substituting indole with strong electron withdrawing groups at the 3, 5, 6-positions that makes this donor comparable with cationic **D2**[+].[1] On the other hand, the complexation constant of *E*-**A2•D3** complex in CD$_2$Cl$_2$ was 7.0 x 10^3 M^{-1} which is the lowest value obtained for the library of AAA-DD(D); approximately thirtyfold less than that of the highest association constant of **A2•D1**[+]. This low K_a value could be attributed to the fewer hydrogen bonding sites and withdrawing groups that in turn decreases the binding affinity for **A2**.

Nearly identical AAA-DDD neutral complexes, **A2•D4** and **A2•D5**, exhibit complexation constants of 2.4 x 10^4 M^{-1} and 1.2 x 10^5 M^{-1} in CDCl$_3$ and CD$_2$Cl$_2$, respectively (Figure 2.13). Among these two donor units, **D5** as discussed earlier proved to be a better donor as it has an extra electron withdrawing NO$_2$ group that can further strengthen the intermolecular interactions between acceptor and donor.

As pictured in Figure 2.14, the complexation constant for **A2•D6** is lower than that for **A2•D1**[+], although both complexes have the same hydrogen bonding arrangement as AAA-DDD.[10,18] The main difference is the lack of a positive charge in the structure of **D6** that can explain the lower binding affinity. The presence of two tautomeric forms of **D6** in CDCl$_3$ at room temperature can also account for the lower value of complexation constant for **A2•D6**.

Overall, *Z*-**A2** proved to have no measurable interaction with our six complementary bond donor arrays. The extrapolation of the titration isotherms to zero concentration of *E*-**A2** gives the chemical shift of the free (uncomplexed) donors that is identical to the chemical shift of the donor in the absence of any acceptor. This can be associated with only one available acceptor site within the molecular structure of **A2** in its *Z* orientation. On the

other hand, *E*-isomer showed to form strong supramolecular interactions with the donors where their complexation constants are ranging from 2.3 x 10^5 M^{-1} to 7.0 x 10^3 M^{-1}.

## 2.6 Experimental Methodology

2.6.1 Generalities

All reagents were purchased from commercially available vendors such as Sigma Aldrich, Alfa Aesar or Oakwood Chemical, and used as received without further purification. When required, solvents were dried using an Innovative Technology Inc. Controlled Atmospheres Solvent Purification System that utilizes dual alumina columns (SPS-400-5). Most of the synthetic procedures and manipulations were performed under ambient condition unless otherwise stated. In the case of air and moisture sensitive reactions, a nitrogen atmosphere using standard Schlenk techniques was applied. Light sensitive compounds were stored in foil-wrapped vials and all the experiments took place in near dark to prevent any potential photoisomerization unless photoswitching was desired. The progress of the reactions was monitored by thin layer chromatography (TLC) using pre-coated TLC-sheets POLYGRAM®SIL G/UV254 and visualized with short-wavelength UV light (254 nm). Column chromatography was carried out using SiliCycle®SiliaFlash® F60, 40-63 μm 60 Å. NMR spectra were obtained on either Varian INOVA 400 MHz (^{1}H=399.76 MHz, ^{13}C=100.52 MHz), Varian INOVA 600 MHz (^{1}H=599.20 MHz, ^{13}C=150.69 MHz) or Bruker 400 MHz (^{1}H=400.08 MHz, ^{13}C=100.61 MHz) spectrometers. Chemical Shifts (δ) are reported in ppm where the residual non-deuterated NMR solvent signals for ^{1}H NMR and the deuterated solvent for ^{13}C spectra were referenced to their corresponding literature values with respect to TMS (^{1}H: CHCl$_3$, δ = 7.26 ppm, CHDCl$_2$, δ = 5.32 ppm; ^{13}C {1H}: CDCl$_3$, δ = 77.2 ppm, CHDCl$_2$, δ = 54.0 ppm). All ^{1}H NMR titration experiments were performed on a Varian Inova 600 MHz spectrometer. For two isomers of (*Z*)-6-(hexyloxy)-2-(2-oxoacenaphthylen-1(2H)-ylidene)benzo[b]thiophen-3(2H)-one (*Z*-**A2**) and (*E*)-6-(hexyloxy)-2-(2-oxoacenaphthylen-1(2H)-ylidene)benzo[b]thiophen-3(2H)-one (*E*-**A2**), all ^{1}H and ^{13}C NMR signals were assigned using two-dimensional NMR protocols

(gCOSY, HSQC, HMBC and NOESY NMR spectroscopy). Deuterated solvents for NMR spectroscopy (Chloroform-*d* and DCM-*d₂*) were purchased from Cambridge Isotope Laboratories and Sigma-Aldrich and dried over 4Å (chloroform) molecular sieves before use. X-ray diffraction data were collected by Dr. Paul Boyle on a Bruker-Nonius Apex II diffractometer using graphite monochromatic Cu-K$_\alpha$ radiation ($\gamma = 1.54178$ Å) source and Kappa CCD detector at a temperature of 110 K. Mass spectra were recorded on a Finnigan MAT 8400 where the samples were analyzed by Electron impact ionization (EI). The chemical composition of samples are reported as mass to charge units (m/z).

## 2.6.2 Synthetic Methods
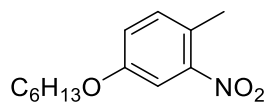
Synthesis of 4-(hexyloxy)-1-methyl-2-nitrobenzene (2) Under an N_2 atmosphere, hexyliodide (5.20 mL, 0.04 mol, 1.1 eq.) was added via a syringe to a solution of 4-methyl-3-nitrophenol (5.00 g, 0.03 mol, 1 eq.) and K_2CO_3 (5.31 g, 0.04 mol, 1.2 eq.) in 125 mL dry DMF at 50 ˚C. The reaction mixture was stirred at 50 ˚C overnight. The reaction mixture was cooled to room temperature and poured into 200 mL water. Liquid-liquid extractions were performed with diethyl ether (2×100 mL) and the entire collected organic layer was poured back into a separatory funnel and washed with water (2×100 mL) and then 50 mL brine. The separated organic phase was dried over anhydrous $MgSO_4$, filtered and the solvent removed under reduced pressure. The product was purified via column chromatography with a mixture of *n*-hexane-ethyl acetate (4.25:0.75) as eluent to yield a clear yellow oily liquid. Yield: 7.34 g, 97%. ^{1}H NMR (600 MHz, CDCl$_3$) δ 7.49 (d, *J*= 2.7 Hz, 1H), 7.20 (d, *J*= 8.5 Hz, 1H), 7.05 (dd, *J*= 8.5 Hz, 2.7 Hz, 1H), 3.98 (t, *J*= 6.5 Hz, 2H), 2.52 (s, 3H), 1.81-1.76 (m, 2H), 1.48-1.43 (m, 2H), 1.35-1.33 (m, 4H), 0.91 (t, *J*= 7.1 Hz, 3H). ^{13}C NMR (100 MHz, CDCl$_3$): δ 157.8, 149.5, 133.5, 125.4, 120.5, 109.8, 68.8, 31.7, 29.1, 25.8, 22.7, 19.8, 14.1. EI-HRMS: Calc. for C$_{13}$H$_{19}$NO$_3$: 237.1365, Found: 237.13688.
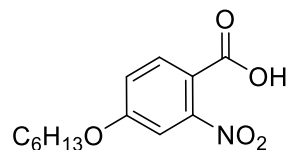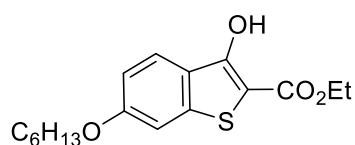
Synthesis of 4-(hexyloxy)-2-nitrobenzoic acid (3) Step 1: To a 500 mL round-bottomed flask equipped with 5.00 g of 4-(hexyloxy)-1-methyl-2-nitrobenzene (0.02 mol, 1 eq.) in 300 mL water:pyridine (1:1), 3.33 g of potassium permanganate ($KMnO_4$) was added (0.02 mol, 1 eq.). The solution was heated to 100 ˚C and kept well-stirred for 1 hour. After that, 4 more equivalents of $KMnO_4$ (16.66 g, 0.1055 mol, 5 eq. in total) were added portionwise during 5 hours every 15 to 20 minutes. Once all $KMnO_4$ was added, the reaction mixture was stirred for another hour at the same temperature (100 ˚C). The cooled reaction mixture was filtered through a thin pad of celite, followed by the addition of a mixture of 120 mL water:pyridine (1:3) to the filtrate. The entire solution was then transferred to a 1000 mL flask in which approximately 100-200 mL water were poured to further dilute the filtrate. The flask was equipped with a large stirbar and cooled in an ice bath where the solution was acidified by slow addition of concentrated HCl. Upon acidification, a white to pale yellow solid precipitated, and was vacuum filtered. The solid obtained was rinsed with cold, 1 M dilute HCl and left overnight to dry. The crude solid was a mixture of product **3** and starting material **2** and was used for the next step without any further purification.
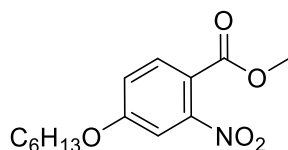

Synthesis of methyl 4-(hexyloxy)-2-nitrobenzoate (4) Step 2: Dimethyl sulfate (1.95 mL, 0.02 mol, 1.1 eq.) was added slowly to a 150 mL round-bottomed flask containing a mixture of compounds **2** and **3** (5.00 g, 0.02 mol, 1 eq.) and K_2CO_3 (2.84 g, 0.02 mol, 1.1 eq.) in 100 mL dry acetone. The well-stirred mixture under N_2, was heated gently to reflux for 2 hours and then cooled to room temperature. The reaction mixture was diluted with 150 mL water and extracted twice with 100 mL diethyl ether. The organic phases were combined, washed with water (2 × 100 mL), dried using $MgSO_4$ and the solvent was removed under reduced pressure. The resulting crude was subjected to column

chromatography where a mixture of *n*-hexane-ethyl acetate (4.25:0.75) was used as eluent to give <u>yellow oily</u> liquid. Equivalents of reagents used for this procedure were calculated as if only pure compound **3** was present. Yield: 2.34 g, 40% over two steps. ^{1}H NMR (400 MHz, CDCl$_3$): δ 7.77 (d, *J*= 8.7 Hz, 1H), 7.22 (d, *J*= 2.5 Hz, 1H), 7.08 (dd, *J*= 8.7 Hz, 2.5 Hz, 1H), 4.03 (t, *J*= 6.5 Hz, 2H), 3.87 (s, 3H), 1.84-1.77 (m, 2H), 1.50-1.42 (m, 2H), 1.37-1.32 (m, 4H), 0.91 (t, *J*= 7.0 Hz, 3H). ^{13}C NMR (100 MHz, CDCl$_3$): δ 165.1, 162.1, 150.9, 132.1, 117.9, 117.7, 109.8, 69.3, 53.0, 31.6, 28.9, 25.7, 22.7, 14.1. EI-HRMS: Calc. for C$_{14}$H$_{19}$NO$_5$: 281.1263, Found: 281.12625.

Synthesis of ethyl 6-(hexyloxy)-3-hydroxybenzo[b]thiophene-2-carboxylate (5). Under an N$_2$ atmosphere, to a cold solution of methyl 4-(hexyloxy)-2-nitrobenzoate (0.50 g, 2 mmol, 1 eq.) and ethyl thioglycolate (0.33 mL, 3.00 mmol, 1.47 eq.) in 75 mL dry DMF, KOH (0.37 g, 6.60 mmol, 3.33 eq.) was added portionwise over the course of 30 minutes at 0 ˚C. The reaction mixture was allowed to stir for another 30 minutes in an ice bath and then at room temperature for approximately 4.5 to 5 hours. The progress of the reaction was monitored by TLC utilizing a mixture of *n*-hexane-ethyl acetate (4.25:0.75) as eluent. Once the reaction was complete, the suspension was poured into an ice-water mixture and subsequently acidified with concentrated HCl. The resulting precipitate was filtered to yield compound **5** as a pale yellow solid. Yield: 0.526 g, 96%. ^{1}H NMR (600 MHz, CDCl$_3$) δ 10.25 (bs, 1H), 7.80 (d, *J*= 8.9 Hz, 1H), 7.14 (d, *J*= 2.2 Hz, 1H), 7.00 (dd, *J*= 8.9 Hz, 2.2 Hz, 1H), 4.40 (q, *J*= 7.2 Hz, 2H), 4.03 (t, *J*= 6.6 Hz, 2H), 1.85-1.80 (m, 2H), 1.51-1.46 (m, 2H), 1.41 (t, *J*= 7.2 Hz, 3H), 1.37-1.35 (m, 4H), 0.92 (t, *J*= 7.0 Hz, 3H). ^{13}C NMR (101 MHz, CDCl$_3$) δ 167.5, 160.7, 159.9, 141.1, 124.2, 123.9, 115.5, 105.7, 99.6, 68.6, 61.3, 31.7, 29.3, 25.9, 22.7, 14.5, 14.2. EI-HRMS: Calc. for C$_{17}$H$_{22}$O$_4$S: 322.1239, Found: 322.1244.
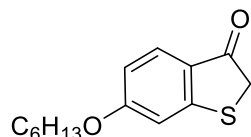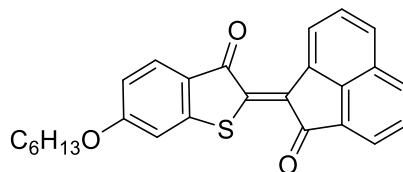
Synthesis of 6-(hexyloxy)benzo[b]thiophen-3(2H)-one (6) In a 250 ml round-bottomed flask, a solution of ethyl 6-(hexyloxy)-3-hydroxybenzo[b]thiophene-2-carboxylate (**5**) (1.00 g, 3.00 mmol, 1 eq.) and KOH (15.00 g, 15% mol) in 100 mL EtOH/H$_2$O (1:1) was heated to reflux for 24 hours under N$_2$ atmosphere. After cooling in an ice bath, the solution was slowly treated with cold HCl 8% aq (pH= 3). Then liquid-liquid extractions with diethyl ether were performed (2 × 100 mL). The combined organic layers were washed with water (3 × 100 mL) and brine (1 × 100 mL), followed by drying over MgSO$_4$. After solvent removal, compound **6** was obtained as a red to orange oil that was carried to the next step without further purification. Yield: 0.68 g, 87%. ^{1}H NMR (600 MHz, CDCl$_3$) δ 7.69 (d, *J*= 8.7 Hz, 1H), 6.84 (d, *J*= 2.2 Hz, 1H), 6.74 (dd, *J*= 8.7 Hz, 2.2 Hz, 1H), 4.03 (t, *J*= 6.5 Hz, 2H), 3.78 (s, 2H), 1.83-1.78 (m, 2H), 1.49-1.44 (m, 2H), 1.36-1.33 (m, 4H), 0.91 (t, *J*= 7.0 Hz, 3H). ^{13}C NMR (101 MHz, CDCl$_3$) δ 198.2, 165.8, 157.4, 128.1, 124.2, 113.9, 108.0, 68.8, 39.8, 31.6, 29.1, 25.7, 22.7, 14.1. EI-HRMS: Calc. for C$_{14}$H$_{18}$O$_2$S: 250.1028, Found: 250.1036.
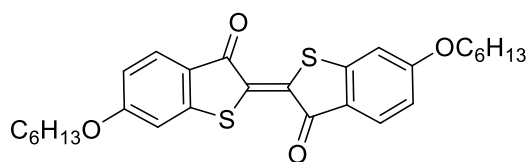

Synthesis of (*E*)-6,6'-bis(hexyloxy)-3H,3'H-[2,2'-bibenzo[b]thiophenylidene]-3,3'-dione (A1). Piperidine (1 mL, 10.40 mmol, 4 eq.) was added to a 150 mL round bottomed flask containing 6-(hexyloxy)benzo[b]thiophen-3(2H)-one (**6**) (0.65 g, 26.00 mmol, 1 eq.) dissolved in 30 mL isopropanol. The mixture was heated to 70 ˚C and a solution of K$_3$Fe(CN)$_6$ (3.42 g, 10.4 mmol, 4 eq.) in 30 mL water was added. The formed suspension was maintained at the same temperature for 30 minutes and then cooled to room temperature to stir for another 30 minutes. 100 mL of water was added to the flask to dissolve any piperidine, K$_3$Fe(CN)$_6$ and propanol residual. A small amount of CH$_2$Cl$_2$ (50 mL) was added and the resulting red solid was vacuum filtered using less porous filter

paper (Whatman 3, 55mm). The solid was washed with water and allowed to dry under vacuum in the dark to give red compound **7**. Yield: 0.25 g, 19%. ^{1}H NMR (600 MHz, CDCl$_3$) δ 7.84 (d, J= 8.6 Hz, 2H), 6.96 (d, J= 2.1 Hz, 2H), 6.82 (dd, J= 8.6 Hz, 2.1 Hz, 2H), 4.08 (t, J= 6.6 Hz, 4H), 1.85-1.80 (m, 4H), 1.51-1.46 (m, 4H), 1.37-1.34 (m, 8H), 0.92 (t, J= 7.1 Hz, 6H). ^{13}C NMR (100 MHz, CD$_2$Cl$_2$): δ 128.6, 114.7, 111.5, 109.1, 107.9, 69.7, 32.1, 29.5, 26.1, 23.2, 14.4. EI-HRMS: Calc. for C$_{28}$H$_{32}$O$_4$S$_2$: 496.1742, Found: 496.17416.

Synthesis of (Z)-6-(hexyloxy)-2-(2-oxoacenaphthylen-1(2H)-ylidene)benzo[b]thiophen-3(2H)-one(Z-A2). To a solution of compound **6** (0.66 g, 2.60 mmol, 1 eq.) dissolved in 75 mL of anhydrous DMF, was added 0.36 g of potassium carbonate (2.60 mmol, 1eq.) and 0.48 g of acenaphthoquinone (2.60 mmol, 1eq.). In the foil-wrapped round-bottomed flask, the reaction mixture was stirred for 2 h at room temperature under a nitrogen atmosphere. The red precipitate obtained was filtered through a less porous–filter paper (Whatman 3, 55 mm) and washed thoroughly with water to remove any trace of DMF. The resulting solid was dried under vacuum protected from light to yield approximately 1.09 g of compound **A2**. ^{1}H NMR (600 MHz, CDCl$_3$) δ 9.53 (d, J= 7.34 Hz, 1H), 8.15 (d, J= 8.03 Hz, 1H), 8.10 (d, J= 7.03 Hz, 1H), 8.01 (d, J= 8.26 Hz, 1H), 7.86 (d, J= 8.55 Hz, 1H), 7.78 (dd, J= 8.26 Hz, J= 7.34 Hz, 1H), 7.75 (dd, J= 8.03 Hz, J= 7.03 Hz, 1H), 6.97 (d, J= 2.1 Hz, 1H), 6.83 (dd, J= 8.55 Hz, J= 2.1 Hz, 1H), 4.10 (t, J= 6.51 Hz, 2H), 1.87-1.82 (m, 2H), 1.52-1.47 (m, 2H), 1.38-1.36 (m, 4H), 0.94-0.92 (t, J= 7.08 Hz, 3H). ^{13}C NMR (101 MHz, CDCl$_3$) δ 194.4, 189.6, 166.0, 151.1, 141.0, 139.1, 133.0, 132.1, 132.0, 131.5, 130.6, 129.1, 128.5, 127.9, 127.6, 126.8, 122.9, 122.0, 114.1, 108.4, 69.0, 31.7, 29.1, 25.8, 22.7, 14.2. EI-HRMS: Calc. for C$_{26}$H$_{22}$O$_3$S: 414.1290, Found: 414.12799.
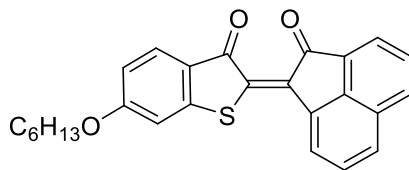
Synthesis of (*E*)-6-(hexyloxy)-2-(2-oxoacenaphthylen-1(2H)-ylidene)benzo[b]thiophen-3(2H)-one (*E*-A2). In a 250 mL round-bottomed flask, 50 mg of compound *Z*-**A2** was dissolved in 125 mL chloroform and purged with nitrogen while it was under irradiation at 520 nm light at room temperature for approximately two hours. The conversion of *Z*- to *E*-isomer was monitored by ^{1}H NMR until reached to the maximum amount of converted *E* possible (63%). The solvent was evaporated to 10 mL by blowing air on the flask. Then, the solution was loaded on a preparatory TLC plate and chloroform was used as eluent to yield an orange to yellow solid. The whole procedure was performed in the dark since the ambient light can affect the isomerization. ^{1}H NMR (600 MHz, CDCl$_3$) δ 8.08-8.04 (m, 3H), 7.96 (d, *J*= 8.21 Hz, 1H), 7.86 (d, *J*= 8.50 Hz, 1H), 7.76-7.74 (m, 2H), 6.91 (d, *J*= 2.11 Hz, 1H), 6.82 (dd, *J*= 8.50 Hz, *J*= 2.11 Hz, 1H), 4.07 (t, *J*= 6.54 Hz, 2H), 1.86-1.81 (m, 2H), 1.51-1.46 (m, 2H), 1.38-1.35 (m, 4H), 0.94-0.91 (t, *J*= 6.99 Hz, 3H). ^{13}C NMR (151 MHz, CDCl$_3$) δ 186.2, 184.2, 165.5, 144.9, 140.8, 140.3, 136.5, 134.8, 133.0, 130.7, 130.2, 129.2, 128.5, 128.5, 127.3, 123.7, 123.5, 122.0, 114.0, 108.4, 69.0, 31.7, 29.1, 25.8, 22.7, 14.2.

2.6.3 ^{1}H NMR Titration Procedure

2.6.3.1 Preparation of **A2** Solution as the Acceptor

At least one day prior to perform the titration experiment, a specific concentration of **A2** (4 mM or 8 mM) in 10 mL of the selected solvent (CHCl$_3$ or CH$_2$Cl$_2$) was prepared in a clean and dry round-bottomed flask. Upon being completely dissolved, a volume of 500 μL of the solution was transferred directly into dry and clean small vials wrapped with aluminum foil to prevent any exposure to light. The solvent in vials was then allowed to

evaporate at room temperature. The entire procedure of solution preparation and transferring was performed in the absence of light.

2.6.3.2   Preparation of Different Donors

In a similar fashion to the preparation of acceptor (**A2**), in a 50 mL round-bottomed flask, a 1mM solution of each of the donor **D1**, **D2**, **D4** and **D6** was prepared in 20 mL of CHCl$_3$. once the solids were completely dissolved, 1 mL of each solution was taken out and transferred to a prelabeled vial. Then at room temperature, the solvent in the vials was allowed to evaporate. Due to the low solubility of **A3** and **A5** in CHCl$_3$, the solutions of 1 mM **D3** and 0.75 mM **D5** were prepared in CH$_2$Cl$_2$.

2.6.3.3   Titration of **A2** with Different Donors (**Dx**)

At the time of titration, to the dry vials containing the required mass of 4 mM **A2** and 1 mM of the selected donor, 0.5 mL and 1 mL of the selected deuterated solvent were added respectively. The addition of deuterated solvent to the **A2** vial was carried out in the dark and the vial kept wrapped in foil for the entire preparation time. Both vials were sealed using black tape and were shaken thoroughly or sonicated to ensure the desired concentration. A 250 µL aliquot of donor solution was transferred via syringe to a clean and dry NMR tube containing 250 µL of CDCl$_3$ to produce 0.5 mL of 0.5 mM solution of the specific donor. The NMR tube was shaken to obtain a consistent concentration inside, and the ^{1}H NMR spectrum was recorded to obtain the chemical shifts for the free donor. In another clean and dry NMR tube, 250 µL of **A2** as the acceptor and 250 µL of the donor solution were added to make a 500 µL solution of 2 mM and 0.5 mM (4:1) **A2·Dx** mixture. The mixture was shaken to produce a homogenous solution and a ^{1}H NMR spectrum was recorded. As an exception, for the titration of **D5** due to its low solubility (0.75 mM in CD$_2$Cl$_2$), 150 µL and 400 µL of 8 mM **A2** and 0.75 mM **D5**, respectively, were injected into a NMR tube containing 50 µL deuterated CD$_2$Cl$_2$ to produce a solution of 600 µL of 2 mM of **A2** and 0.5 mM **D5** (4:1). The samples were taken out of the instrument and

exposed to room light from 20 seconds to 20 minutes (depending on the rate of photoisomerization) to induce photoswitching and the conversion to *E*-isomer. ^{1}H NMR spectra were acquired for the solution over time after each light exposure and the chemical shifts of the NH or NH_2 protons of the donors were recorded.

2.7 References

1. Wang, H.-B.; Mudraboyina, B. P.; Wisner, J. A. *Chem. Eur. J.* **2012**, *18* (5), 1322-1327.

2. Linares Mendez, I. J.; Wang, H.-B.; Yuan, Y.-X.; Wisner, J. A. *Macromol. Rap, Commun.* **2017**, in press, DOI: marc.201700619R1.

3. Rosengaus, J.; Willner, I. *J. Phys.Org. Chem.* **1995**, *8* (1), 54-62.

4. Williamson, W. *J. Chem. Soc.* **1852**, *106*, 229-239.

5. Schwink, L.; Stengelin, S.; Gossel, M.; Hessler, G.; Haack, T.; Lennig, P. Novel azacycly-substituted arylthienopyrimidinones, process for their preparation and their use as medicaments. WO2007093363 A1, August 23. 2007.

6. Ballini, R.; Carotti, A. *Synth. Commun.* **1983**, *13* (14), 1197-1201.

7. Beck, J. R. *J. Org. Chem.* **1973**, *38* (23), 4086-4087.

8. Vlahakis, J. Z.; Maly, K. E.; Lemieux, R. P. *J. Mater. Chem.* **2001**, *11*, 2459-2464.

9. Schulz, M.; Christoffers, J. *Tetrahedron* **2013**, *69* (2), 802-809.

10. Blight, B. A.; Camara-Campos, A.; Djurdjevic, S.; Kaller, M.; Leigh, D. A.; McMillan, F. M.; McNab, H.; Slawin, A. M. Z. *J. Am. Chem. Soc.* **2009**, *131* (39), 14116–14122.

11. Kim, H. Y.; Oh, K. *Org. Lett.* **2011**, *13* (6), 1306–1309.

12. Robertson, W. M.; Kastrinsky, D. B.; Hwang, I.; Boger, D. L. *Bioorganic Med. Chem. Lett.* **2010**, *20*, 2722-2725.

13. Xu, G.; Zheng, L.; Dang, Q.; Bai, X. *Synthesis* **2013**, *45*, 743-752.

14. Murray, T. J.; Zimmerman, S. C. Kolotuchin, S. V. *Tetrahedron* **1995**, *51* (2), 635-648.

15. Thordarson, P. *Chem. Soc. Rev.,* **2011**, *40* (3), 1305-1323.

16. Bisson, A. P.; Carver, F. J.; Eggleston, D. S.; Haltiwanger, R. C.; Hunter, C. A.; Livingstone, D. L.; McCabe, J. F.; Rotger, C.; Rowan, A. E. *J. Am. Chem. Soc.* **2000,** *122* (37), 8856-8868.

17. https://www.originlab.com/

18. Hargrove, A. E.; Zhong, Z.; Sessler, J. L.; Anslyn, E. V. *New J Chem.* **2010**, *34*, 348-354.

19. Han, Y.-F.; Chen, W.-Q.; Wang, H.-B.; Yuan, Y.-X.; Wu, N.-N.; Song, X.-Z.; Yang, L. *Chem. Eur. J.* **2014**, *20* (51), 16980-16986.

20. Blight, B. A.; Hunter, C. A.; Leigh, D. A.; McNab, H.; Thomson, P. I. T. *Nat. Chem.* **2011**, *3*, 244-248.

Chapter 3

3   Conclusions and Future Work

3.1   Conclusions

The work in this thesis describes synthesis, photoisomerization studies and binding properties of thioindigos as viable acceptor arrays in supramolecular complexes. The work began by synthesizing symmetrical **A1** aiming at incorporating this molecule in a complementary hydrogen bond complex AAA-DD(D). Although it proved to form a stable supramolecular complex, the solubility impeded proper evaluation of the proposed system. To solve the issue, another derivative of thioindigo, unsymmetrical **A2**, was synthesized through a six-step procedure identical to **A1** except for the last step. An extensive study of the photophysical properties of **A2** in both its isomeric forms was conducted using ^{1}H NMR and UV-Vis spectroscopy. These spectroscopic studies revealed that irradiating at different wavelengths, the reversible interconversion between *Z*- and *E*-**A2** took place wherein the latter isomeric form was assumed to function as a feasible acceptor array. This assumption was due to the linear arrangement of carbonyl groups in *E*-isomer that provides an electron rich spot favorable for hydrogen bonding. The assumption was examined by incorporating the *E*-**A2** in six different complementary hydrogen bond complexes, AAA-DD(D). Herein lies the novelty of the project that ^{1}H NMR studies of **A2•Dx** proved that *E*-**A2** is a versatile acceptor array that shows high binding affinity towards different donors with distinctive arrangement of hydrogen bonding sites and inherent tendency towards the acceptor entity. As shown in Figure 3.1, the complexation constants obtained using ^{1}H NMR titration studies are ranged from 2.3×10^5 M^{-1} to 7.0×10^3 M^{-1} that can be translated to free energies between -30.60 kJ mol^{-1} and -22.00 kJ mol^{-1}. The most stable supramolecular complex **A2•D1$^+$** demonstrated an association constant of 2.3×10^5 M^{-1}. The high stability of this complex is a direct outcome of number of hydrogen bonding sites and the presence of a positively charged heteroatom ($^+$NH) in the structure of donor entity (**D1$^+$**). On the other hand, fewer sites available for hydrogen bonding in **D3** leads to the lowest value obtained for **A2•D3**.
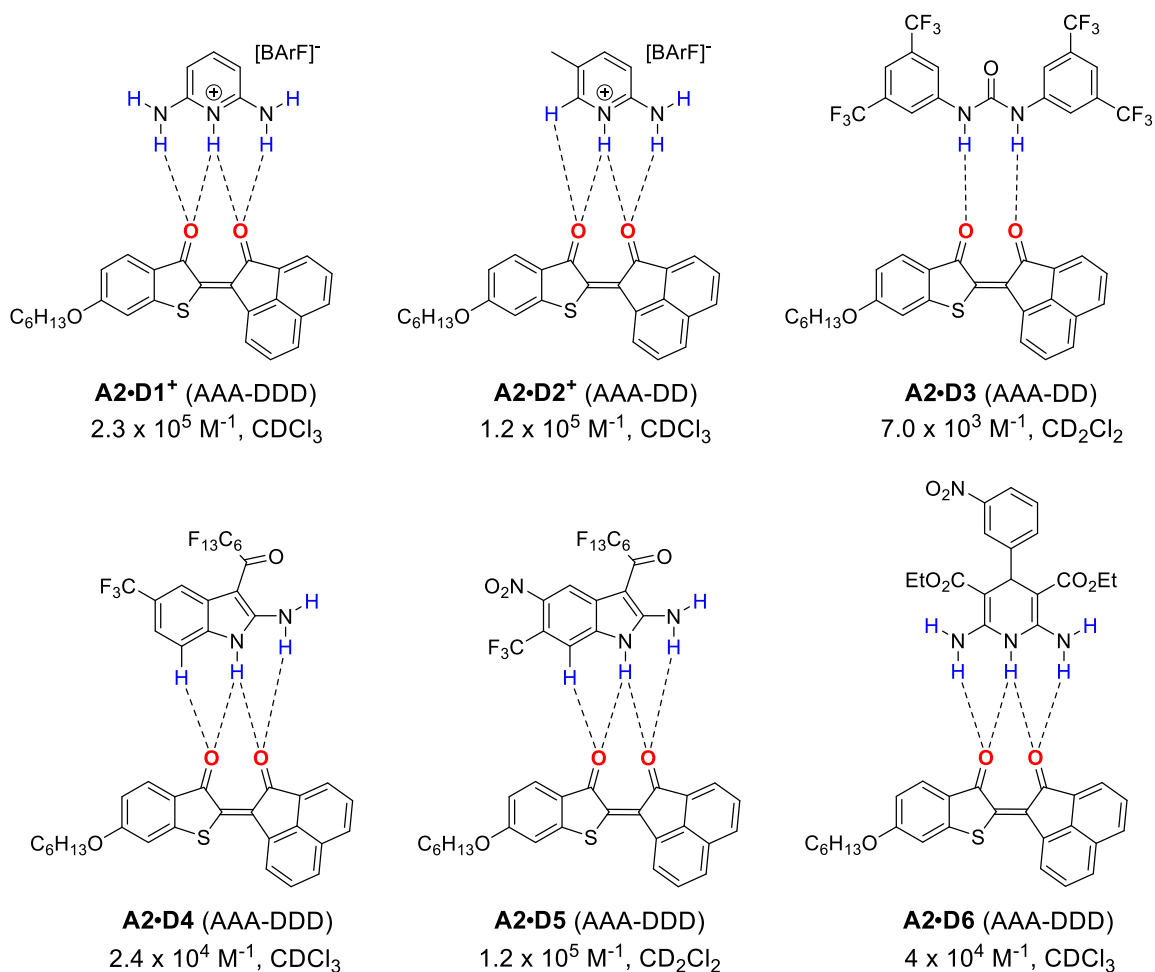
Figure 3.1 Different AAA-DD(D) hydrogen bond complexes with their complexation values.

It is also important to note that *Z*-**A2** was demonstrated to be unable to form measurable hydrogen bonding interactions. We concluded this because the extrapolations of the titration curves obtained for six supramolecular complexes reveal that at zero concentration of *E*-**A2** where the solution is pure *Z*-**A2** there is no change in the chemical shift of the donor proton.

3.2 Future Work

Given the complexation constants for six different supramolecular complexes examined in this project, thioindigo derivatives proved to be potential acceptors that have been explored in the context of supramolecular chemistry. The main problem related to these photoswitches is their poor solubility that retards further development in their characterizations and applications. However, if this impediment can be removed, as in the case of **A2**, various kinds of supramolecular polymers can be designed and synthesized. This purpose can be achieved by substituting specifically the phenyl rings of acenaphthylene-1,2-dione before condensing it with 6-(hexyloxy)benzo[b]thiophen-3(2H)-one (Scheme 3.1). Since the phenyl rings of acenaphthylene-1,2-dione tend to be more reactive to nucleophilic aromatic substitution, a wide array of substitutions such as nitration, halogenation, Friedel-Crafts acylation and alkylation can be performed to build a library of thioindigo acceptors. However, only those electron donating substitutions that increase the electron density on oxygen atoms are worthwhile to consider.

X: Br, OH, NH_2, OPh, OCH_3 ... etc.
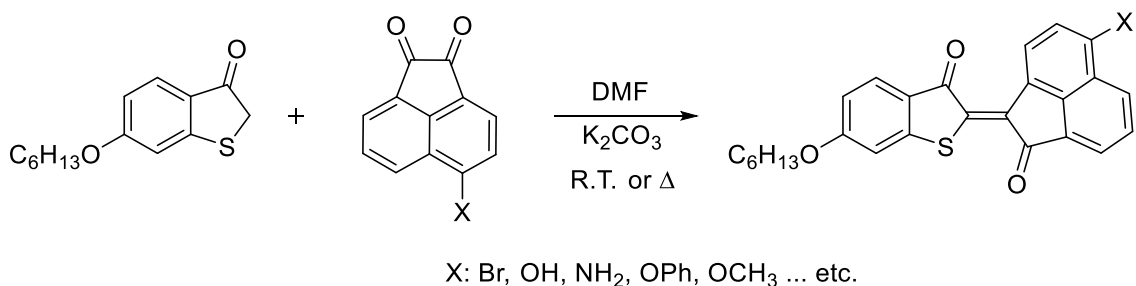
Scheme 3.1 A plausible synthetic procedure for preparing different **A2** derivatives.

Ideally, if these thioindigo derivatives show high solubility, their photophysical properties could be probed. Once these hypothetically soluble acceptors show photoisomerization to *E*-isomer which provides a linear arrangement of carbonyl groups for hydrogen bonding, they can be introduced to different donors (Figure 3.2). It is anticipated that these supramolecular complexes exhibit comparable or greater stability as those obtained for **A2•Dx.**
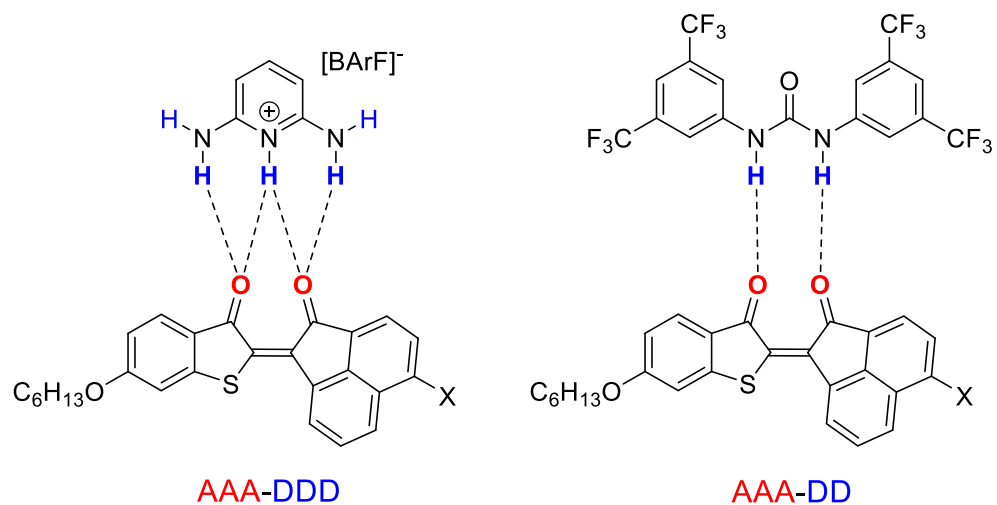
X: Br, OH, NH$_2$, OPh, OCH$_3$ ... etc.

Figure 3.2 The anticipated complexation between proposed thioindigo derivatives and **D1**[+] and **D3**.

Appendices
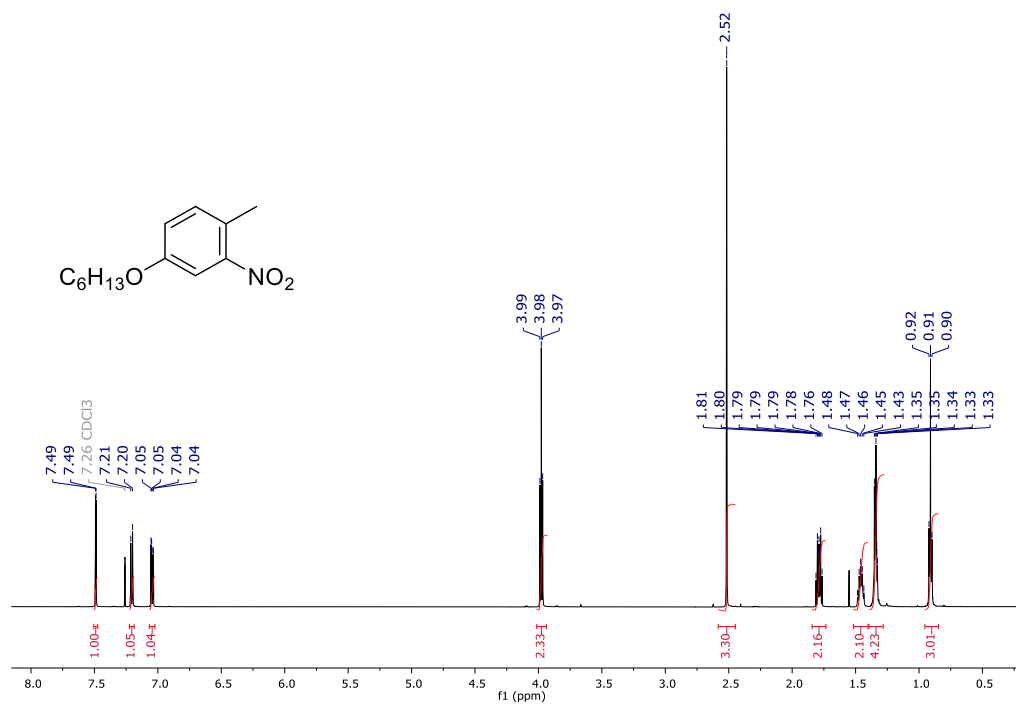
Figure A.1 ^{1}H NMR spectrum of 4-(hexyloxy)-1-methyl-2-nitrobenzene (**2**) in CDCl$_3$.
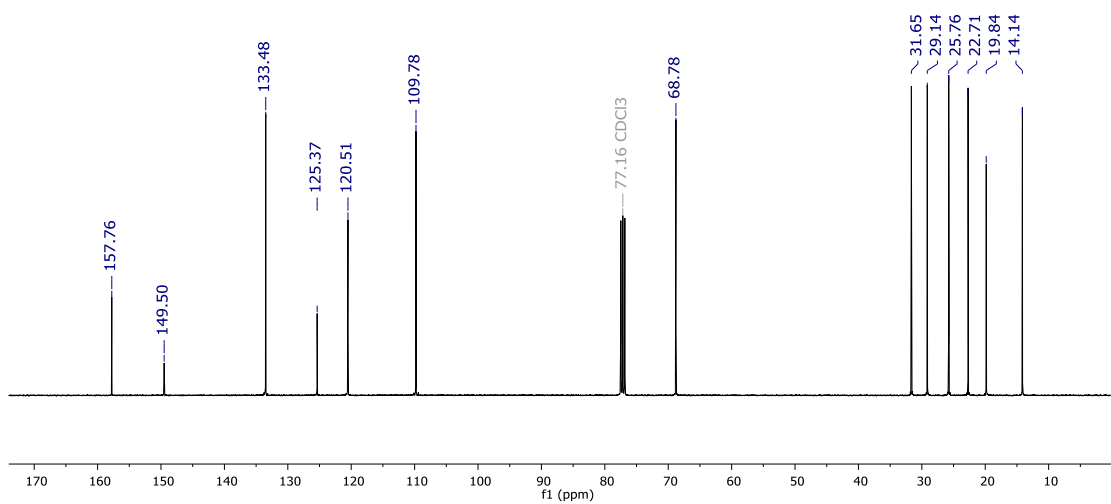
Figure A.2 ^{13}C{1H} NMR spectrum 4-(hexyloxy)-1-methyl-2-nitrobenzene (**2**) in CDCl$_3$.
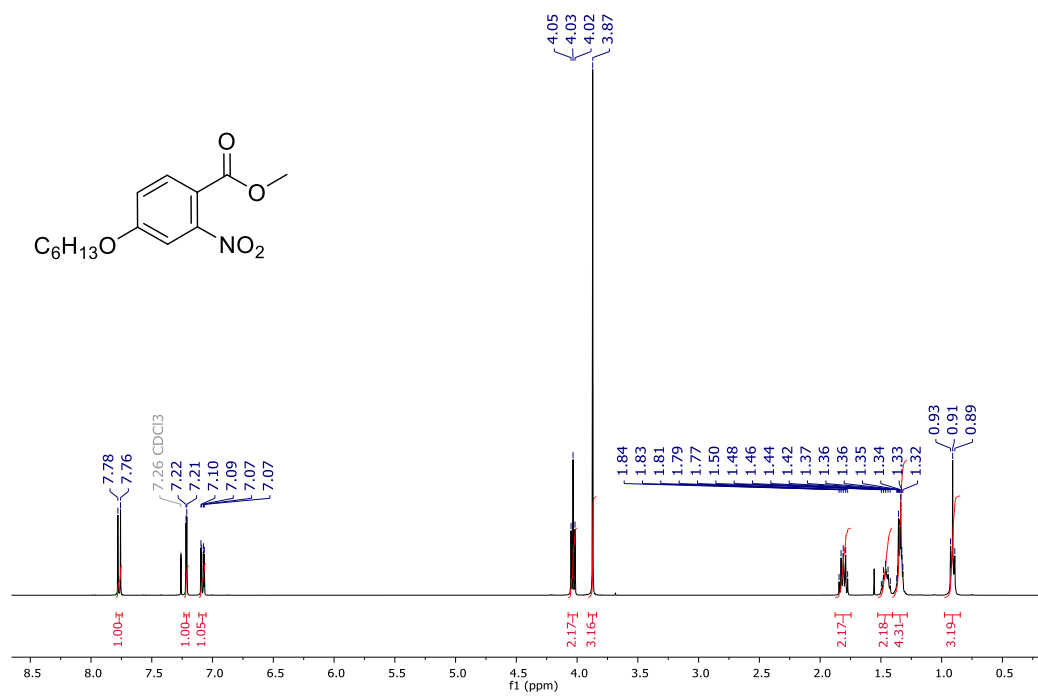
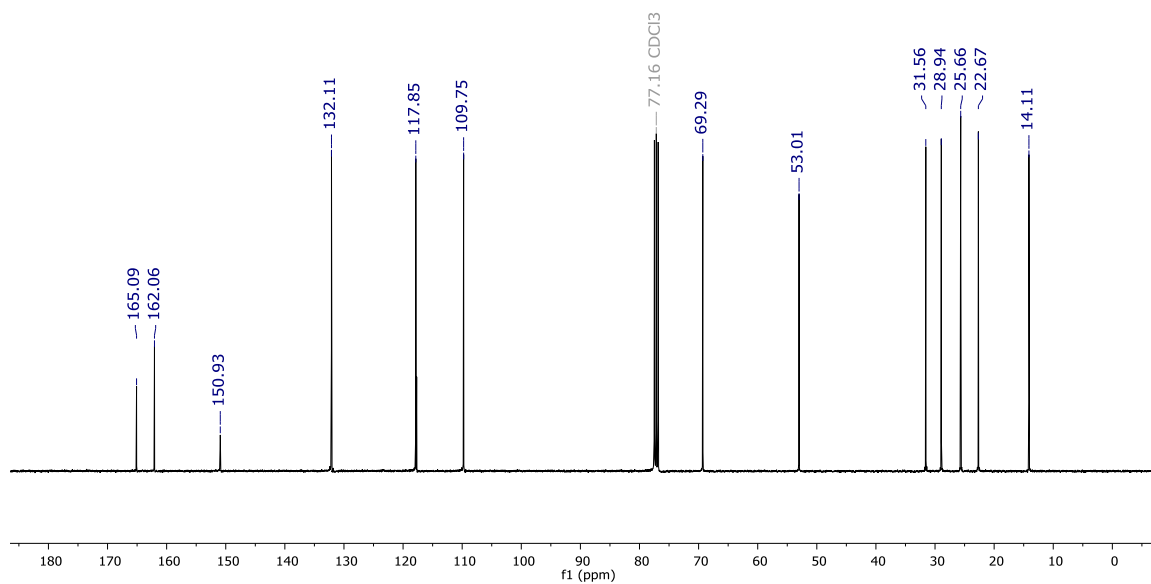**Figure A.3** ^{1}H NMR spectrum of methyl 4-(hexyloxy)-2-nitrobenzoate (**4**) in CDCl$_3$.

Figure A.4 ^{13}C{1H} NMR spectrum of methyl 4-(hexyloxy)-2-nitrobenzoate (**4**) in CDCl$_3$.
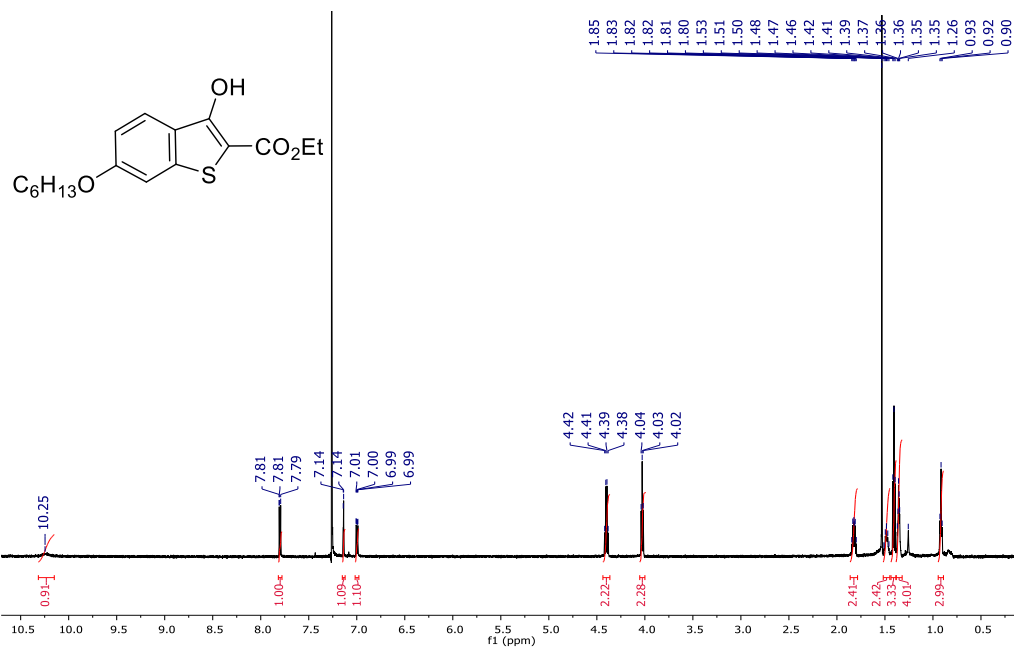
Figure A.5 ^{1}H NMR spectrum of ethyl 6-(hexyloxy)-3-hydroxybenzo[b]thiophene-2-carboxylate (**5**) in CDCl$_3$.
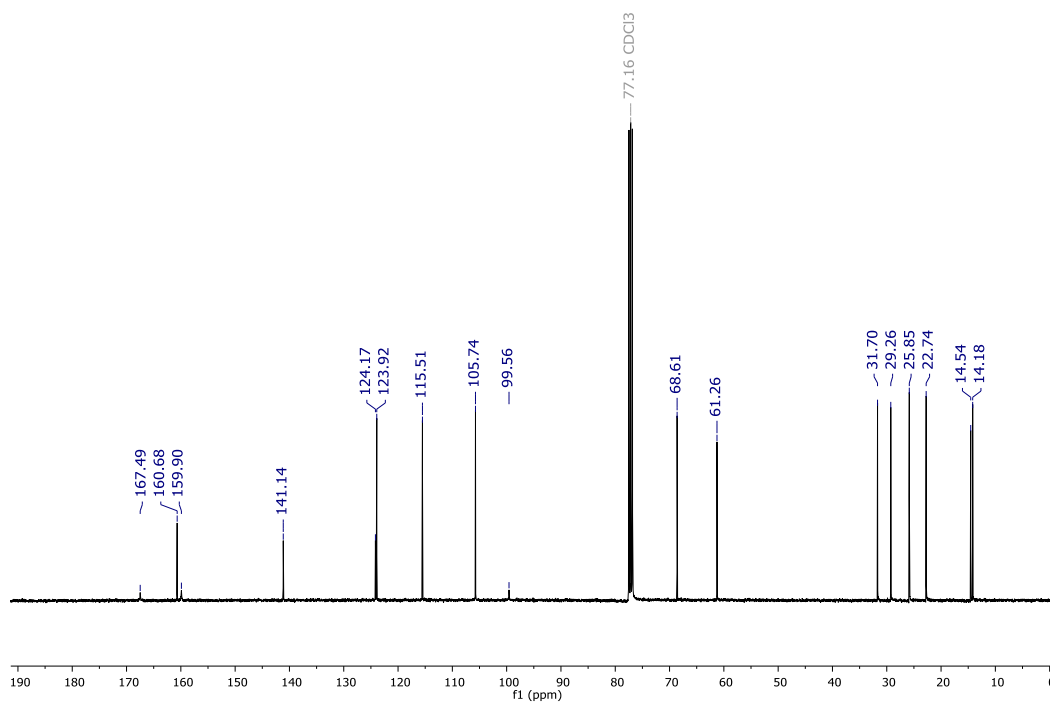
Figure A.6 ^{13}C{1H} NMR spectrum of ethyl 6-(hexyloxy)-3-hydroxybenzo[b]thiophene-2-carboxylate (**5**) in CDCl$_3$.
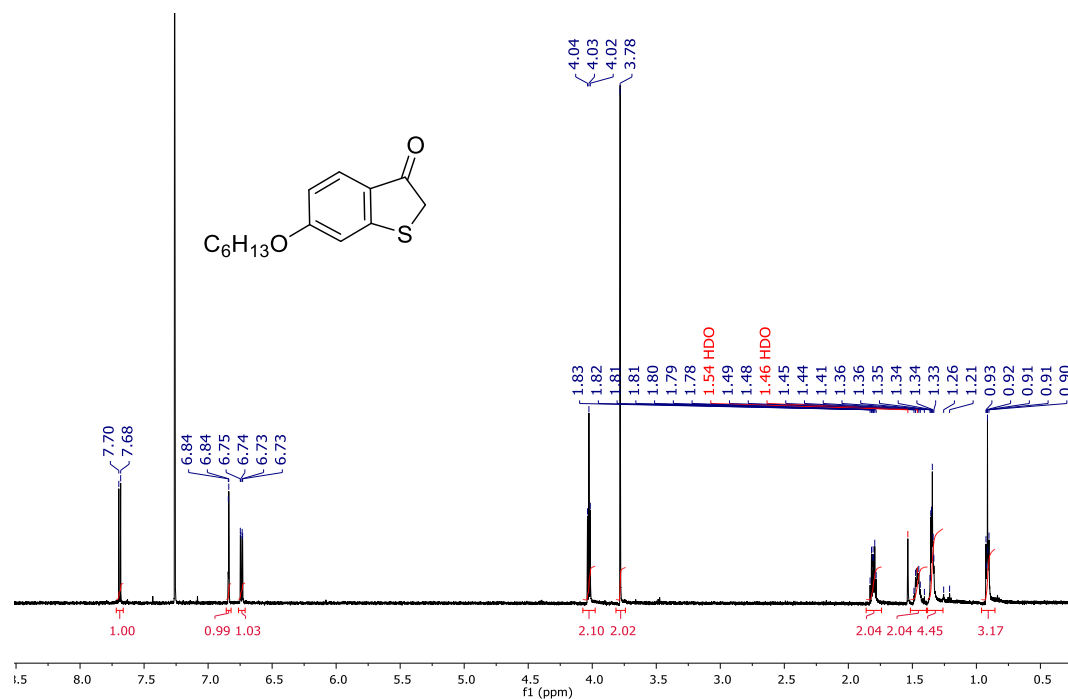
Figure A.7 ^{1}H NMR spectrum of 6-(hexyloxy)benzo[b]thiophen-3(2H)-one (**6**) in CDCl$_3$.
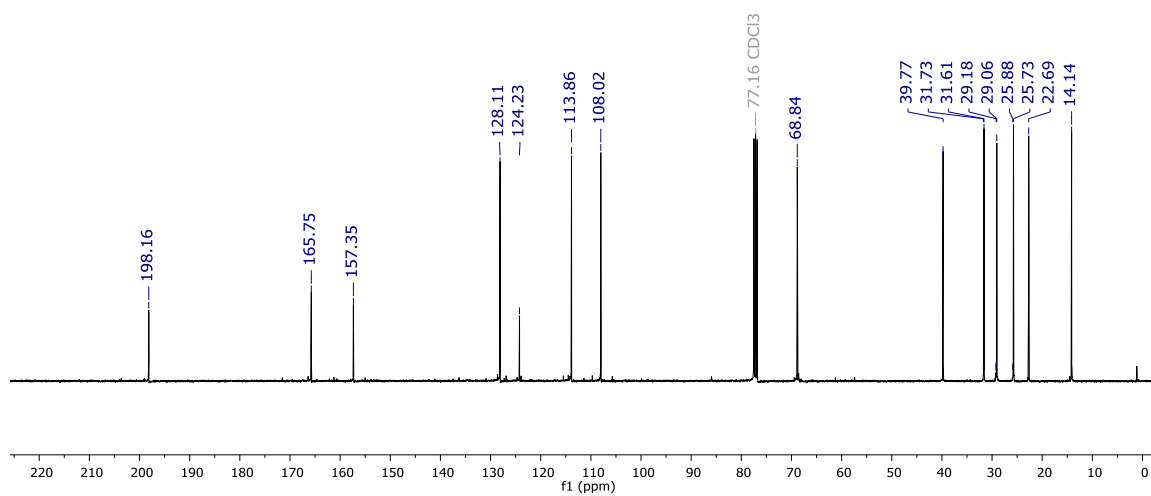
Figure A.8 ^{13}C{1H} NMR spectrum of 6-(hexyloxy)benzo[b]thiophen-3(2H)-one (**6**) in CDCl$_3$.
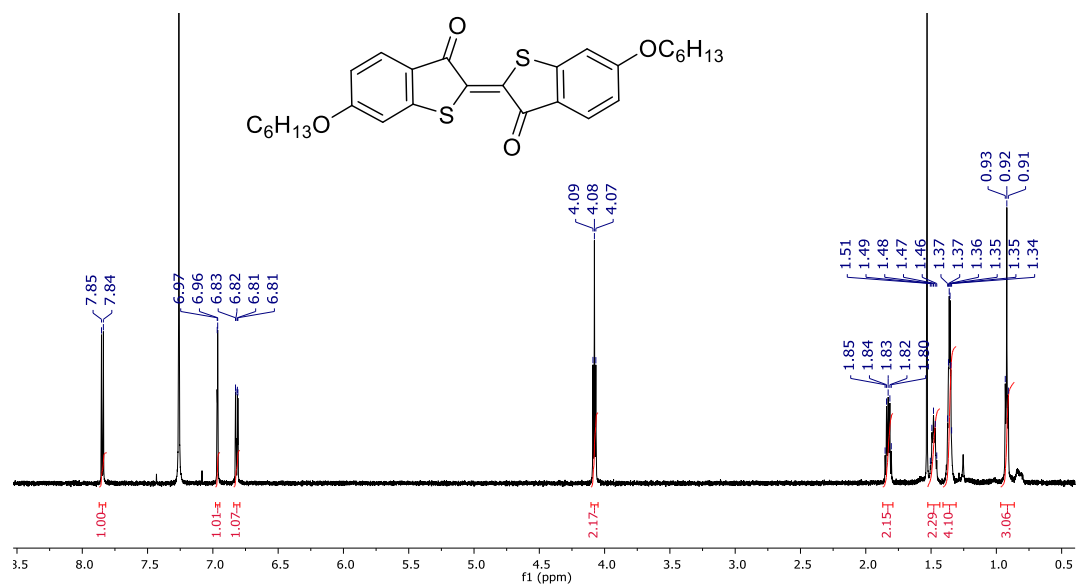
Figure A.9 ^{1}H NMR spectrum of (*E*)-6,6'-bis(hexyloxy)-3H,3'H-[2,2'-bibenzo[b]thiophenylidene]-3,3'-dione (**A1**) in CDCl$_3$.
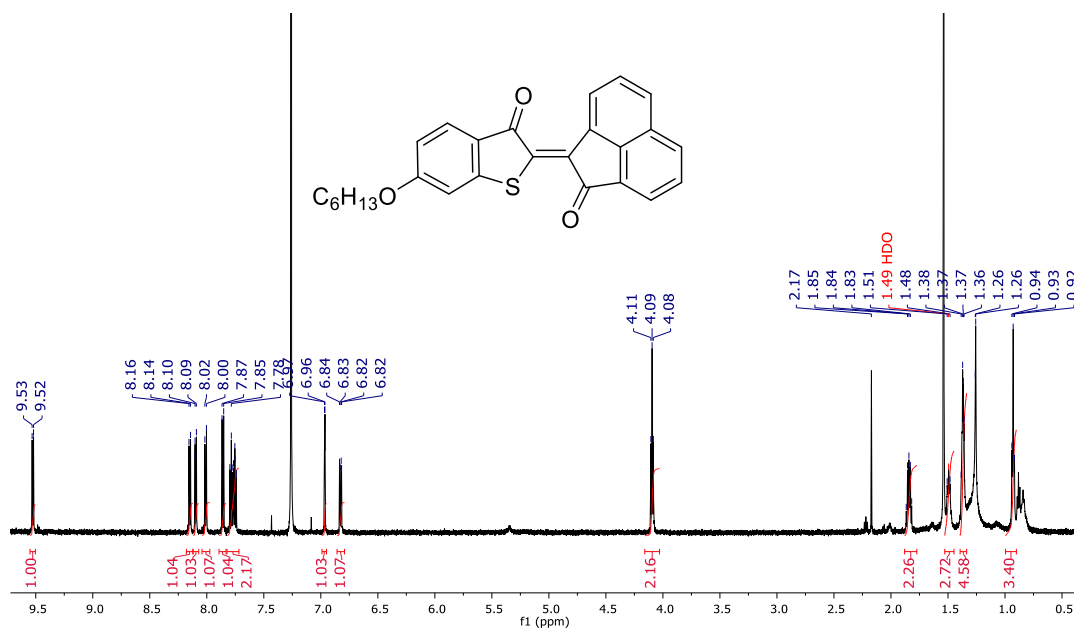
Figure A.10 ^{1}H NMR spectrum of (*Z*)-6-(hexyloxy)-2-(2-oxoacenaphthylen-1(2H)-ylidene)benzo[b]thiophen-3(2H)-one(Z-**A2**) in CDCl$_3$.
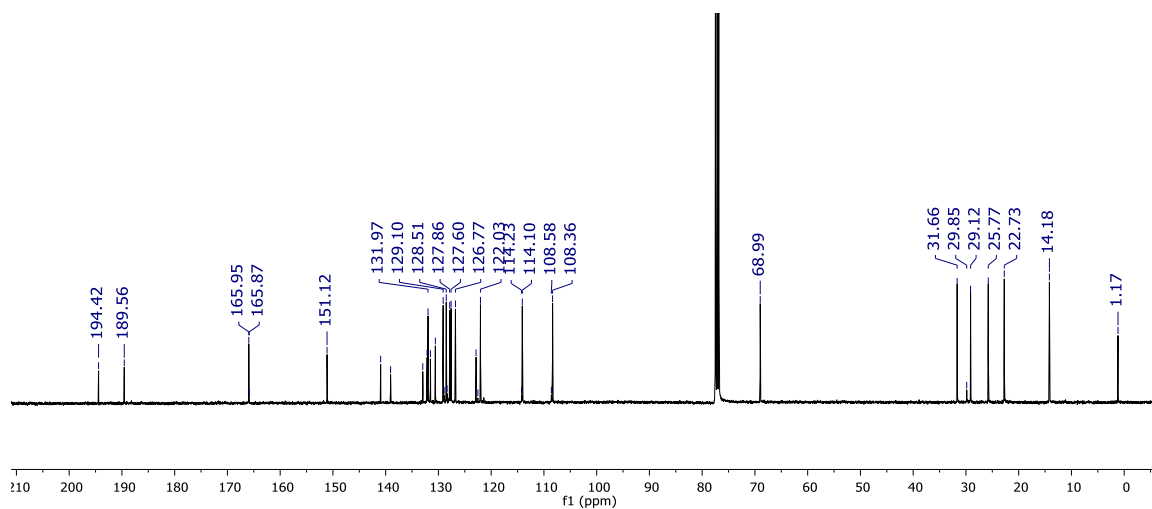
Figure A.11 ^{13}C{1H} NMR spectrum of (*Z*)-6-(hexyloxy)-2-(2-oxoacenaphthylen-1(2H)-ylidene)benzo[b]thiophen-3(2H)-one(Z-**A2**) in CDCl$_3$.
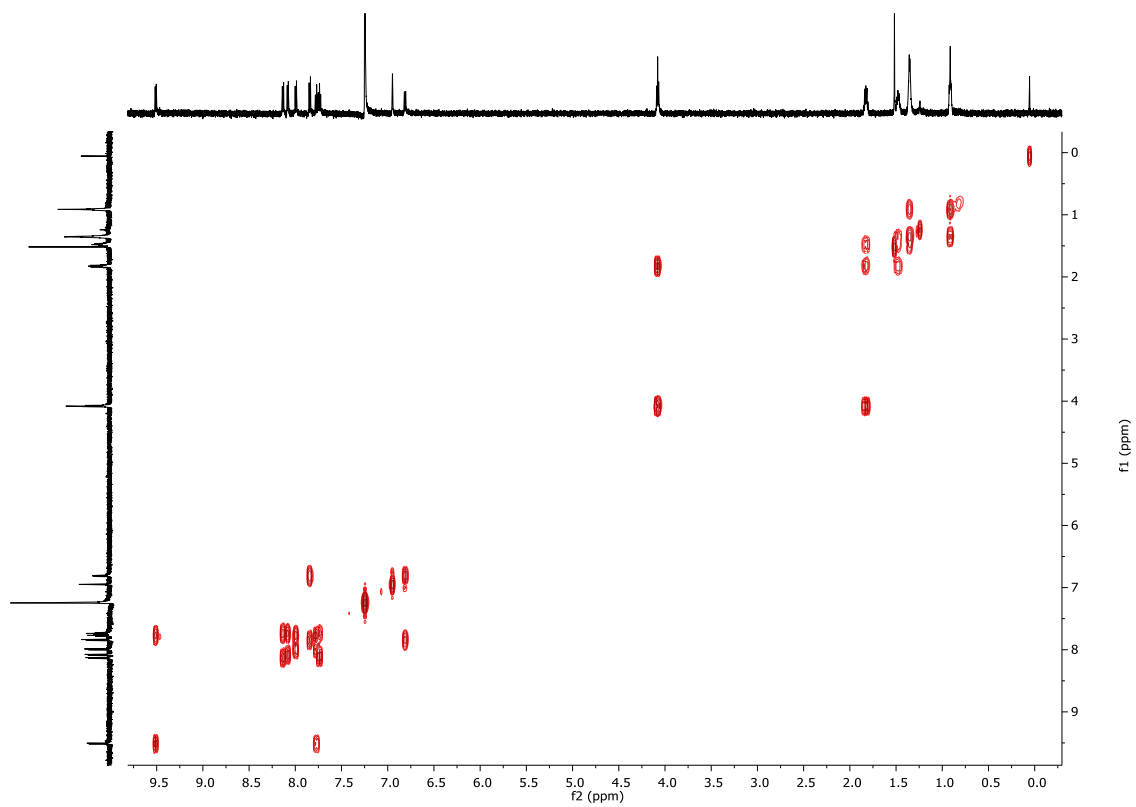
Figure A.12 gCOSY NMR spectrum of Z-**A2** in CDCl₃.
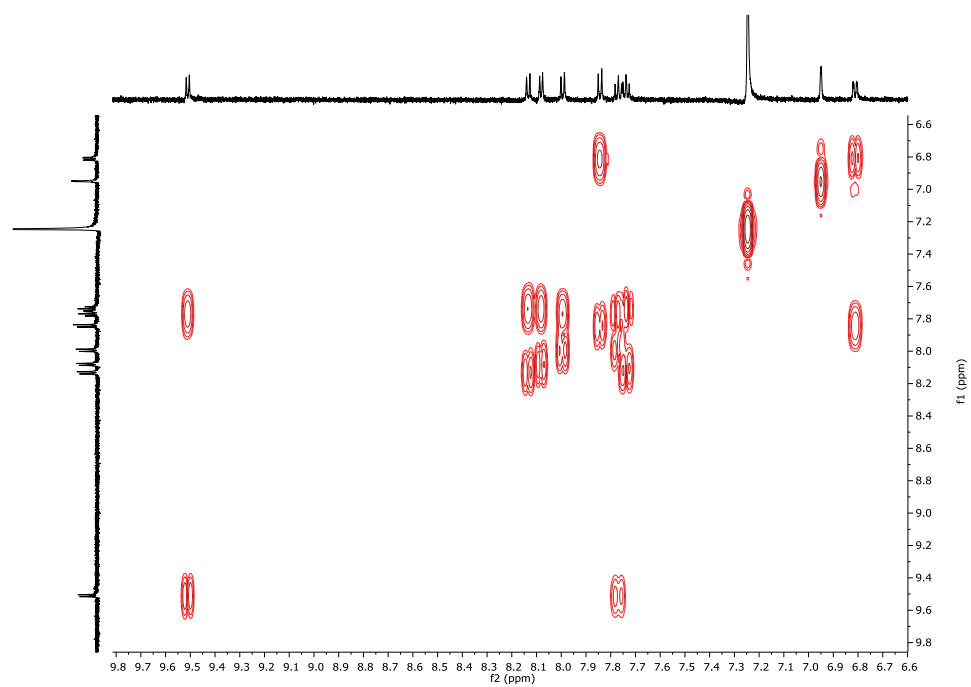
Figure A.13 gCOSY NMR spectrum of *Z*-**A2** in CDCl₃ (crowded region).
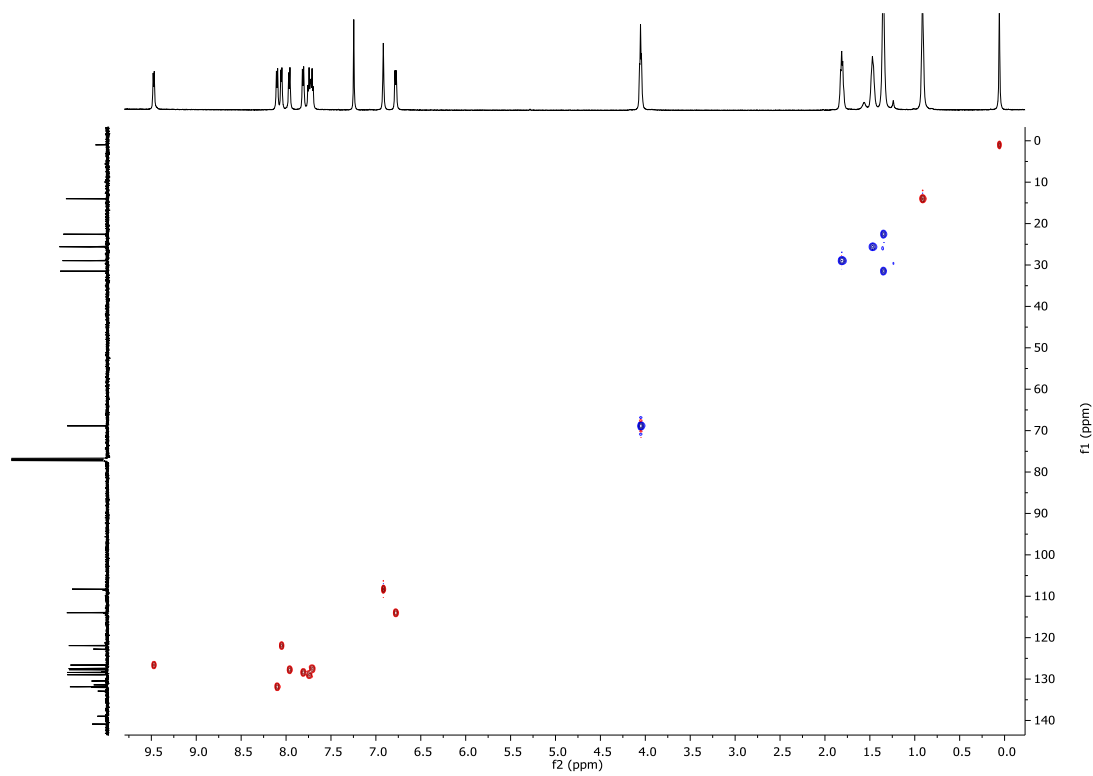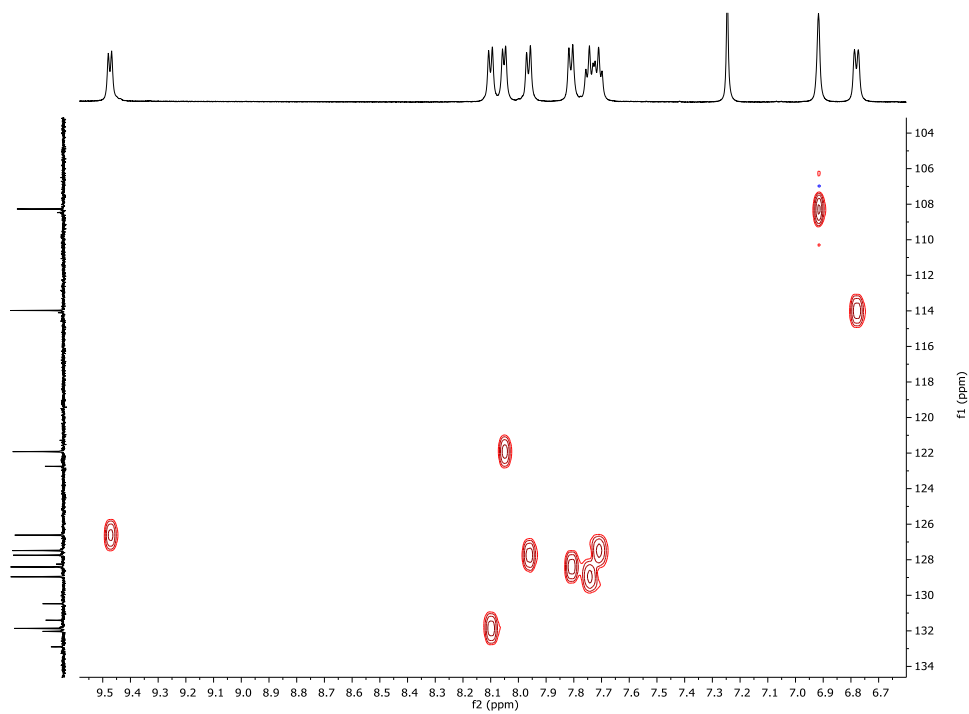
Figure A.14 HSQCAD NMR spectrum of Z-**A2** in CDCl₃.

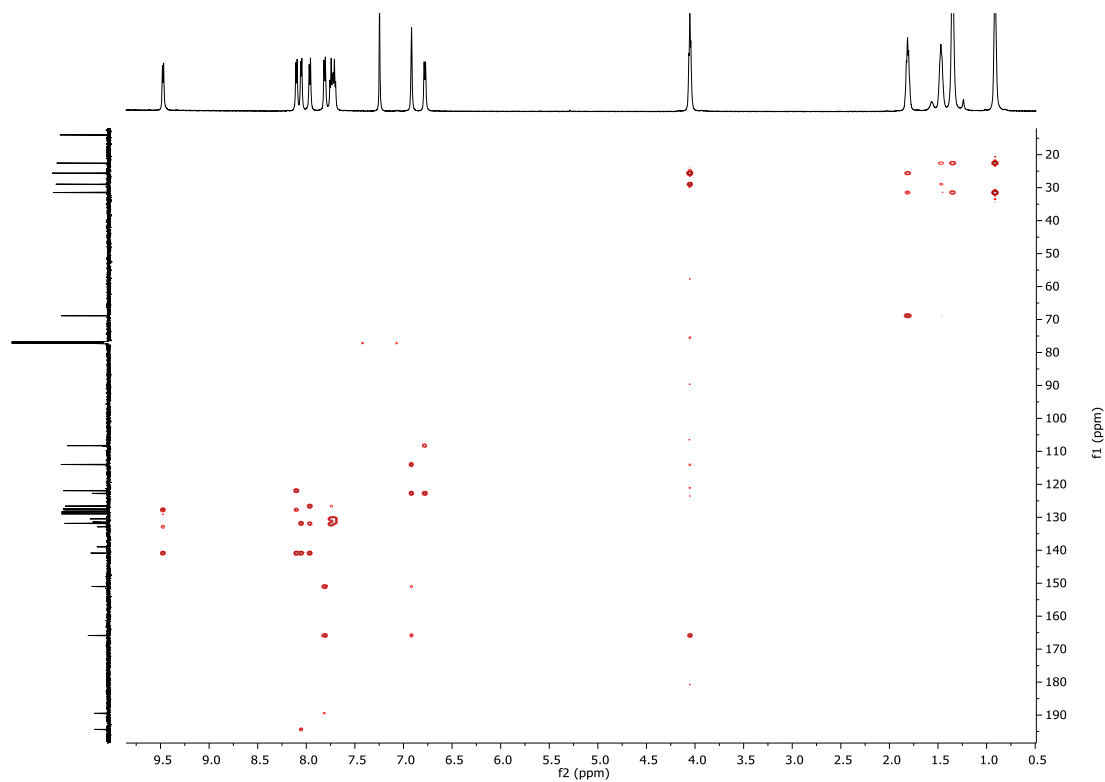**Figure A.15** HSQCAD NMR spectrum of Z-**A2** in CDCl₃ (crowded region).
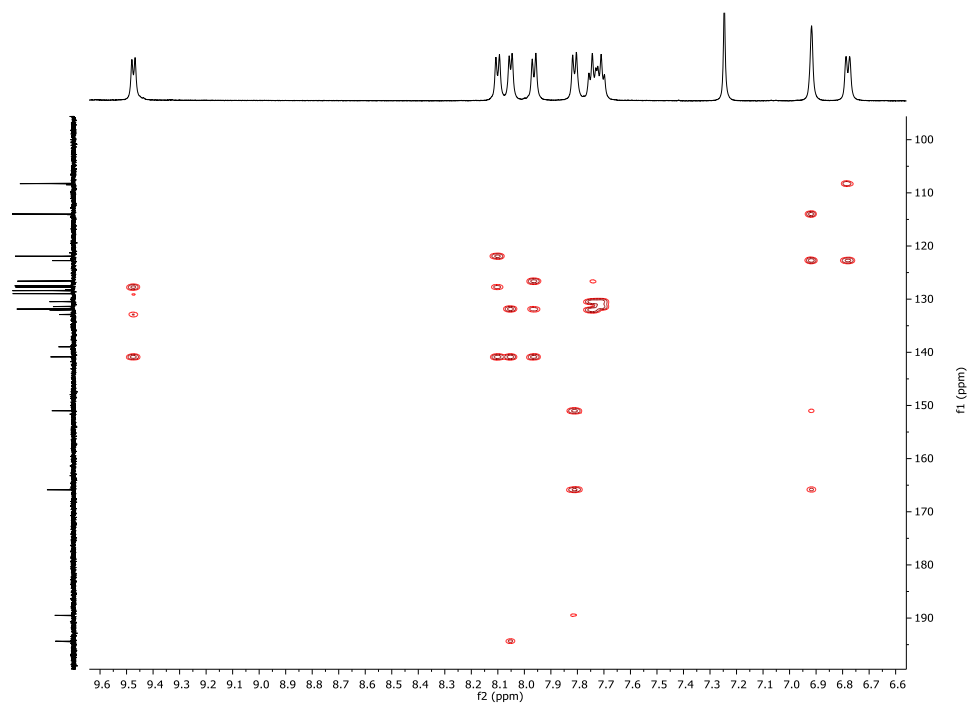
Figure A.16 HMBC NMR spectrum of *Z*-**A2** in CDCl₃.

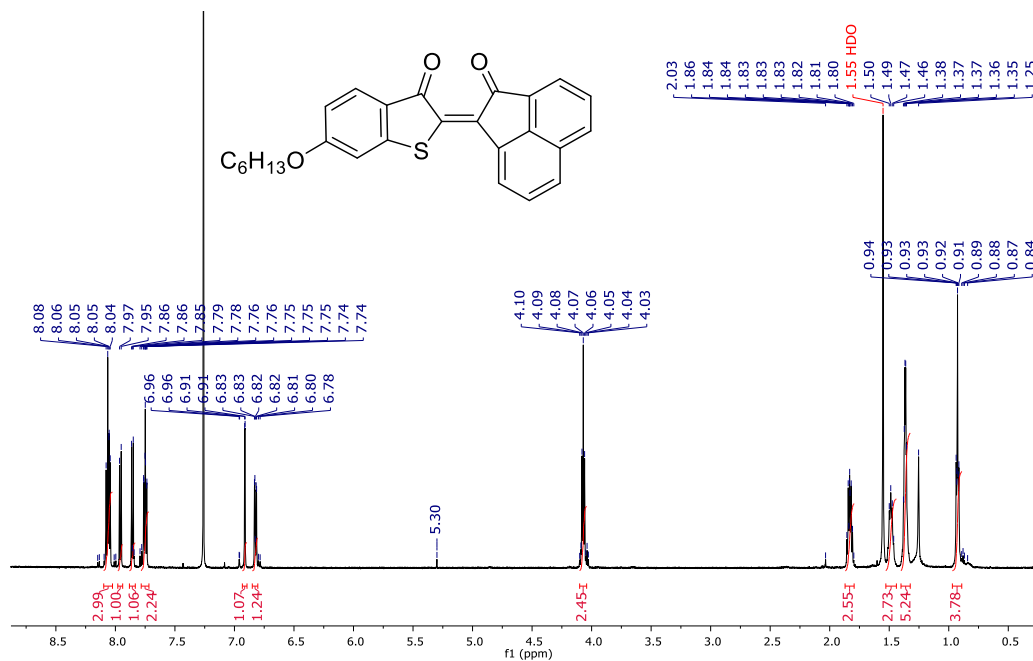**Figure A.17** HMBC NMR spectrum of *Z*-**A2** in CDCl₃ (crowded region).

Figure A.18 ^{1}H NMR spectrum of (*E*)-6-(hexyloxy)-2-(2-oxoacenaphthylen-1(2H)-ylidene)benzo[b]thiophen-3(2H)-one (*E*-**A2**) in CDCl$_3$.
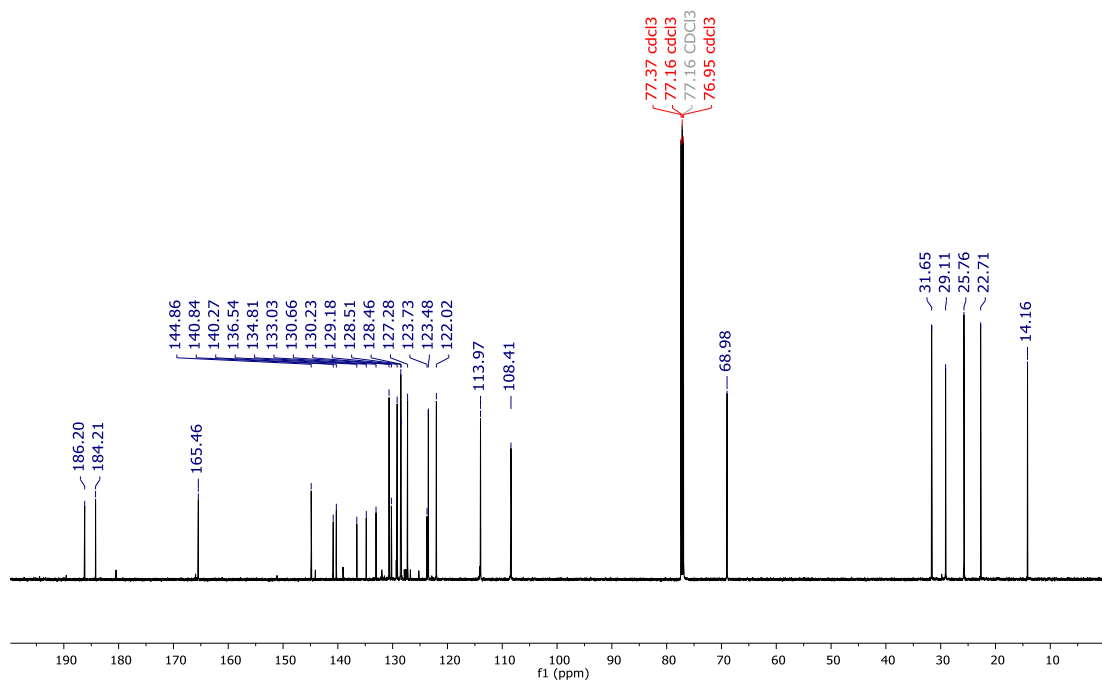

Figure A.19 ^{13}C{1H} spectrum of (*E*)-6-(hexyloxy)-2-(2-oxoacenaphthylen-1(2H)-ylidene)benzo[b]thiophen-3(2H)-one (*E*-**A2**) in CDCl$_3$.
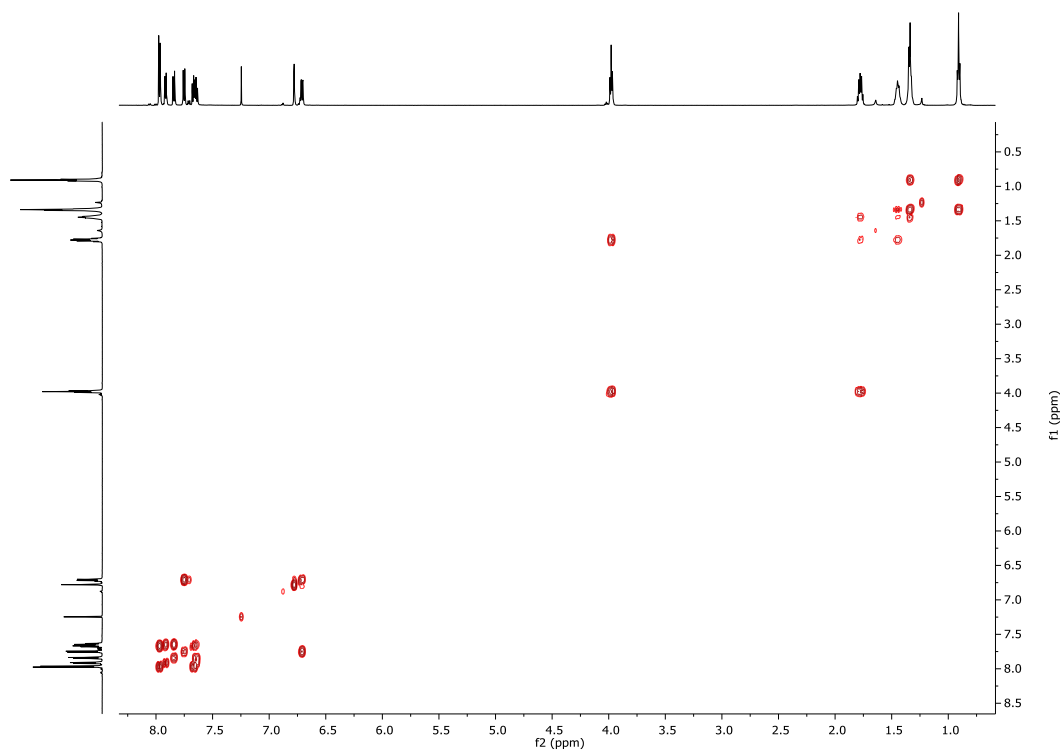
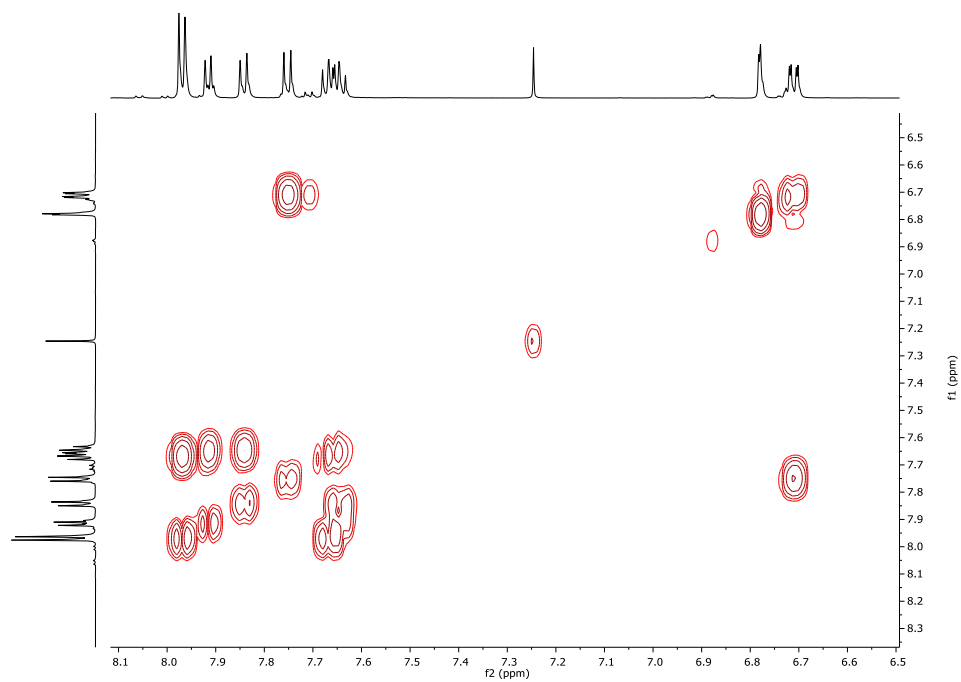**Figure A.20** gCOSY NMR spectrum of *E*-**A2** in CDCl₃.

Figure A.21 gCOSY NMR spectrum of *E*-**A2** in CDCl₃ (crowded region).
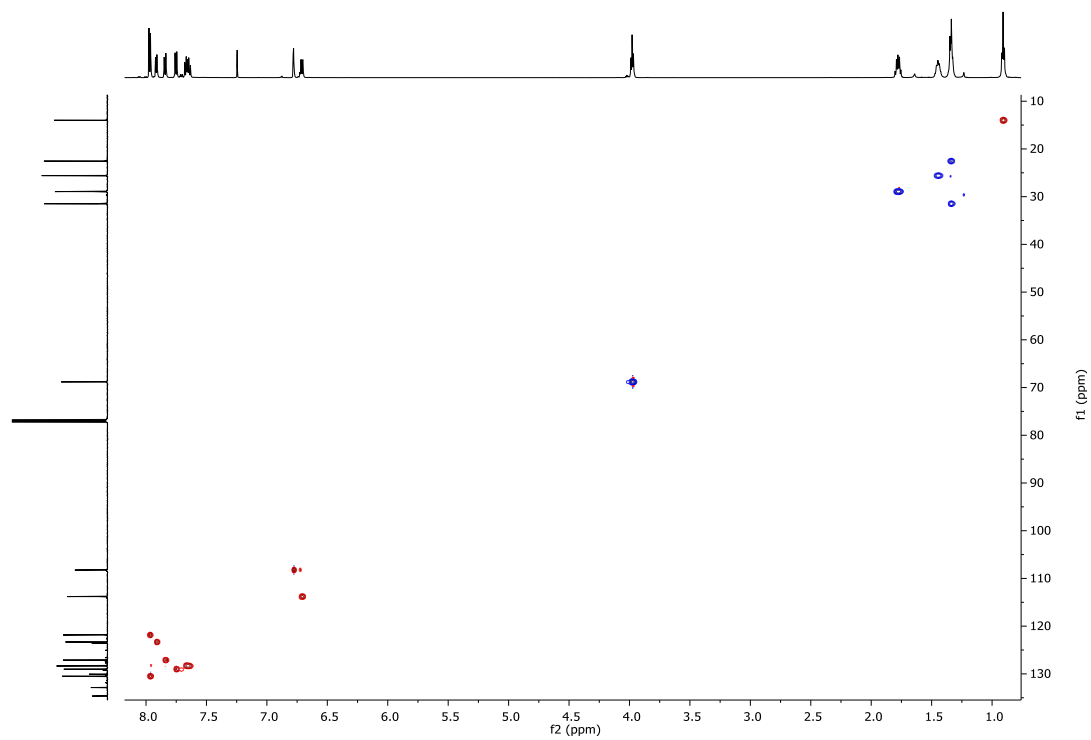
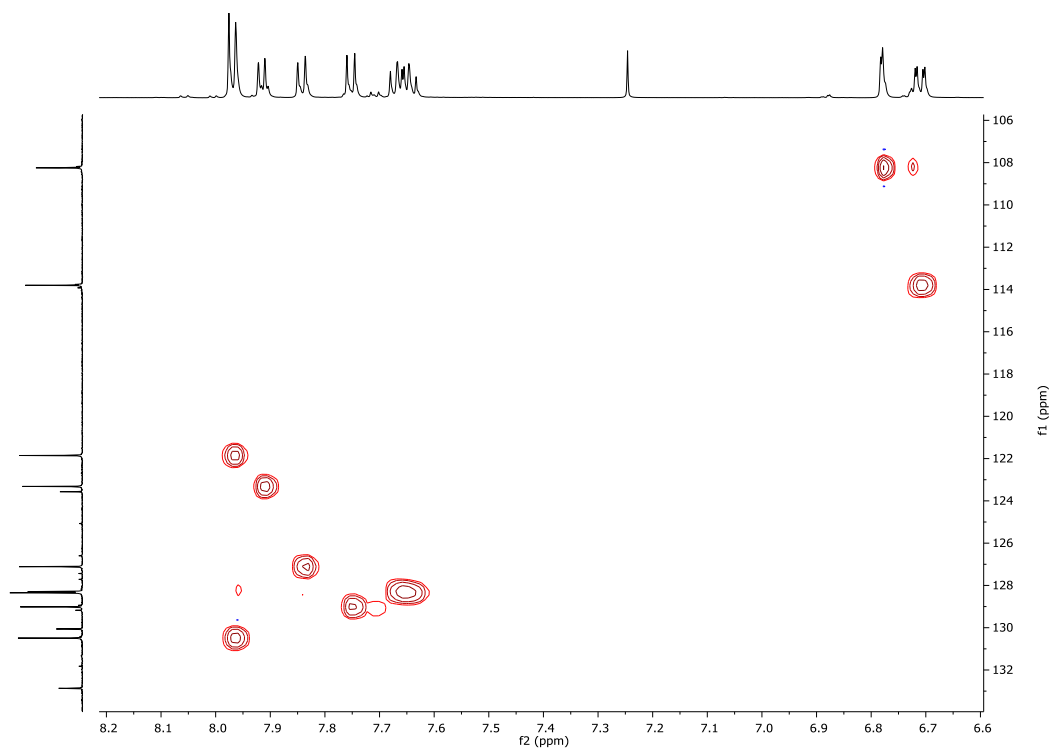**Figure A.22** HSQCAD NMR spectrum of *E*-**A2** in CDCl₃.

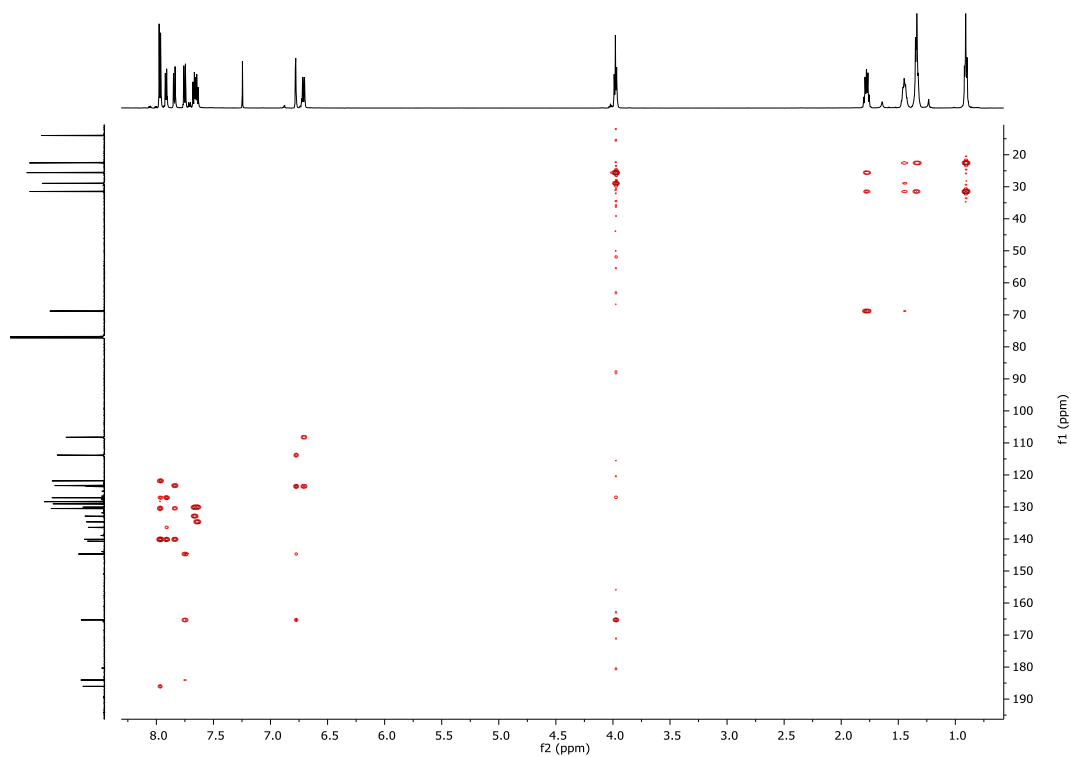**Figure A.23** HSQCAD NMR spectrum of *E*-**A2** in CDCl₃ (crowded region).

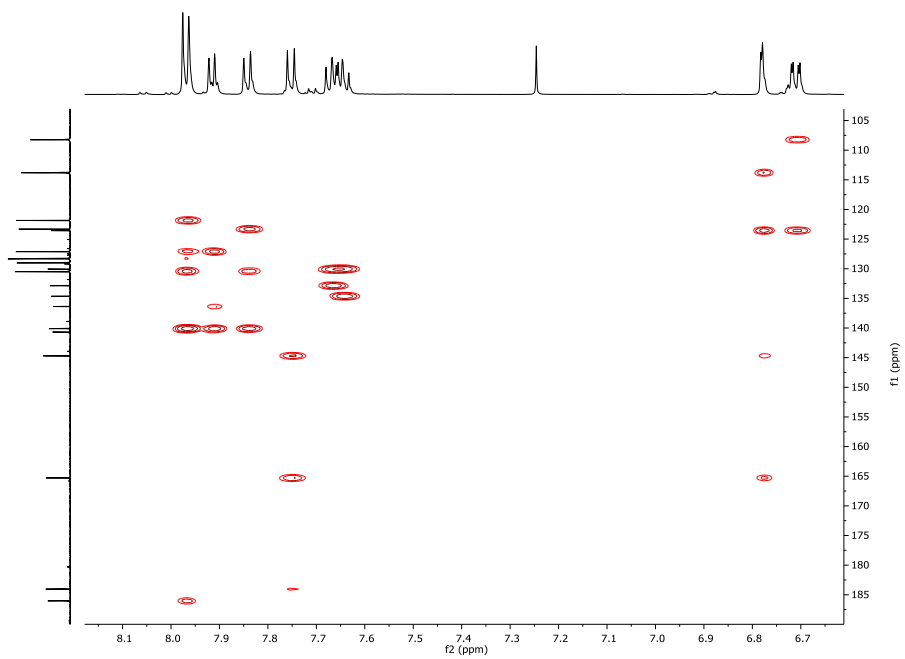**Figure A.24** HMBC NMR spectrum of *E*-**A2** in CDCl₃.

Figure A.25 HMBC NMR spectrum of *E*-**A2** in CDCl₃ (crowded region).

Curriculum Vitae

Name: Fereshteh Davoud

Post-secondary   Science and Research Branch, IAU
Education and   Ahvaz, Khouzestan, Iran
Degrees: 2010-2012 M.Sc.

                        Shahid Chamran University
                        Ahvaz, Khouzestan, Iran
                        2005-2009 B.Sc.

Honours and   Western Graduate Research Scholarship (WGRS)
Awards: 2016-2018

                        Iran Nanotechnology Initiative Council Award

Related Work   Teaching Assistant
Experience   University of Western Ontario
                        2016-2018

                        Research Assistant
                        ACECR-Production Technology Research Institute
                        Ahvaz, Khouzestan, Iran
                        Sep. 2014-June 2015

                        Research Assistant
                        Petroleum University of Technology
                        Ahvaz, Khouzestan, Iran
                        2013-2014

Publications:

Saghanezhad, S. J.; Nazari, Y.; **Davod**, **F**. Cucurbit[6]uril-OSO$_3$H: a Novel Acidic Nanocatalyst for the One-Pot Preparation of 14-aryl-14H-dibenzo[a,j]xanthenes and 1,8-dioxo-octahydro-xanthenes *RSC Adv.* **2016**, *6*, 25525–25530.

Davod, F.; Kiasat, A. R.; Enjilzadeh, M.; Cheraghchi, M. One-Pot Synthesis of 14-Aryl-14 H-dibenzo[*a,j*]xanthene derivatives Catalyzed by Nano-Alumina Sulfuric Acid Through Solvent-Free Conditions *Lett. Org. Chem.* **2016**, *3*, 58-66.

Conference Presentations:
Davoud, **F**.; Wisner, J. A. Thioindigo Derivatives as Photoswitchable Hydrogen Bond Acceptor Arrays, 100th Canadian Chemistry Conference and Exhibition, Toronto, Ontario, Canada, May 28-June 1, 2017(Poster).

Farhadi, A.; **Davod**, **F**.; Enjilzadeh, M.; Takassi, M. A.; Hamoule, T. Synthesis of DHPMs Catalyzed by N-ASA Under Solvent-Free Conditions", First National Conference of New Technologies in Chemical and Petrochemical, Tehran, Iran, April 17, 2014 (Poster).

Farhadi, A.; Takassi, M. A.; Hejazi, L.; **Davod**, **F**.; Enjilzadeh, M. Synthesis of 1,2,3,4-Tetrahydropyrimidin-one Using N-ZrO$_2$. First National Conference of New Technologies in Chemical and Petrochemical, Tehran, Iran, April 17, 2014 (Poster).

Montazeri, N.; **Davod**, **F**. Multi Component Reactions (MCRs) as a Green Approach Towards the Synthesis of Xanthene Derivatives. 1th National conference on Multi-Component Reactions, Kerman, Iran, May 30-31, 2012 (Poster).

Mahdavi Rad, R.; **Davod**, **F**. The Synthesis of Highly Functionalized 4H-Pyrans via a Three Component Reaction of Isocyanides. 1th National conference on Multi-Component Reactions, Kerman, Iran, May 30-31, 2012 (Poster).